



universität
wien

DIPLOMARBEIT

Titel der Diplomarbeit

„Geometry of GHZ type quantum states“

verfasst von

Mag. Dr. Gabriele Uchida

angestrebter akademischer Grad

Magistra der Naturwissenschaften (Mag. rer. nat.)

Wien, 2013

Studienkennzahl lt. Studienblatt:

A 411

Studienrichtung lt. Studienblatt:

411 Diplomstudium Physik UniStG

Betreuer:

Ao. Univ.-Prof. Dr. Reinhold A. Bertlmann

Acknowledgement

I would like to express my gratitude to the many people who saw me through this book and to all those who provided support and assistance.

First and foremost I want to thank my supervisor Reinhold A. Bertlmann for his continued support, encouragement and his time for fruitful discussions.

Furthermore I would like to acknowledge my indebtedness to Prof. Paul Wagner who guided my first steps and with his lively and capturing lectures tempted me into more seriously studying physical sciences.

Long and intensive discussions with colleagues, especially Philipp Köhler and many others gave me much energy and inspiration.

Especially I would like to thank my husband whose unconditional love and support enabled and encouraged me to complete this work.

Contents

1	Introduction	1
2	Basics and mathematical formalism	3
2.1	Quantum states	3
2.2	Density matrices	5
2.3	Bloch sphere	6
3	Bipartite systems	9
3.1	Vector states	9
3.2	Operators, Density matrices	10
3.3	Schmidt decomposition	12
3.4	Separability and entanglement	13
3.4.1	Entanglement of pure states	13
3.4.2	Entanglement of mixed states	14
3.4.3	Positive Partial Transpose Criterion	16
3.5	Entanglement measures	18
3.5.1	Entanglement measures for pure states	19
3.5.2	Entanglement measures for mixed states	21
3.5.2.1	Entanglement of formation	21
3.5.2.2	Concurrence	22
3.5.2.3	Entanglement cost	23
3.5.2.4	Entanglement of distillation	23
3.5.2.5	Hilbert-Schmidt distance	23
3.5.2.6	Negativity	24
3.5.2.7	Entanglement witness	24
3.6	EPR and Bell inequality	26
3.6.1	EPR "Paradoxon"	26
3.6.2	Bell inequality	27
3.7	Bloch decomposition	28

4	Tripartite and especially GHZ type states	33
4.1	Types of entanglement, GHZ and W states	33
4.2	Generalized Schmidt Decomposition	37
4.3	EPR and GHZ Theorem	37
4.4	Geometry and entanglement	39
4.4.1	Partial Traces	39
4.4.2	Entanglement measures	40
4.4.2.1	Entropy	40
4.4.2.2	3-tangle and concurrence	43
4.4.2.3	Negativity	46
4.4.2.4	Entanglement witnesses	47
4.4.3	Entanglement type for GHZ symmetric states	49
4.4.4	Unitary transformations	52
4.5	Entangled Entanglement	54
4.5.1	Eight entangled entanglement 2x2x2 states	55
4.5.2	Local unitary transformation of entangled entanglement states	57
4.5.3	Entanglement construction	60
4.6	Bloch representation in the tripartite case	61
4.6.1	Unitary 2x2x2 transformations and density matrices	61
4.6.2	Pure 2x2x2 states	62
4.6.3	States with entangled entanglement	67
4.6.4	Entanglement in the magic simplex	71
5	Conclusion	75
A	Mathematica Tool	77
B	Unitary transformation matrices	85
C	Bloch representation and pure states	87
	References	92

Chapter 1

Introduction

Greenberger-Horne-Zeilinger or GHZ states are a superposition of two maximally distinct three-qubit states [1]. In some sense they can be considered as maximally entangled. They have been studied intensively in the last years and many interesting applications have emerged:

- quantum teleportation [2],
- quantum entanglement swapping [3],
- quantum computing [4],
- quantum cryptography [5] and
- quantum information [6].

Moreover it could be shown in [7] that GHZ states violate local realism in an extreme form, leading to a Bell inequality check that can be effectuated in only one experiment.

In the three qubit case states have a much richer structure than two qubit states. Whereas two qubits can be separable or entangled, in the three qubit case we have a larger spectrum of possibilities; states can here be completely separable, biseparable or tripartite entangled and there are even two classes of tripartite entanglement: GHZ or W type states. These tripartite entanglement classes are not equivalent!

The association to one of these entanglement classes is much more difficult to establish, and especially the well known PPT criterion – widely used in the two qubit case – is not a necessary and sufficient condition in the tripartite qubit case.

In the last years many entanglement measures have been developed for this case, at least for quite a lot of special cases [8], [9].

Studying geometrical properties can give us new ideas and insights to (sometimes very strange) properties and applications of quantum states. Especially interesting are geometrical connections between states of different entanglement or separability types, since structures are more sophisticated for multipartite situations. Different geometrical representations and perspectives can give us a broader understanding of the complicated structures.

In this work we will give a very short overview of the basic mathematical formalism, a very concise overview of the bipartite situation and finally a collection of different findings regarding the three-qubit case.

Throughout the work, but especially for the last chapter, Wolfram Mathematica Software has been used to perform calculations and drawings. Most, but not all of these calculations could have been made without this software, but since done by hand tend to be very time consuming, it made life much easier.

Chapter 2

Basics and mathematical formalism

2.1 Quantum states

The state of a quantum mechanical system is represented by a vector in a Hilbert space \mathcal{H} , meaning a complex vector space equipped with an inner product. In this work we will consider quantum systems where corresponding physical quantities allow only a limited number of results as outcome of their measurements. Therefore we use a finite dimensional Hilbert space for the mathematical representation [10].

Our main focus will be restricted to studying two-state systems, so that pure states $|\psi\rangle$ can be represented by vectors in the two dimensional Hilbert space $\mathcal{H} = \mathbb{C}^2$. The spin of an electron or the polarization of a single photon are well studied examples of this type.

Vectors of this two dimensional space can be written as linear combinations of two vectors forming a basis of the corresponding Hilbert space. Often these basis vectors are written as $|0\rangle$ and $|1\rangle$ and it is assumed that they are normalized and orthogonal:

$$\langle 0|0\rangle = 1, \langle 1|1\rangle = 1 \text{ and } \langle 0|1\rangle = 0 \quad (2.1.1)$$

The notation $|0\rangle$ and $|1\rangle$ suggests an analogy to a bit in information theory, so in quantum theory two-state systems are often called *qubits*. But there are some serious differences: whereas in a two-state quantum system, vectors like the superposition $\frac{1}{\sqrt{2}}(|0\rangle + i|1\rangle)$ can be interpreted as a state with a physical meaning, ordinary bits in information theory can only take the values 0 or 1.

In the context of concrete physical systems we come up with different notations.

For example:

- In experiments with spin $\frac{1}{2}$ particles instead of $|0\rangle, |1\rangle$, the basis vectors $|\uparrow\rangle, |\downarrow\rangle$ (for spin up and spin down) are used in an absolutely equivalent way. More precisely, if S_x, S_y, S_z are the corresponding components of the angular momentum (measured in units of \hbar), $|0\rangle = |\uparrow\rangle$ corresponds to $S_z = +\frac{1}{2}$ and $|1\rangle = |\downarrow\rangle$ to $S_z = -\frac{1}{2}$. For the x- and y-components we obtain the following correspondences:

$$\begin{aligned} S_x = +\frac{1}{2} &\leftrightarrow \frac{1}{\sqrt{2}}(|0\rangle + |1\rangle), & S_x = -\frac{1}{2} &\leftrightarrow \frac{1}{\sqrt{2}}(|0\rangle - |1\rangle) \\ S_y = +\frac{1}{2} &\leftrightarrow \frac{1}{\sqrt{2}}(|0\rangle + i|1\rangle), & S_y = -\frac{1}{2} &\leftrightarrow \frac{1}{\sqrt{2}}(|0\rangle - i|1\rangle) \end{aligned} \quad (2.1.2)$$

- In quantum optics, polarization of photons is noted as $|H\rangle, |V\rangle$ for polarization in horizontal or vertical direction respectively. In this context some rotated bases are frequently used and the following representation can be taken for bases $|0\rangle, |1\rangle$ or correspondingly $|H\rangle, |V\rangle$ in \mathbb{C}^2 .

$$|H\rangle = |0\rangle = \begin{pmatrix} 1 \\ 0 \end{pmatrix}, \quad |V\rangle = |1\rangle = \begin{pmatrix} 0 \\ 1 \end{pmatrix} \quad (2.1.3)$$

The rotated basis for photons polarized along $\pm 45^\circ$ is written as

$$\begin{aligned} | +45^\circ \rangle &= |+\rangle = \frac{1}{\sqrt{2}}(|H\rangle + |V\rangle) = \frac{1}{\sqrt{2}} \begin{pmatrix} 1 \\ 1 \end{pmatrix}, \\ | -45^\circ \rangle &= |-\rangle = \frac{1}{\sqrt{2}}(|H\rangle - |V\rangle) = \frac{1}{\sqrt{2}} \begin{pmatrix} 1 \\ -1 \end{pmatrix} \end{aligned} \quad (2.1.4)$$

and right $|R\rangle$ and left $|L\rangle$ circularly polarized photons take the form

$$\begin{aligned} |R\rangle &= \frac{1}{\sqrt{2}}(|H\rangle + i|V\rangle) = \frac{1}{\sqrt{2}} \begin{pmatrix} 1 \\ i \end{pmatrix}, \\ |L\rangle &= \frac{1}{\sqrt{2}}(|H\rangle - i|V\rangle) = \frac{1}{\sqrt{2}} \begin{pmatrix} 1 \\ -i \end{pmatrix} \end{aligned} \quad (2.1.5)$$

similar to the correspondences in the spin $\frac{1}{2}$ particle case.

2.2 Density matrices

Vectors in a Hilbert space \mathcal{H} represent pure states, which are well suited for isolated systems. In a general quantum mechanical system, we also need to describe mixed states. The following mixture of quantum states $|\psi_i\rangle$ with respective probabilities p_i , will be represented by a $\mathbb{C}^2 \times \mathbb{C}^2$ density matrix (see for example [11])

$$\rho = \sum_i p_i |\psi_i\rangle \langle \psi_i|, \quad p_i \geq 0, \quad \sum_i p_i = 1 \quad (2.2.1)$$

To make sure that the density matrix ρ corresponds to physical states, the following properties must be fulfilled:

- $\rho \geq 0$: ρ is a "positive" matrix in the sense that all its eigenvalues are non-negative (actually this means the matrix is positive semi-definite)
- $\rho = \rho^\dagger$: ρ is self-adjoint
- $\text{tr } \rho = 1$: The trace of a density matrix is equal to 1
- $\text{tr } \rho^2 \leq 1$: The trace of the square of a density matrix is smaller than or equal to 1
- $\rho^2 = \rho$: the square of the density matrix equals the density matrix if the state is pure and therefore, in this case only, $\text{tr } \rho^2 = \text{tr } \rho = 1$
 Remark: $1 - \text{tr } \rho^2$ could therefore be used as measure for mixedness.

Actually states represented in this form are elements of the Hilbert-Schmidt space; the space of operators acting on vectors of the corresponding Hilbert space \mathcal{A} . And indeed, for pure states the density matrix $\rho = |\psi\rangle \langle \psi|$ is an operator of this form, namely just the projector onto the corresponding vector state $|\psi\rangle$.

The trace operation is defined as

$$\text{tr } A = \sum_i A_{ii} = \sum_i \langle i | A | i \rangle \quad (2.2.2)$$

with an orthogonal basis $\{|i\rangle\}$ and A_{ii} the matrix elements in the diagonal of A. The value of the trace is independent of the choice of the basis and equal to the sum of the eigenvalues λ_i of A

$$\text{tr } A = \sum_i \lambda_i \quad (2.2.3)$$

The trace operator provides an inner product of two elements A, B of the Hilbert-Schmidt space:

$$\langle A, B \rangle = \text{Tr}(A^\dagger B) \quad (2.2.4)$$

and also a norm

$$\|A\| = \sqrt{\langle A, A \rangle} = \sqrt{\text{Tr}(A^\dagger A)}. \quad (2.2.5)$$

The Hilbert-Schmidt distance is then defined as

$$d(A, B) = \|A - B\|. \quad (2.2.6)$$

Considering an observable O for a quantum state ρ , its expectation value is given by

$$\langle O \rangle_\rho = \text{tr}(\rho O). \quad (2.2.7)$$

For a pure quantum state with density matrix $\rho = |\psi\rangle\langle\psi|$, the expectation value is given by

$$\langle O \rangle_\rho = \text{tr}(\rho O) = \langle \psi | O | \psi \rangle. \quad (2.2.8)$$

This shows that the density matrix contains all the information that is physically important.

The matrix elements of the density matrix can easily be obtained using the standard basis $\{|i\rangle\}$ as

$$\rho_{ij} = \langle i | \rho | j \rangle, \quad (2.2.9)$$

allowing us to write the density matrix for a qubit in the following way:

$$\rho = \begin{pmatrix} \langle 0 | \rho | 0 \rangle & \langle 0 | \rho | 1 \rangle \\ \langle 1 | \rho | 0 \rangle & \langle 1 | \rho | 1 \rangle \end{pmatrix} \quad (2.2.10)$$

2.3 Bloch sphere

In two-level quantum systems (qubits) pure states can be geometrically represented as points on a Bloch sphere (in optics called Poincaré sphere).

A pure state $|\psi\rangle$ can be written as a superposition of the basis vectors $\{|0\rangle, |1\rangle\}$

$$|\psi\rangle = a|0\rangle + b|1\rangle, \quad a, b \in \mathbb{C}, \quad |a|^2 + |b|^2 = 1. \quad (2.3.1)$$

The representation can also be given in spheric coordinates (see Figure 2.1 below) assigning to a state $|\psi\rangle$ the point with the following coordinates:

$$\begin{aligned} x &= \sin 2\theta \cos \phi \\ y &= \sin 2\theta \sin \phi \\ z &= \cos 2\theta \end{aligned}$$

with $-\frac{\pi}{2} \leq \theta < \frac{\pi}{2}$ and $0 \leq \phi < 2\pi$.

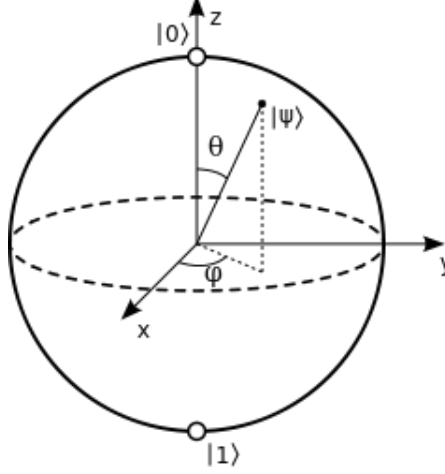


Figure 2.1: Bloch sphere (image from Wikimedia commons)

With this representation we assign the point $\begin{pmatrix} 0 \\ 0 \\ 1 \end{pmatrix}$ to $|0\rangle$ and $\begin{pmatrix} 0 \\ 0 \\ -1 \end{pmatrix}$ to $|1\rangle$ – say as the north- and the south-pole. More generally orthogonal quantum states correspond to antipodes, points on opposite sides of the sphere. Mixed states correspond to points in the interior of the sphere. For qubits the density matrices ρ are complex 2×2 hermitian matrices that can be represented als linear combinations of the two-dimensional Identity matrix and the three hermitian, traceless Pauli-matrices

$$\mathbb{I} = \begin{pmatrix} 1 & 0 \\ 0 & 1 \end{pmatrix}, \sigma_x = \begin{pmatrix} 0 & 1 \\ 1 & 0 \end{pmatrix}, \sigma_y = \begin{pmatrix} 0 & -i \\ i & 0 \end{pmatrix}, \sigma_z = \begin{pmatrix} 1 & 0 \\ 0 & -1 \end{pmatrix}$$

$$\rho = \frac{1}{2}(\mathbb{I} + \vec{a} \cdot \vec{\sigma}) \quad (2.3.2)$$

The three-dimensional Bloch vector \vec{a} now represents a point in the Bloch-sphere. This means every 2×2 density matrix can be thought of as a point on or inside a sphere. Points on the hull of the sphere represent pure states and points inside the sphere correspond to mixed states with the point in the center corresponding to the origin $\begin{pmatrix} 0 \\ 0 \\ 0 \end{pmatrix}$, representing the maximally mixed state $\frac{1}{2}\mathbb{I}$. The density matrix

$|0\rangle\langle 0| = \begin{pmatrix} 1 & 0 \\ 0 & 0 \end{pmatrix}$ corresponding to the pure state $|0\rangle$ is obviously again related to the point $\vec{a} = \begin{pmatrix} 0 \\ 0 \\ 1 \end{pmatrix}$, for in this case we obtain

$$\frac{1}{2}(\mathbb{I} + \vec{a} \cdot \vec{\sigma}) = \frac{1}{2}(\mathbb{I} + \sigma_z) = \frac{1}{2}\left(\begin{pmatrix} 1 & 0 \\ 0 & 1 \end{pmatrix} + \begin{pmatrix} 1 & 0 \\ 0 & -1 \end{pmatrix}\right) = \begin{pmatrix} 1 & 0 \\ 0 & 0 \end{pmatrix}. \quad (2.3.3)$$

Eigenvalues of ρ are given by $\frac{1}{2}(1 \pm |\vec{a}|)$. Since ρ has to be positive semidefinite, we need $|\vec{a}| \leq 1$ to obtain physical states.

Points on the surface of the Bloch sphere fulfill $|\vec{a}| = 1$ which is in accordance with $\text{tr } \rho^2 = \text{tr } \rho = 1$, since $\text{tr } \rho^2 = \frac{1}{2}(1 + |\vec{a}|^2)$ equal to 1 exactly if and only if $|\vec{a}| = 1$, which is right on the surface of the Bloch sphere.

Chapter 3

Bipartite systems

3.1 Vector states

Instead of one qubit, let us now consider a quantum system of two subsystems. Let \mathcal{H}_A and \mathcal{H}_B be Hilbert spaces of the two subsystems of observer *Alice* and *Bob*. State vectors of composite systems are suitably described by elements of the composite Hilbert space which is the tensor product of the Hilbert spaces of the subsystems: $\mathcal{H}_{AB} = \mathcal{H}_A \otimes \mathcal{H}_B$.

The dimension of the new Hilbert space is the product of the dimensions of the subsystems:

$$\dim \mathcal{H}_{AB} = \dim \mathcal{H}_A \cdot \dim \mathcal{H}_B, \quad (3.1.1)$$

in case of two qubits the dimension is $\dim \mathcal{H}_{AB} = 2 \cdot 2 = 4$.

Remark 3.1.1 *In situations where there is no ambiguity, we often omit the indices A and B .*

The Hilbert space \mathcal{H}_{AB} consists of all the vectors of the form

$$|\psi\rangle = \sum_i \sum_j c_{ij} |a_i\rangle \otimes |b_j\rangle \quad (3.1.2)$$

for some coefficients c_{ij} , where $\{|a_i\rangle\}$ and $\{|b_j\rangle\}$ are orthonormal bases of \mathcal{H}_A and \mathcal{H}_B . So $\{|a_i\rangle \otimes |b_j\rangle\}$ form obviously a basis in \mathcal{H}_{AB} . In the special case of two qubits the composite Hilbert space consists of the vectors

$$|\psi\rangle = c_{00} |0\rangle \otimes |0\rangle + c_{01} |0\rangle \otimes |1\rangle + c_{10} |1\rangle \otimes |0\rangle + c_{11} |1\rangle \otimes |1\rangle. \quad (3.1.3)$$

For convenience we often write the tensor product $|a\rangle \otimes |b\rangle$ using the shorter form $|a\rangle |b\rangle$ or even shorter as $|ab\rangle$, giving us the compact form

$$|\psi\rangle = c_{00} |00\rangle + c_{01} |01\rangle + c_{10} |10\rangle + c_{11} |11\rangle. \quad (3.1.4)$$

The inner product in \mathcal{H}_{AB} is given by

$$\langle \psi_A \otimes \psi_B | \phi_A \otimes \phi_B \rangle = \langle \psi_A | \phi_A \rangle \langle \psi_B | \phi_B \rangle, \quad \psi_A, \phi_A \in \mathcal{H}_A, \psi_B, \phi_B \in \mathcal{H}_B \quad (3.1.5)$$

using again as a shorter notation $|\phi_A \otimes \phi_B\rangle = |\phi_A\rangle \otimes |\phi_B\rangle$.

A vector state or pure state $|\psi\rangle \in \mathcal{H}_{AB}$ that can actually be written as $|\psi\rangle = |\psi_A\rangle \otimes |\psi_B\rangle$ is called a *product state*. States that cannot be written in this form are called *entangled states*.

In most cases it is not really evident whether a vector state written in the form of (3.1.2) is a product state or not, because $|\psi_A\rangle$ as well as $|\psi_B\rangle$ could be linear combinations of basis states.

Example 3.1.1 *The state $|00\rangle + |01\rangle + |10\rangle + |11\rangle$ can be written as $(|0\rangle + |1\rangle) \otimes (|0\rangle + |1\rangle)$ and therefore is a product state.*

Physically the definition of a product state means that states are uncorrelated. If Alice measures an observable A and Bob an observable B, the measurement outcome of Alice does not depend on Bob's outcome.

3.2 Operators, Density matrices

Operators acting on vectors of the Hilbert space \mathcal{H}_{AB} form themselves a Hilbert space called the Hilbert-Schmidt space \mathcal{A}_{AB} . The tensor product of operators is defined by their action on vectors (of a basis). Let $A \in \mathcal{A}_A$ and $B \in \mathcal{A}_B$ be operators of the Hilbert-Schmidt spaces associated to \mathcal{H}_A and \mathcal{H}_B :

$$(A \otimes B)(|a_i\rangle \otimes |b_j\rangle) = A|a_i\rangle \otimes B|b_j\rangle. \quad (3.2.1)$$

Any operator $O \in \mathcal{A}_{AB}$ can be expressed as linear combination of tensor products of operators in the subspaces:

$$O = \sum_i \sum_j o_{ij} A_i \otimes B_j, \quad A_i \in \mathcal{A}_A, B_j \in \mathcal{A}_B. \quad (3.2.2)$$

Observables A and B of the subspaces can be integrated in the Hilbert-Schmidt space \mathcal{A}_{AB} in the following way:

$$A \otimes \mathbb{I}_B \quad (3.2.3)$$

$$\mathbb{I}_A \otimes B \quad (3.2.4)$$

with \mathbb{I}_A and \mathbb{I}_B the identity operators in the corresponding subspaces.

In section (2.2) we introduced density matrices to represent states and especially mixed states, noting that for pure states the density matrix $\rho = |\psi\rangle\langle\psi|$ is an operator of the Hilbert-Schmidt space. Again, the density matrix for composite systems is an operator acting on $\mathcal{H}_A \otimes \mathcal{H}_B$, meaning it is an element of \mathcal{A}_{AB} . For two-state systems the dimension is $\dim \mathcal{H}_{AB} = 4$, so our density matrices are complex 4×4 -matrices. If subsystems A and B are uncorrelated, the density matrix of the composite system is given by the tensor product of the density matrices ρ^A and ρ^B of the subsystems:

$$\rho = \rho^{AB} = \rho^A \otimes \rho^B. \quad (3.2.5)$$

The expectation value of the tensor product of operators is then given by

$$\langle A \otimes B \rangle_\rho = \text{tr}(A \otimes B)\rho = \text{tr}(A\rho^A \otimes B\rho^B). \quad (3.2.6)$$

Let us define the trace of an operator $O \in \mathcal{A}_{AB}$ as

$$\sum_{i,j} \langle a_i | \otimes \langle b_j | O | a_i \rangle \otimes | b_j \rangle \quad (3.2.7)$$

and the partial traces over the respective subspaces as

$$\text{tr}_B O = \sum_j \langle b_j | O | b_j \rangle \quad (3.2.8)$$

or

$$\text{tr}_A O = \sum_i \langle a_i | O | a_i \rangle. \quad (3.2.9)$$

It then is easily seen that the partial traces of a product operator are given by

$$\text{tr}_A(A \otimes B) = \text{tr}_A(A)B \quad \text{and} \quad \text{tr}_B(A \otimes B) = \text{tr}_B(B)A \quad (3.2.10)$$

and the trace of a product operator is just the product of the partial traces

$$\text{tr}(A \otimes B) = \sum_i \langle a_i | A | a_i \rangle \cdot \sum_j \langle b_j | B | b_j \rangle = \text{tr}_A(A) \cdot \text{tr}_B(B). \quad (3.2.11)$$

For the expectation value of equation (3.2.6) we then obtain

$$\langle A \otimes B \rangle_\rho = \text{tr}_A A \rho^A \cdot \text{tr}_B B \rho^B = \langle A \rangle_{\rho^A} \cdot \langle B \rangle_{\rho^B}. \quad (3.2.12)$$

Especially for a density matrix $\rho \in \mathcal{A}_{AB}$ we can just obtain *reduced density matrices* which describe states on the subsystems with the help of partial traces:

$$\rho^A = \text{tr}_B \rho \in \mathcal{A}_A \quad (3.2.13)$$

$$\rho^B = \text{tr}_A \rho \in \mathcal{A}_B. \quad (3.2.14)$$

The reduced density matrix ρ^A describes completely statistical properties of the subsystem A for observables $O = O_A \otimes \mathbb{I}_B$ (where O_A is the part concerning the subsystem A):

$$\langle O \rangle_\rho = \text{tr} O \rho = \text{tr}(O_A \otimes \mathbb{I}_B) \rho = \text{tr}_A O_A \rho^A = \langle O_A \rangle_{\rho^A} \quad (3.2.15)$$

For a concise overview of operators and partial traces see [12], Chapter 6.

3.3 Schmidt decomposition

Vectors $|\psi\rangle \in \mathcal{H}_{AB} = \mathcal{H}_A \otimes \mathcal{H}_B$ describe bipartite pure states. For every such vector, orthonormal bases exist (not necessarily unique) – called the Schmidt-bases – in the Hilbert space \mathcal{H}_A $\{|\chi_i\rangle_A \in \mathcal{H}_A\}$ as well as in the second Hilbert space \mathcal{H}_B $\{|\chi_i\rangle_B \in \mathcal{H}_B\}$ such that

$$|\psi\rangle = \sum_i c_i |\chi_i\rangle_A \otimes |\chi_i\rangle_B \quad (3.3.1)$$

where $c_i \in \mathbb{C}$ are called the Schmidt coefficients. In fact – resulting from the singular value decomposition theorem [13] – a basis can be found so that c_i take non-negative real values. These real values are the square roots of the eigenvalues of the matrix CC^\dagger , where matrix $C = (c_{ij})$ contains the coefficients from equation (3.1.2). See for example Nielsen/Chuang [14].

The Schmidt decomposition of a pure state allows definition of the *Schmidt rank* $r_S(\rho)$, which is the number of positive coefficients c_i in the Schmidt decomposition. This Schmidt rank is an invariant under local unitary transformations, meaning that it does not depend on a particular Schmidt basis.

Remark 3.3.1 *Pure product states have Schmidt rank one. This fact can be used to determine if a pure state is separable or not (see below).*

Remark 3.3.2 *For a pure state ρ the reduced density matrices $\rho^A = \text{tr}_B \rho$ and $\rho^B = \text{tr}_A \rho$ have the same eigenvalues [14].*

3.4 Separability and entanglement

3.4.1 Entanglement of pure states

A pure state in a composite system $|\psi\rangle_{AB} \in \mathcal{H}_A \otimes \mathcal{H}_B$ is called a *separable* state iff it can be written as tensor product of two state vectors of the composing subsystems $|\psi\rangle_A \in \mathcal{H}_A$ and $|\psi\rangle_B \in \mathcal{H}_B$

$$|\psi\rangle_{AB} = |\psi\rangle_A \otimes |\psi\rangle_B. \quad (3.4.1)$$

The density matrix $\rho^{AB} = \rho^A \otimes \rho^B$ can then be associated to the state $|\psi\rangle_{AB}$.

A state is called *entangled* if it is not separable.

Using the Schmidt decomposition, we can say that the state $|\psi\rangle_{AB}$ is entangled if the Schmidt number $N_S > 1$, else if $N_S = 1$ the state $|\psi\rangle_{AB}$ is separable, it is a product state.

If for a given density matrix ρ of a pure state, a subsystem $\rho^A = \text{tr}_B \rho$ or $\rho^B = \text{tr}_A \rho$ is mixed, then ρ was entangled. This result is a characteristic feature of entanglement: tracing a pure entangled state over subsystems results in a mixed state.

For a test of purity or mixedness of the subsystem, we could check if $\text{tr}(\rho^A)^2 < 1$.

Remark 3.4.1 *If the system is in a pure state $\rho = |\psi\rangle\langle\psi|$, the corresponding reduced density matrices ρ^A and ρ^B have the same eigenvalues (see [15]).*

A very special basis of $\mathcal{H}_A \otimes \mathcal{H}_B$ is the Bell basis consisting of four orthonormal, maximally entangled pure Bell states:

$$|\phi^-\rangle = \frac{1}{\sqrt{2}}(|0\rangle|0\rangle - |1\rangle|1\rangle) \quad (3.4.2)$$

$$|\phi^+\rangle = \frac{1}{\sqrt{2}}(|0\rangle|0\rangle + |1\rangle|1\rangle) \quad (3.4.3)$$

$$|\psi^-\rangle = \frac{1}{\sqrt{2}}(|0\rangle|1\rangle - |1\rangle|0\rangle) \quad (3.4.4)$$

$$|\psi^+\rangle = \frac{1}{\sqrt{2}}(|0\rangle|1\rangle + |1\rangle|0\rangle) \quad (3.4.5)$$

These states are maximally entangled in the sense that tracing over one of the constituting subspaces gives a maximally mixed state $\frac{1}{2}\mathbb{I}_2$.

The density matrices for the Bell states are given by

$$\omega^\pm = |\phi^\pm\rangle\langle\phi^\pm| = \frac{1}{2} \begin{pmatrix} 1 & 0 & 0 & \pm 1 \\ 0 & 0 & 0 & 0 \\ 0 & 0 & 0 & 0 \\ \pm 1 & 0 & 0 & 1 \end{pmatrix} \quad (3.4.6)$$

and

$$\rho^\pm = |\psi^\pm\rangle\langle\psi^\pm| = \frac{1}{2} \begin{pmatrix} 0 & 0 & 0 & 0 \\ 0 & 1 & \pm 1 & 0 \\ 0 & \pm 1 & 1 & 0 \\ 0 & 0 & 0 & 0 \end{pmatrix} \quad (3.4.7)$$

3.4.2 Entanglement of mixed states

For density matrices a state ρ is said to be a *product state* if states ρ^A for Alice and ρ^B for Bob exist, such that the state can be written as

$$\rho = \rho^A \otimes \rho^B. \quad (3.4.8)$$

Generally, for the mixed case, we extend the pure state definition of separability so that we can define a mixed state as separable if it can be written as

$$\rho = \sum_i p_i \rho_i^A \otimes \rho_i^B, \quad p_i \geq 0, \quad \sum_i p_i = 1. \quad (3.4.9)$$

We could interpret this in the sense that Alice and Bob "produce" states ρ_i^A and ρ_i^B locally, based on the outcome i of a shared random number generator. Therefore, using only local operations and classical communication (LOCC) they finally produce the state $\rho_i^A \otimes \rho_i^B$ with probability p_i .

If such a formulation is not possible, the mixed state is called entangled.

Remark 3.4.2 *The set of separable states is obviously a convex set, because they are defined in (3.4.9) as a convex combination of pure product states. The set of separable states is thus the convex hull of the pure product states.*

Unfortunately in this case simply checking mixedness of subsystems to confirm entanglement does not suffice.

Example 3.4.1 *Take $\rho = \frac{1}{4}\mathbb{I} = \frac{1}{4}(|0\rangle\langle 0| \otimes |0\rangle\langle 0| + |0\rangle\langle 0| \otimes |1\rangle\langle 1| + |1\rangle\langle 1| \otimes |0\rangle\langle 0| + |1\rangle\langle 1| \otimes |1\rangle\langle 1|)$ and evidently $\rho^A = \text{Tr}_B \rho = \frac{1}{2}\mathbb{I}_A$, a mixed state, while the original state ρ is the maximally mixed state and obviously separable and not entangled.*

This means that we have to find more sophisticated ways to discriminate between separable and entangled states in the mixed case. The general problem to determine whether a mixed state is entangled or separable is a very difficult task (see for example [16]).

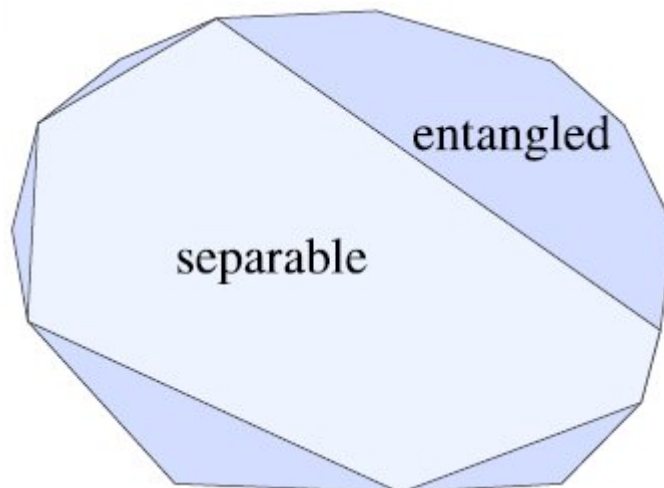


Figure 3.1: Schematic picture of the set of all states with the set of separable states as a convex subset. It should be stressed that the extremal points of the set of separable states (the pure product states), are also extremal points of the set of all physical states (taken from Gühne/Toth's review article [17])

In case of 2×2 and 2×3 a necessary and sufficient condition for separability is known, which we will discuss in the next section. For all other cases no general necessary and sufficient condition is known. Instead, entanglement measures are calculated or geometric techniques like entanglement witnesses are used (see section (3.5)) to analyse entanglement and separability properties.

Important examples for mixed states (in $\mathbb{C}^2 \otimes \mathbb{C}^2$) :

1. The maximally mixed state $\rho = \frac{1}{4}\mathbb{I}_4 = \frac{1}{4}\mathbb{I}_2 \otimes \mathbb{I}_2$ is separable (see previous example)
2. The so-called Werner states [18], a mixture of the maximally mixed and one of the Bell states, for example

$$\rho_W = \alpha |\phi^+\rangle \langle \phi^+| + \frac{1-\alpha}{4} \mathbb{I}_2 \otimes \mathbb{I}_2 \quad (3.4.10)$$

Werner states are invariant under the transformation $U \otimes U$, if U is unitary [19]. Isotropic states are a similar family, where transformations of the form $U \otimes U^*$ let the state be invariant (U^* denotes complex conjugate).

3. States with density matrices being diagonal in the Bell basis are called Bell-diagonal states, meaning they are a mixture of the four Bell states:

$$p_1 |\psi^-\rangle \langle \psi^-| + p_2 |\psi^+\rangle \langle \psi^+| + p_3 |\phi^-\rangle \langle \phi^-| + p_4 |\phi^+\rangle \langle \phi^+| \quad (3.4.11)$$

with $\sum p_i = 1$. The corresponding density matrix is of a very symmetric form

$$\frac{1}{2} \begin{pmatrix} p_4 + p_3 & 0 & 0 & p_4 - p_3 \\ 0 & p_2 + p_1 & p_2 - p_1 & 0 \\ 0 & p_2 - p_1 & p_2 + p_1 & 0 \\ p_4 - p_3 & 0 & 0 & p_4 + p_3 \end{pmatrix} \quad (3.4.12)$$

and the geometry of these states will be studied in section 3.7

3.4.3 Positive Partial Transpose Criterion

The positive partial transpose (PPT) test is most useful to discriminate between entanglement and separability of bipartite states. It is a necessary condition for separability as first noted by Asher Peres [20] and was also shown sufficient for systems composed of two qubits or one qubit and one qutrit 1996 by Michał, Paweł and Ryszard Horodecki [21]. For higher dimensions it is still useful as a necessary condition for separability of bipartite states.

To state the criterion we need the following definitions:

Definition 3.4.1 A linear map $M : \mathcal{H} \rightarrow \mathcal{H}$ is called positive if and only if M maps positive operators of the Hilbert space \mathcal{H} onto positive operators of \mathcal{H} , i.e.

$$A \geq 0 \Rightarrow M(A) \geq 0, \forall A \in \mathcal{H} \quad (3.4.13)$$

Definition 3.4.2 A positive linear map $M : \mathcal{H} \rightarrow \mathcal{H}$ is called completely positive if under every extension to higher dimensions it remains positive, i.e. if

$$M \otimes \mathbb{I}_k : \mathcal{H} \otimes \mathcal{M}_k \rightarrow \mathcal{H} \otimes \mathcal{M}_k \quad (3.4.14)$$

is again a positive map for $k = 2, 3, \dots$, where \mathcal{M}_k is the matrix space of $k \times k$ complex matrices and \mathbb{I}_k its identity matrix.

Definition 3.4.3 Let ρ be the density matrix of a state acting on $\mathcal{H}^A \otimes \mathcal{H}^B$: We can represent ρ as

$$\rho = \sum_{i,j,k,l} p_{kl}^{ij} |i\rangle \langle j| \otimes |k\rangle \langle l|. \quad (3.4.15)$$

Partial transposition (with respect to B) applied to ρ , $\rho^{TB} = (\mathbb{I} \otimes T)\rho$ acts on the A party as an identity map and on the B party as a transposition map.

A very nice illustration of process and meaning of partial transposition can be found in [22].

It was noted by Peres [20] and especially the Horodecki's [21], that for a separable state $\rho_{sep} = \sum_i \rho_i^A \otimes \rho_i^B$ positive maps, extended to higher dimensions, preserve positivity, but for entangled states ρ_{ent} this need not be true

$$(M \otimes \mathbb{I}_k)\rho_{sep} = \sum_i M\rho_i^A \otimes \rho_i^B \geq 0. \quad (3.4.16)$$

For entangled states we can find a positive, but not completely positive map, such that

$$(M \otimes \mathbb{I}_k)\rho_{ent} \leq 0. \quad (3.4.17)$$

Moreover, Peres noticed that partial transposition is such a positive map, where a distinction between separable and entangled states is possible, at least for dimensions 2×2 or 2×3 .

Now we can formulate the following Theorem

Theorem 3.4.1 (*The PPT Criterion*). *For a bipartite separable state ρ the partial transposition is a positive operator*

$$\rho^{T_B} = (\mathbb{I} \otimes T)\rho \geq 0. \quad (3.4.18)$$

If for a given state, after partial transposition, negative eigenvalues occur, we know that the state has to be entangled. The criterion is even necessary and sufficient, but only for low dimensional cases.

Theorem 3.4.2 (*Horodecki Theorem*). *If ρ is a state operating on $\mathcal{H}_2 \otimes \mathcal{H}_2$ or $\mathcal{H}_2 \otimes \mathcal{H}_3$, then $\rho^{T_B} \geq 0$ also implies that ρ is separable.*

For higher dimensions the criterion is only necessary for separability. States – in higher dimensions – exist, that fulfill the PPT criterion, but are nevertheless entangled. These states are called *bound entangled states*.

Example 3.4.2 *An interesting one-parametric family are the Werner states [18] defined in section 3.4.2. In the 2×2 qubit case the density matrix is of the form*

$$\rho_{W_\alpha} = \begin{pmatrix} \frac{1-\alpha}{4} & 0 & 0 & 0 \\ 0 & \frac{1+\alpha}{4} & \frac{-\alpha}{2} & 0 \\ 0 & \frac{-\alpha}{2} & \frac{1+\alpha}{4} & 0 \\ 0 & 0 & 0 & \frac{1-\alpha}{4} \end{pmatrix} \quad (3.4.19)$$

if we take the mixture of the maximally mixed state and the $|\psi^-\rangle$ Bell state. Since the Eigenvalues are then $\lambda_1 = \lambda_2 = \lambda_3 = \frac{1-\alpha}{4}$ and $\lambda_4 = \frac{1+3\alpha}{4}$, the state is physically defined for $-\frac{1}{3} \leq \alpha \leq 1$.

Taking the partial transposition of ρ_{W_α} as in Definition 3.4.3, we obtain the matrix

$$\rho_{W_\alpha}^{T_B} = \begin{pmatrix} \frac{1-\alpha}{4} & 0 & 0 & \frac{-\alpha}{2} \\ 0 & \frac{1+\alpha}{4} & 0 & 0 \\ 0 & 0 & \frac{1+\alpha}{4} & 0 \\ \frac{-\alpha}{2} & 0 & 0 & \frac{1-\alpha}{4} \end{pmatrix} \quad (3.4.20)$$

with the eigenvalues: $\lambda_1^{T_B} = \lambda_2^{T_B} = \lambda_3^{T_B} = \frac{1+\alpha}{4}$ and $\lambda_4^{T_B} = \frac{1-3\alpha}{4}$.

The first three eigenvalues are non-negative for the whole allowed interval of the parameter $-\frac{1}{3} \leq \alpha \leq 1$, but $\lambda_4^{T_B}$ can take negative values. So considering the PPT criterion 3.4.1, we obtain:

$$\begin{aligned} -\frac{1}{3} \leq \alpha \leq \frac{1}{3} & \Rightarrow \lambda_4^{T_B} \geq 0 \Rightarrow \rho_{W_\alpha} \text{ is separable} \\ \frac{1}{3} < \alpha \leq 1 & \Rightarrow \lambda_4^{T_B} < 0 \Rightarrow \rho_{W_\alpha} \text{ is entangled} \end{aligned}$$

3.5 Entanglement measures

In the last section a useful criterion to discriminate between separable and entangled states was introduced, but in a fully satisfying way it only works in low-dimensional cases 2×2 or 2×3 . For higher dimensions we would like to find some measures to decide if and how much quantum states are entangled. To this end, several entanglement measures, meaning mappings E from density matrices into non-negative real numbers, have been suggested. To be useful as an entanglement measure, E should fulfill several requirements, but it is not clear if all of the properties below are really necessary. None of the suggested entanglement measures fulfill all of these requirements (see [23], [24], [25]):

- *Zero entanglement for separable states:* If ρ is separable the entanglement measure should be zero; the entanglement measure should not show any entanglement in a separable state
 ρ is separable $\Leftrightarrow E(\rho) = 0$
- *Invariance under local unitary transformation:* Local unitary operations U_A, U_B leave $E(\rho)$ invariant, i.e.
 $E(\rho) = E(U_A \otimes U_B \rho U_A^\dagger \otimes U_B^\dagger)$.

- *No increase under LOCC*: Entanglement measures cannot increase under local operations and classical communication (LOCC) Θ :
 $E(\rho) \geq E(\Theta\rho)$
- *Continuity*: The entanglement measure should be continuous. If the Hilbert-Schmidt distance between two states vanishes, the difference between their entanglement should also go towards zero
 $E(\rho_1) - E(\rho_2) \rightarrow 0$ for $\|\rho_1 - \rho_2\| \rightarrow 0$
- *Additivity*: Entanglement of a composite system is equal to the sum of the entanglements of the constituting systems
 $E(\rho \otimes \sigma) = E(\rho) + E(\sigma)$
- *Subadditivity*: Additivity is sometimes considered as being too strong. Instead then subadditivity can be required
 $E(\rho \otimes \sigma) \leq E(\rho) + E(\sigma)$
- *Convexity*: The entanglement measure is convex, meaning
 $E(\lambda\rho_1 + (1 - \lambda)\rho_2) \leq \lambda E(\rho_1) + (1 - \lambda)E(\rho_2), \quad 0 \leq \lambda \leq 1$
- *Normalization*: Entanglement of a maximally entangled state should be 1.
- *Computability*: The entanglement measure should be efficiently computable for every state.

Up to now no entanglement measure is known, that can fulfill all of these requirements. Especially, the computability requirement turns out to be hard to fulfill in higher dimensions. In the following subsections we will consider several suggested entanglement measures for pure and also for mixed states. This overview is of course very incomplete.

3.5.1 Entanglement measures for pure states

For pure states we can readily find entanglement measures considering mixedness and entropy.

Mixedness (see section 2.2) of subsystems can be used as a separability criterion for a pure state $\rho = \rho^A \otimes \rho^B$, meaning that the mixedness of the subsystems ρ^A and ρ^B can help us quantify entanglement. From a high degree of mixedness of reduced density matrices one can derive a strong entanglement of the original state. Entanglement can be seen as the amount of information contained in the system, but not in the subsystems.

Mixedness of the subsystems or information contained therein can be measured with different types of entropy. From there we can deduce a measure for entanglement of the composite system.

- Mixedness of the subsystems could be measured using $M(\rho) = 1 - \text{tr}(\rho^2)$, also called linear entropy, which takes values between 0 for a pure state and $1 - \frac{1}{d}$ (d dimension of ρ) for the maximally mixed state. Normalized as $\frac{d}{d-1}(1 - \text{tr}(\rho^2))$ it will take values between 0 and 1.

Remark: Linear entropy is a first order approximation of von Neumann entropy (see below).

- A natural extension of Shannon entropy in classical information theory – $-\sum_i p_i \log p_i$ (p_i discrete probability distribution with $p_i \geq 0$ and $\sum p_i = 1$) is the von Neumann entropy in quantum mechanics for a given density matrix ρ

$$S(\rho) = -\text{tr}(\rho \log(\rho)). \quad (3.5.1)$$

If λ_i are the eigenvalues of ρ , the von Neumann entropy of ρ is the Shannon entropy of the eigenvalues of ρ

$$S(\rho) = -\sum \lambda_i \log \lambda_i. \quad (3.5.2)$$

The range of von Neumann Entropy is $0 \leq S(\rho) \leq 1$ (with log to base d) for all density matrices ρ , with $S(\rho) = 0$ for pure states and $S(\rho) = 1$ for the totally mixed state $\rho = \frac{1}{d}\mathbb{I}_d$.

For general mixed states ρ with spectral decomposition $\sum p_i |\phi_i\rangle \langle \phi_i|$ the von Neumann entropy coincides with Shannon entropy.

Remark: Moreover, von Neumann Entropy is invariant under unitary transformation U : $S(U\rho U^\dagger) = S(\rho)$. So under unitary transformation pure states remain pure and mixed states remain mixed!

- A generalization of Shannon entropy is the Renyi- α -entropy, which is used as a measurement for diversity, or randomness in a system and can be used in the quantum version as a measurement of entanglement for quantum states. In its quantum version it is defined as

$$S_\alpha(\rho) = \frac{1}{1-\alpha} \log \text{tr}(\rho^\alpha) \quad (3.5.3)$$

with $\alpha \geq 0, \alpha \neq 1$.

For pure states ρ the Renyi entropy is again $S_\alpha(\rho) = 0$ and for mixed states $S_\alpha(\rho) > 0$.

Remark: Taking the limit of the Renyi-Entropy for $\alpha \rightarrow 1$, we obtain the von Neumann entropy: $\lim_{\alpha \rightarrow 1} S_\alpha(\rho) = S(\rho)$

Therefore we can define the following measure for entanglement

Definition 3.5.1 For a pure bipartite state $\rho = \rho^A \otimes \rho^B$ the following measure

$$\mathcal{E}(\rho) := S(\rho^A) = S(\rho^B) \quad (3.5.4)$$

is called entropy of entanglement.

Remark 3.5.1 If ρ is a product state, $\mathcal{E}(\rho) = 0$, that means the minimum value of the entropy measure is 0.

For product states (pure, separable) $S(\rho^A) = S(\rho^B)$ and therefore $\mathcal{E}(\rho) = 0$ is a consequence of the very remarkable fact, that the eigenvalues of the reduced density operators ρ^A and ρ^B are identical, see section 3.3 for the Schmidt decomposition.

For entangled states – again because of the Schmidt decomposition – we have $S(\rho^A) = S(\rho^B) > 0$.

Remark 3.5.2 The maximal value is $\log d$. Take for example

$$|\psi\rangle = \frac{1}{\sqrt{d}}(|0\rangle_A \otimes |0\rangle_B + |1\rangle_A \otimes |1\rangle_B + \cdots + |d-1\rangle_A \otimes |d-1\rangle_B). \quad (3.5.5)$$

Alternatively we could formulate this with help of the Schmidt rank for pure states:

$$r_S(\rho) = 1 \Leftrightarrow \rho \text{ is separable}$$

$$r_S(\rho) > 1 \Leftrightarrow \rho \text{ is entangled}$$

and take $\mathcal{E}_S = r_S(\rho) - 1$ as an entanglement measure.

3.5.2 Entanglement measures for mixed states

3.5.2.1 Entanglement of formation

To detect and quantify entanglement for mixed states, we use the entropy of entanglement $\mathcal{E}(\rho)$ defined in section 3.5.1 in calculating its infimum over all ensembles

$\{(p_i, |\phi_i\rangle)\}$ of pure states $|\phi_i\rangle$ and probability distributions $\{p_i\}$ realizing the state $\rho = \sum_i p_i |\phi_i\rangle \langle \phi_i| = \sum_i p_i \rho_i$

$$E_F(\rho) = \inf_{\{(p_i, \rho_i)\}} \sum_i p_i \mathcal{E}(\rho_i) \quad (3.5.6)$$

calling this quantity the "Entanglement of formation" [26], [27].

This technique, to calculate the infimum of quantities defined for pure states over ensembles and thus extending the definition to mixed states, is called a *convex roof construction*.

Since we usually do not know the possible (not unique) decompositions of a general mixed state into pure state ensembles, the calculation of the corresponding infimum can be very difficult.

3.5.2.2 Concurrence

In the special case of a two qubits state, the entanglement of formation can be written as

$$E_F(\rho) = E(C) = H\left(\frac{1 + \sqrt{1 - C^2}}{2}\right), \quad (3.5.7)$$

where H is the Shannon entropy function

$$H(x) = -x \log_2 x - (1 - x) \log_2 (1 - x). \quad (3.5.8)$$

C is a quantity defined below, called the concurrence. The concurrence C is another quantity that can be used as an entanglement measure [27], [28], [29], since it is monotonically increasing and ranges from 0 to 1.

The concurrence C of a pure 2-qubit state $|\psi\rangle$ is defined as

$$C(\psi) = |\langle \psi | \tilde{\psi} \rangle|, \quad (3.5.9)$$

with $|\tilde{\psi}\rangle = (\sigma_y \otimes \sigma_y) |\psi^*\rangle$ where a spin flip operation (σ_y is the second of the Pauli matrices) has been applied to the complex conjugate of $|\psi\rangle$.

For a mixed 2-qubit state ρ the concurrence is defined in the convex roof construction way as in section 3.5.2.1 as

$$C(\rho) = \inf \sum_i p_i C(\psi_i) \quad (3.5.10)$$

where $\rho = \sum_i p_i |\psi_i\rangle \langle \psi_i|$.

There exists an explicit formula for the concurrence given by

$$C(\rho) = \max\{0, \lambda_1 - \lambda_2 - \lambda_3 - \lambda_4\}, \quad (3.5.11)$$

where λ_i denote the squareroots of eigenvalues of $\rho\tilde{\rho}$ in decreasing order, with $\tilde{\rho} = (\sigma_y \otimes \sigma_y)\rho^*(\sigma_y \otimes \sigma_y)$.

3.5.2.3 Entanglement cost

Entanglement cost $E_C(\rho)$ [22], [30] quantifies how expensive it is to create a given state ρ from a maximally entangled state via LOCC operations. That is, we minimize the ratio of the number of copies $n_{|\Phi\rangle^{in}}$ of maximally entangled input states $|\Phi\rangle$ over the produced output states over all LOCC operations. In the limit we obtain (infinitely many outputs)

$$E_C(\rho) = \inf_{\{\Lambda_{LOCC}\}} \lim_{n_{\rho} \rightarrow \infty} \frac{n_{|\Phi\rangle^{in}}}{n_{\rho}^{out}}. \quad (3.5.12)$$

3.5.2.4 Entanglement of distillation

On the other hand, if we are now interested in how much entanglement can be extracted from an entangled state ρ via LOCC, we maximize the ratio of the number of maximally entangled output states $|\Phi\rangle$ over the needed input states over all LOCC operations [22], [31]. In the limit we obtain (infinitely many inputs)

$$E_D(\rho) = \sup_{\{\Lambda_{LOCC}\}} \lim_{n_{\rho} \rightarrow \infty} \frac{n_{|\Phi\rangle^{out}}}{n_{\rho}^{in}}. \quad (3.5.13)$$

Entanglement of distillation and entanglement of cost are in some way dual to each other [30] and the quantities E_D and E_C are in a way extreme, because the distillable entanglement is a lower, and entanglement cost is an upper bound for any entanglement measure $E(\rho)$ [22], at least for pure states

$$E_D(\rho) \leq E(\rho) \leq E_C(\rho) \quad (3.5.14)$$

3.5.2.5 Hilbert-Schmidt distance

Keeping in mind that the set of separable states S is convex, a very intuitive measure of entanglement is to determine the nearest separable state σ for a state ρ and to calculate their distance. A suitable choice would be the Hilbert-Schmidt distance [32]:

$$D(\rho, \sigma) = \|\rho - \sigma\| = \sqrt{\text{tr}(\rho - \sigma)^2}. \quad (3.5.15)$$

So the entanglement measure could be defined as

$$E(\rho) = \min_{\sigma \in S} D(\rho, \sigma). \quad (3.5.16)$$

To find the nearest separable state can be a difficult task which we will also encounter in the context of entanglement witnesses in section 3.5.2.7.

3.5.2.6 Negativity

Negativity [33] is another entanglement measure very easy to calculate

$$N = \frac{\|\rho^{TA}\|_1 - 1}{2} \quad (3.5.17)$$

where $\|A\|_1$ is the trace norm

$$\|A\|_1 = \text{tr} \sqrt{A^\dagger A}. \quad (3.5.18)$$

which is the sum of the singular values of the operator A .

In our case it corresponds to the absolute value of the sum of negative eigenvalues of ρ^{TA} and can be equivalently written as

$$N = \sum_i \frac{|\lambda_i| - \lambda_i}{2} \quad (3.5.19)$$

with λ_i being all the eigenvalues, positive and negative ones.

N measures by how much the partially transposed density matrix ρ^{TA} fails to be positive definite. For all PPT states $N = 0$ and for maximally entangled states $N = 1$.

This measure has some drawbacks because it vanishes for some entangled states. Its main advantage though is that it can easily be computed and that it must not be restricted to two-level systems, but can be generalized for l -level systems ($l > 2$).

3.5.2.7 Entanglement witness

Another way to discriminate between entangled and separable quantum states are entanglement witnesses (see [21], [34]), where the geometry of the state space is analyzed. In the set of physical states, the set of separable states S is a convex subset. With the Hahn-Banach theorem we can state that an entangled state

ρ_{ent} outside of S can be separated from the convex set S of separable states by a hyperplane. This hyperplane can be determined by a hermitian operator A .

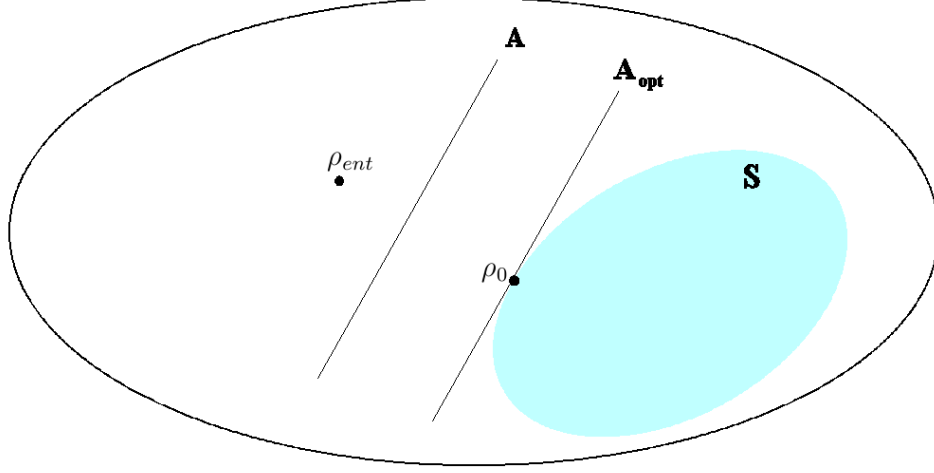


Figure 3.2: Schematic overview for an entanglement witness. The nearest separable state is ρ_0 and the optimal entanglement witness A_{opt}

Theorem 3.5.1 *A state ρ_{ent} is entangled if and only if there exists a hermitian operator A such that:*

$$\begin{aligned} \langle \rho_{ent} | A \rangle &= \text{tr } \rho_{ent} A < 0 & \text{and} \\ \langle \rho | A \rangle &= \text{tr } \rho A \geq 0 & \text{for all } \rho \in S \end{aligned} \quad (3.5.20)$$

This operator A is called an entanglement witness.

An optimal entanglement witness A_{opt} for the entangled state ρ_{ent} can be constructed in the following way [35]

$$A_{opt} = \frac{\rho_0 - \rho_{ent} - \langle \rho_0 | \rho_0 - \rho_{ent} \rangle \mathbb{I}}{\|\rho_0 - \rho_{ent}\|} \quad (3.5.21)$$

with ρ_0 such that $\|\rho_{ent} - \rho_0\| = \min_{\rho \in S} \|\rho_{ent} - \rho\|$ is the nearest separable state (in Hilbert-Schmidt distance).

For such a state $\rho_0 \in S$ we obtain $\langle \rho_0 | A_{opt} \rangle = 0$ and the state ρ_0 is an element of the border of S : $\rho_0 \in \partial S$ (see Fig. 3.2).

3.6 EPR and Bell inequality

3.6.1 EPR "Paradoxon"

In 1935 Albert Einstein, Boris Podolsky und Nathan Rosen (EPR) proposed a Gedankenexperiment to show that the quantum-mechanical description of physical reality is incomplete. To this end some plausible requirements were formulated, that a consistent and complete theory should fulfill [36]:

1. *Completeness: Every element of the physical reality must have a counterpart in the physical theory.*
2. *Reality: If, without in any way disturbing a system, we can predict with certainty (i.e., with probability equal to unity) the value of a physical quantity, then there exists an element of physical reality corresponding to this physical quantity.*
3. *Locality: If two systems do not interact (anymore), then changes in one of the systems cannot entail real changes in the second system (no instantaneous action at a distance is possible, this would violate the fact that information cannot be propagated faster than the speed of light).*

Let us now consider the following physical system with a pair of two-state particles (for example spin $\frac{1}{2}$). A source emits two particles into opposite directions. They can move arbitrarily far away from the source and end up finally at the observers Alice and Bob, see Figure 3.3.

The corresponding quantum state is entangled:

$$|\Psi\rangle = \frac{1}{\sqrt{2}}(|+\rangle|-\rangle + |-\rangle|+\rangle) \quad (3.6.1)$$

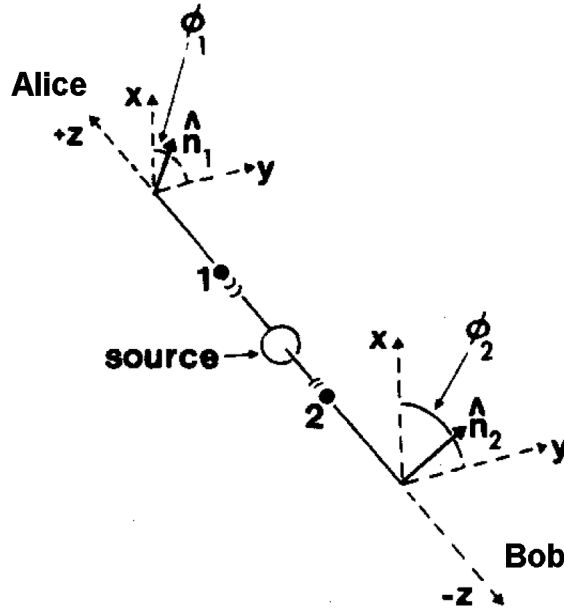


Figure 3.3: Source emitting two particles, from [7] (slightly adapted)

If Alice and Bob now measure along the same direction, there is perfect anti-correlation. This means, if for example Alice measures $+$ along the x -direction, then Bob will measure $-$, again along the x -direction. Einstein, Podolsky and Rosen argued now in the following way:

If Alice and Bob are far enough away from each other, Alice's measurement cannot influence Bob's (Locality). But Alice's measurement determines Bob's result (perfect anti-correlation). Without another interaction in the system, Bob's result is determined (with probability 1) and known, so it must be an element of reality.

Analogous considerations can be made for the y - and z -directions. However the quantum mechanical formalism cannot determine such a state, so Einstein, Podolsky and Rosen concluded that quantum mechanics must be incomplete and the effects, which the theory could not explain, had to come from some hidden variables.

3.6.2 Bell inequality

In 1964 John Bell established an inequality [37] that must always be fulfilled under the locality and reality requirements. On the other hand, in quantum mechanics one can construct situations where this inequality is violated.

With that in mind, one obtains – in principle – a testable statement, that could bring about a decision between local-realistic theories (LRT, see Einstein, Podolsky and Rosen [36]) and quantum mechanics.

Starting from these considerations some experimental studies were started (for example 1972 by Freedman and Clauser [38] or later in 1982 by Aspect et al. [39]) using for example many pairs of entangled photons, that showed that Bell's inequalities can indeed be violated and so that the assumptions of locality and reality (at least jointly) are unsustainable.

A special form of Bell's inequality was developed 1969 by Clauser, Horne, Shimony und Holt (CHSH) [40]. In this form experimental tests are more accessible [41], especially the following form of Bell's inequality

$$S(a, b, a', b') = |E(a, b) + E(a, b')| + |E(a', b) - E(a', b')| \leq 2 \quad (3.6.2)$$

where $E(a, b)$ is the expectation of a series of measurements with two detector settings a and b . The value $S(a, b, a', b') = 2$ cannot be exceeded in LRT, but in quantum mechanics detector settings can be adjusted in such a way that Bell's inequality is violated. Especially for the so-called Bell angles $a = 0^\circ, a' = 45^\circ, b = 22,5^\circ, b' = 67,5^\circ$ the violation is maximal with $S(a, b, a', b') = 2\sqrt{2}$, this value being clearly higher than the LRT upper bound of 2.

Bell's inequality provides an upper bound for the average of measurements that can be exceeded in certain special quantum mechanical situations.

So with the predictions from Bell's theorem, a disagreement between the EPR statement and the quantum mechanical theory can be shown experimentally. The decision between LRT and quantum mechanics was finally clearly – due to experimental tests – provided in favor of quantum mechanics. Quantum mechanical predictions were correct and so instead of proving incompleteness, quantum mechanics was confirmed with the help of Bell's inequalities.

3.7 Bloch decomposition

Two qubit states can be represented in a Hilbert-Schmidt basis in the following way (see for example [42], [43])

$$\rho = \frac{1}{4}(\mathbb{I} \otimes \mathbb{I} + \vec{a} \cdot \vec{\sigma} \otimes \mathbb{I} + \mathbb{I} \otimes \vec{b} \cdot \vec{\sigma} + \sum_{m,n} t_{nm} \sigma_n \otimes \sigma_m) \quad (3.7.1)$$

where \vec{a} and \vec{b} are three-dimensional real vectors and $\vec{\sigma}$ the vector incorporating the three Pauli matrices. The coefficients t_{nm} form a real 3×3 matrix T .

The condition $\text{tr}(\rho^2) \leq 1$ (see section 2.2) implies that

$$\sum_i (a_i^2 + b_i^2) + \sum_{m,n} t_{nm}^2 \leq 3 \quad (3.7.2)$$

and equality is achieved for pure states.

The matrix T can be diagonalized and since the unitary transformations needed keep the properties separable or entangled invariant, an equivalent representation with less parameters is possible

$$\rho = \frac{1}{4}(\mathbb{I} \otimes \mathbb{I} + \vec{a} \cdot \vec{\sigma} \otimes \mathbb{I} + \mathbb{I} \otimes \vec{b} \cdot \vec{\sigma} + \sum_i t_{ii} \sigma_i \otimes \sigma_i). \quad (3.7.3)$$

A special one-parametric family of states are isotropic states

$$\rho_\alpha = \alpha |\phi^+\rangle \langle \phi^+| + \frac{1-\alpha}{4} \mathbb{I}, \quad \alpha \in \mathbb{R}, \quad -\frac{1}{3} \leq \alpha \leq 1. \quad (3.7.4)$$

For this family the terms $\vec{a} \cdot \vec{\sigma} \otimes \mathbb{I}$ and $\mathbb{I} \otimes \vec{b} \cdot \vec{\sigma}$ vanish (see [44]) and the representation takes the form

$$\rho = \frac{1}{4}(\mathbb{I} \otimes \mathbb{I} + \sum_{m,n} t_{nm} \sigma_n \otimes \sigma_m) \quad (3.7.5)$$

or in diagonalized form

$$\rho = \frac{1}{4}(\mathbb{I} \otimes \mathbb{I} + a \cdot \sigma_x \otimes \sigma_x + b \cdot \sigma_y \otimes \sigma_y + c \cdot \sigma_z \otimes \sigma_z) \quad (3.7.6)$$

with finally only three real parameters a, b, c left.

From there it is easily seen that these states have to fulfill the following four inequalities (due to positivity of eigenvalues) to be physical states

$$\begin{aligned} \frac{1}{4}(1 - a - b - c) &\geq 0 \\ \frac{1}{4}(1 + a + b - c) &\geq 0 \\ \frac{1}{4}(1 + a - b + c) &\geq 0 \\ \frac{1}{4}(1 - a + b + c) &\geq 0 \end{aligned} \quad (3.7.7)$$

thus forming a tetrahedron [45], [46] in three-dimensional space (see Figure 3.4) with the maximally mixed state $\frac{1}{4}\mathbb{I}_4$ at its center, sometimes called the "magic tetrahedron".

The states in this tetrahedron are just the Bell-diagonal states (3.4.11) from section 3.4.2.

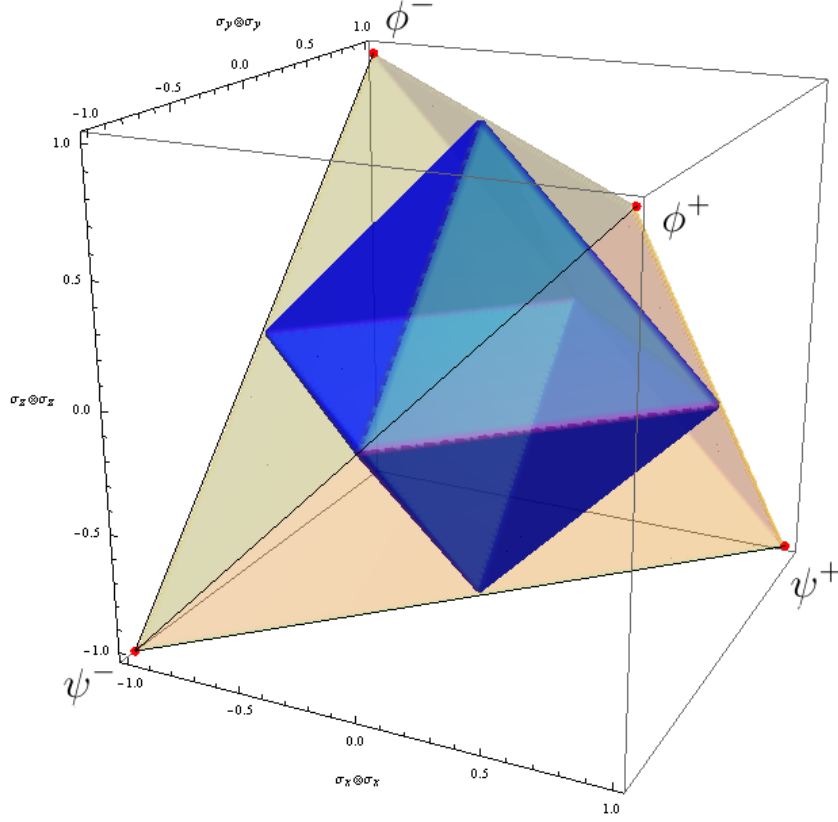


Figure 3.4: Magic tetrahedron

The corners are associated to the Bell states:

$$\begin{aligned}
 \frac{1}{4}(\mathbb{I} \otimes \mathbb{I} - \sigma_x \otimes \sigma_x - \sigma_y \otimes \sigma_y - \sigma_z \otimes \sigma_z) &= |\psi^-\rangle \langle \psi^-| \\
 \frac{1}{4}(\mathbb{I} \otimes \mathbb{I} + \sigma_x \otimes \sigma_x + \sigma_y \otimes \sigma_y - \sigma_z \otimes \sigma_z) &= |\psi^+\rangle \langle \psi^+| \\
 \frac{1}{4}(\mathbb{I} \otimes \mathbb{I} - \sigma_x \otimes \sigma_x + \sigma_y \otimes \sigma_y + \sigma_z \otimes \sigma_z) &= |\phi^-\rangle \langle \phi^-| \\
 \frac{1}{4}(\mathbb{I} \otimes \mathbb{I} + \sigma_x \otimes \sigma_x - \sigma_y \otimes \sigma_y + \sigma_z \otimes \sigma_z) &= |\phi^+\rangle \langle \phi^+|
 \end{aligned} \tag{3.7.8}$$

Note: General separable states can be represented by

$$\rho = \frac{1}{4} \sum_k p_k (\mathbb{I} \otimes \mathbb{I} + \vec{a} \cdot \vec{\sigma} \otimes \mathbb{I} + \mathbb{I} \otimes \vec{b} \cdot \vec{\sigma} + \sum_{i,j} a_i b_j \sigma_i \otimes \sigma_j) \tag{3.7.9}$$

with $p_k \geq 0, \sum_k p_k = 1$.

In the magic tetrahedron in the 2×2 case the subset of separable states can be visually represented – via PPT criterion – by the states in the double pyramid in Figure 3.4.

The Bell states at the corners are the only pure states in this graphical representation, because the equality condition in 3.7.2, here $a^2 + b^2 + c^2 = 3$, is only fulfilled for them.

Chapter 4

Tripartite and especially GHZ type states

4.1 Types of entanglement, GHZ and W states

For two qubits we had essentially two possibilities – the qubits were separable or entangled – and in addition the powerful PPT criterion [20] to discern these properties. For three qubits we are confronted with even more possibilities. Often – for pure states – three classes of entanglement are distinguished [47]

- Totally separable states can be written as $|\Psi_S\rangle = |\Phi_A\rangle \otimes |\Phi_B\rangle \otimes |\Phi_C\rangle$.

For example $|000\rangle$ is totally separable, a product state.

- Bi-separable states are states where only two out of the three parts in the system are entangled, the third is in a tensor product with the entangled two, this can be written as A–BC, B–AC or C–AB.

An example could be $\frac{1}{\sqrt{2}}(|0\rangle \otimes (|00\rangle + |11\rangle))$.

- Tripartite entangled states mean states with genuine entanglement of all three subsystems. There exist two subtypes of inequivalent states [48]

- GHZ states, for example $\frac{1}{\sqrt{2}}(|000\rangle + |111\rangle)$

- W states, for example $\frac{1}{\sqrt{3}}(|100\rangle + |010\rangle + |001\rangle)$

The distinction between separable, bi-separable and tripartite entangled is not enough, since the genuinely three-qubit entangled states belong to two inequivalent classes, the GHZ class or the W class, this distinction is also essential.

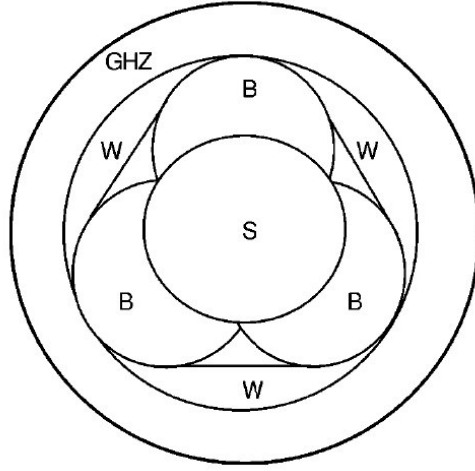


Figure 4.1: Types of tripartite entanglement after [47]

The sets corresponding to the different entanglement classes – S separable states, B bi-separable states, W the W states, GHZ the GHZ states – are embedded into each other in the following way [47]

$$S \subset B \subset W \subset GHZ \quad (4.1.1)$$

where at least the last inclusion $W \subset GHZ$ is at first sight a little surprising.

For mixed states the situation is more difficult and more cases are possible. Distinguishing classes of states with different "flavours" of entanglement could be accomplished using different entanglement measures, although several measures sometimes do not even distinguish between some tripartite entangled and separable states (e.g. 3-tangle, see section 4.4.2.2 below).

The following classification suggested in [49] shows the structural richness of different entanglement types, including distinction of states with different entanglement of their reduced states. Entanglement of reduced states is marked in the following figures 4.2 and 4.3 by a straight line connecting the two states, if tracing over the third qubit results in an entangled state, and without such a line if tracing over the third qubit results in a separable state.

- Type 0-0: totally separable states, no quantum entanglement
- Type 1: biseparable states
 - Subtype 1¹ – 0: Simply biseparable states, with no reduced entanglement. Of the three-qubit state considered, two qubits are entangled,

but tracing over the remaining qubit, the resulting two-qubit state is separable. This subtype is only possible for non-pure mixed states.

Example 4.1.1 *The state $\rho = (|0\rangle\langle 0| \otimes |\psi^-\rangle\langle \psi^-| + |1\rangle\langle 1| \otimes |\psi^+\rangle\langle \psi^+|)/2$ is biseparable and the resulting state after tracing over the first qubit is $(|\psi^-\rangle\langle \psi^-| + |\psi^+\rangle\langle \psi^+|)/2 = (|0\rangle\langle 0| \otimes |1\rangle\langle 1| + |1\rangle\langle 1| \otimes |0\rangle\langle 0|)/2$ which is clearly separable, a very counter-intuitive result.*

- Subtype $1^1 - 1$: simply biseparable states, with reduced entanglement. Tracing over the remaining separable qubit the resulting two-qubit state remains entangled.

Remark 4.1.1 *All pure biseparable states are of this type*

Remark 4.1.2 *There exist also non-pure mixed states of this subtype, see [49].*

- Subtype 1^2 : generalized biseparable states with bipartite entanglements in two pairs of qubits, with or without reduced entanglements. The following subtypes are possible: $1^2 - 0, 1^2 - 1, 1^2 - 2$ depending on the entanglement of the reduced states.
- Subtype 1^3 : generalized biseparable states with bipartite entanglements in three pairs of qubits. Again depending on the entanglement of the reduced states we obtain the following subtypes: $1^3 - 0, 1^3 - 1, 1^3 - 2, 1^3 - 3$

Example 4.1.2 *The state*

$$\rho = \frac{1}{3}(|\phi^+\rangle\langle \phi^+|_{AB} \otimes |0\rangle\langle 0|_C + |\phi^+\rangle\langle \phi^+|_{AC} \otimes |0\rangle\langle 0|_B + |\phi^+\rangle\langle \phi^+|_{BC} \otimes |0\rangle\langle 0|_A) \quad (4.1.2)$$

is an example for the case $1^3 - 3$.

- Type 2: tripartite entangled states
 - Subtype 2-0: all three reduced entanglements are zero \rightarrow GHZ-like states
 - Subtype 2-1: one reduced entanglement is non-zero.
 - Subtype 2-2: two reduced entanglements are non-zero.
 - Subtype 2-3: all three reduced entanglements are non-zero \rightarrow W-like states

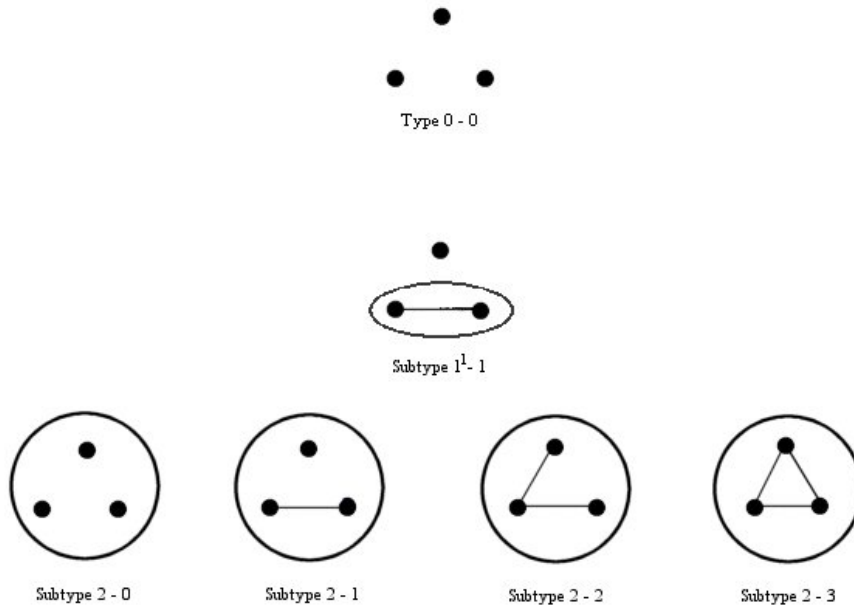


Figure 4.2: Graphic representation of entanglement types in pure states of three-qubit systems

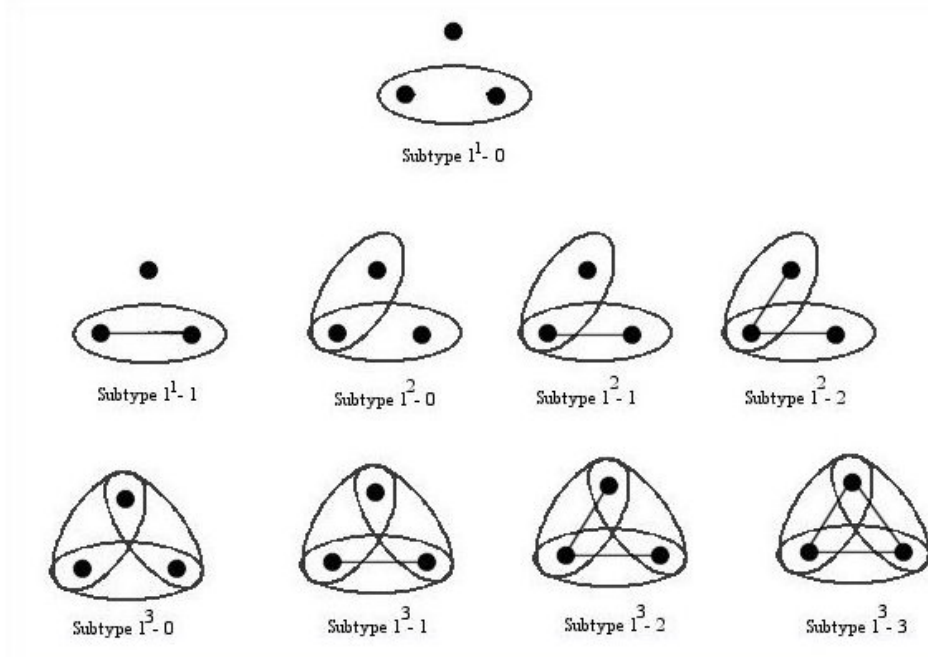


Figure 4.3: Graphic representation of entanglement types in mixed states of three-qubit systems

4.2 Generalized Schmidt Decomposition

A generalization to the Schmidt decomposition in an absolutely similar way as for two qubit states (see section 3.3) is not possible [50] for n -partite systems with $n \geq 3$, because such a decomposition is only possible under certain conditions.

But every pure three qubit state can be transformed by local unitary operations into

$$|\psi\rangle = \lambda_0 |000\rangle + \lambda_1 e^{i\theta} |100\rangle + \lambda_2 |101\rangle + \lambda_3 |110\rangle + \lambda_4 |111\rangle \quad (4.2.1)$$

with five coefficients. The five coefficients consist of six parameters, where the λ_i are real, non-negative, $\sum_i \lambda_i^2 = 1$ and $\theta \in [0; \pi]$ (see [51], [52]). Thus generally for a pure state we need six real parameters to characterize the nonlocal properties.

Especially for the class of W states one finds $\theta = \lambda_4 = 0$. This shows that the set of pure W states is a set of measure zero in the set of all pure states [17].

Some more alternative generalizations of the Schmidt decomposition to the multipartite situation exist with different conditions on the coefficients used to expand the state in terms of a factorizable orthonormal basis [52], [53], [54], [55], [56].

4.3 EPR and GHZ Theorem

With Bell's theorem, predictions can be made which show disagreement between EPR and quantum mechanical theory. Experimental tests using many pairs of entangled photons have shown that quantum mechanical predictions are correct (see section 3.6). By using states of three or four entangled particles, further insights can be gained. Especially testing EPR vs. quantum mechanics can be made with GHZ states in only one experiment and no correlations and expectation values are needed [7].

Let us consider the following Gedankenexperiment [57] for a system consisting of three particles (a,b,c) with spin $\frac{1}{2}$ and a set of three commuting hermitian operators

$$\sigma_x^a \sigma_y^b \sigma_y^c, \quad \sigma_y^a \sigma_x^b \sigma_y^c, \quad \sigma_y^a \sigma_y^b \sigma_x^c. \quad (4.3.1)$$

Since the operators commute, a common eigenstate for all three operators is possible. The square of all three operators gives the unit operator and so the only possible eigenvalues are +1 or -1. If we now choose the following GHZ state as common eigenstate

$$|GHZ^-\rangle = \frac{1}{\sqrt{2}}(|000\rangle - |111\rangle), \quad (4.3.2)$$

then for all three operators the corresponding eigenvalue equals +1. Furthermore $|GHZ^-\rangle$ is also eigenstate of the following operator

$$\sigma_x^a \sigma_x^b \sigma_x^c = -\sigma_x^a \sigma_y^b \sigma_y^c \cdot \sigma_y^a \sigma_x^b \sigma_y^c \cdot \sigma_y^a \sigma_y^b \sigma_x^c, \quad (4.3.3)$$

but now to the eigenvalue -1.

Remembering the EPR argumentation, we can now argue that using three well separated entangled particles with spin $S = \frac{1}{2}$ in the state $|GHZ^-\rangle$, we are taking three measurements (three different operators) on the corresponding three particles a, b, c. After two measurements we already know with probability 1 (perfect correlation) the result of the third measurement.

Again EPR argumentation states, that the measurements at the different particles do not influence the measurements at other particles and instantaneous action at a distance is not possible, but the third result is 100 % predictable. Therefore, after EPR, the above measurement results should be fixed before measurement and the property "spin" would be real for all three particles.

For the operator $\sigma_x^a \sigma_y^b \sigma_y^c$, for example, we know the measurement result m_x^a before measuring, having measured m_y^b for particle b and m_y^c for particle c, since the product of all three measurements in the state $|GHZ^-\rangle$ has to give the (eigen)value +1 (m_x und m_y can take the values ± 1). Analogous considerations for the operators $\sigma_y^a \sigma_x^b \sigma_y^c$ and $\sigma_y^a \sigma_y^b \sigma_x^c$ give an absolutely similar result.

So we can attribute the following values to the operators (after EPR they are real):

$$\sigma_x^a \sigma_y^b \sigma_y^c : \quad m_x^a m_y^b m_y^c = 1 \quad (4.3.4)$$

$$\sigma_y^a \sigma_x^b \sigma_y^c : \quad m_y^a m_x^b m_y^c = 1 \quad (4.3.5)$$

$$\sigma_y^a \sigma_y^b \sigma_x^c : \quad m_y^a m_y^b m_x^c = 1 \quad (4.3.6)$$

Taking the product of these three identities, one obtains

$$m_x^a m_y^b m_y^c \cdot m_y^a m_x^b m_y^c \cdot m_y^a m_y^b m_x^c = m_x^a m_x^b m_x^c (m_y^a)^2 (m_y^b)^2 (m_y^c)^2 = 1 \quad (4.3.7)$$

Thus it follows that the value attributed to the operator from 4.3.3 has to be equal to +1

$$m_x^a m_x^b m_x^c = 1. \quad (4.3.8)$$

This then means that EPR predicts the eigenvalue +1 for the operator $\sigma_x^a \sigma_x^b \sigma_x^c$ – in exact opposition to the quantum mechanics prediction 4.3.3 – where the prediction (eigenvalue) was equal to -1.

More interesting Gedankenexperiments and playful illustrations for two, three or four particles can be found in Mermin [57], Kwiat and Hardy [58] and Aravind [59].

4.4 Geometry and entanglement

4.4.1 Partial Traces

Calculating partial traces, we observe a remarkable difference between GHZ and W states. Whereas the partial traces over one qubit of the GHZ state produce – as anticipated – mixed bipartite separable states, the resulting states of W states stay – quite counter intuitively at first view – entangled.

Example 4.4.1 *The density matrix corresponding to the GHZ state (pure, entangled)*

$$|GHZ\rangle = \frac{1}{\sqrt{2}}(|000\rangle + |111\rangle) \quad (4.4.1)$$

is given as:

$$\rho_{GHZ} = \frac{1}{2} \begin{pmatrix} 1 & 0 & 0 & 0 & 0 & 0 & 0 & 1 \\ 0 & 0 & 0 & 0 & 0 & 0 & 0 & 0 \\ 0 & 0 & 0 & 0 & 0 & 0 & 0 & 0 \\ 0 & 0 & 0 & 0 & 0 & 0 & 0 & 0 \\ 0 & 0 & 0 & 0 & 0 & 0 & 0 & 0 \\ 0 & 0 & 0 & 0 & 0 & 0 & 0 & 0 \\ 0 & 0 & 0 & 0 & 0 & 0 & 0 & 0 \\ 1 & 0 & 0 & 0 & 0 & 0 & 0 & 1 \end{pmatrix} \quad (4.4.2)$$

Taking the trace over **any one** of the subspaces A_i ($i = 1, 2, 3$), we obtain a **NON** entangled mixed states:

$$\text{tr}_{A_i} \rho_{GHZ} = \frac{1}{2}(|00\rangle\langle 00| + |11\rangle\langle 11|) = \frac{1}{2} \begin{pmatrix} 1 & 0 & 0 & 0 \\ 0 & 0 & 0 & 0 \\ 0 & 0 & 0 & 0 \\ 0 & 0 & 0 & 1 \end{pmatrix} \quad (4.4.3)$$

This state is separable, specifically it is the convex combination of two product states.

Example 4.4.2 *The W state*

$$(|100\rangle + |010\rangle + |001\rangle)/\sqrt{3}, \quad (4.4.4)$$

is represented by the corresponding density matrix

$$\rho_W = \frac{1}{3} \begin{pmatrix} 0 & 0 & 0 & 0 & 0 & 0 & 0 & 0 \\ 0 & 1 & 1 & 0 & 1 & 0 & 0 & 0 \\ 0 & 1 & 1 & 0 & 1 & 0 & 0 & 0 \\ 0 & 0 & 0 & 0 & 0 & 0 & 0 & 0 \\ 0 & 0 & 0 & 0 & 0 & 0 & 0 & 0 \\ 0 & 1 & 1 & 0 & 1 & 0 & 0 & 0 \\ 0 & 0 & 0 & 0 & 0 & 0 & 0 & 0 \\ 0 & 0 & 0 & 0 & 0 & 0 & 0 & 0 \end{pmatrix} \quad (4.4.5)$$

and taking now partial traces over any one of the subspaces, we obtain – in contrast – again an entangled state (this can easily be checked via PPT criterion):

$$\text{tr}_{A_i} \rho_W = \frac{1}{3} \begin{pmatrix} 1 & 0 & 0 & 0 \\ 0 & 1 & 1 & 0 \\ 0 & 1 & 1 & 0 \\ 0 & 0 & 0 & 0 \end{pmatrix} \quad (4.4.6)$$

But both states (GHZ, W) are genuinely tripartite entangled, so taking partial traces alone is not too useful to discriminate between entangled and separable states in the tripartite case.

4.4.2 Entanglement measures

In section 3.5 a few entanglement measures for the 2×2 case have been studied. While the bipartite case for two qubits is quite manageable, since we only have to discern between separable and entangled states, the situation in the tripartite case is much more complicated as we have seen in section 4.1.

4.4.2.1 Entropy

In section 3.5.1 we used entropy as an entanglement measure for bipartite states. For tripartite states we can use von Neumann entropy to get insights into entanglement by dividing the tripartite state into two parts, and calculating entropy in the same way as in the bipartite situation [48].

Example 4.4.3 For GHZ states the corresponding entropies can be calculated from the reduced density matrices ρ_A, ρ_B, ρ_C (here with logarithmus dualis) and the result in this case is $S_A = S_B = S_C = 1 > 0$.

Example 4.4.4 If we take generalized GHZ states of the form

$$|GHZ_\theta\rangle = \cos\theta |000\rangle + \sin\theta |111\rangle \quad (4.4.7)$$

the corresponding entropies are then (see also Figure 4.4 below)

$$S_A = S_B = S_C = -(\cos^2\theta \log_2(\cos^2\theta) + \sin^2\theta \log_2(\sin^2\theta)) \quad (4.4.8)$$

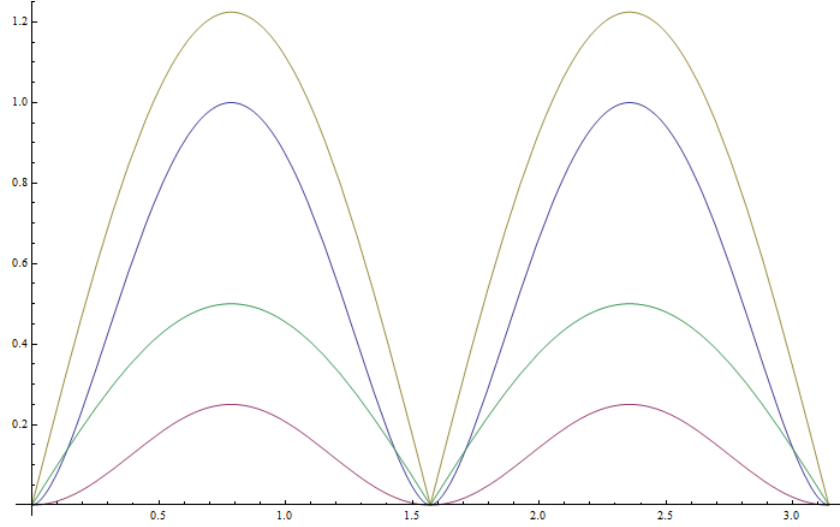


Figure 4.4: Entropy (blue), 3-tangle (red), concurrence (yellow) and negativity (green) of the generalized GHZ state

Example 4.4.5 For W states the entropies are

$$S_A = S_B = S_C = \log_2 \frac{3}{2^{\frac{2}{3}}} = \log_2 3 - \frac{2}{3} \approx 0.918296 > 0. \quad (4.4.9)$$

Example 4.4.6 If we generalize the W states in the following form

$$|W_{\alpha_1, \alpha_2, \alpha_3}\rangle = \alpha_1 |100\rangle + \alpha_2 |010\rangle + \alpha_3 |001\rangle \quad \text{with} \quad \sum_{i=1}^3 \alpha_i^2 = 1 \quad (4.4.10)$$

the entropies are

$$S_A = S_B = S_C = -[\alpha_i^2 \log_2 \alpha_i^2 + (1 - \alpha_i^2) \log_2(1 - \alpha_i^2)] > 0, \quad (4.4.11)$$

with $i = 1$ for A , $i = 2$ for B and $i = 3$ for C .

Example 4.4.7 For another example take the bi-separable state $\psi_{A-BC} = |0\rangle \otimes |\psi^+\rangle$. By separating the state into the two parts A and BC , the corresponding entropy S_A then vanishes in this case, whereas $S_B = S_C = 1 > 0$.

Example 4.4.8 The totally separable state $A - B - C$ has of course all entropies vanishing: $S_A = S_B = S_C = 0$.

For an overall entropy measure for three-qubit states Feng Pan et al. [60] suggested to calculate the arithmetic mean of partial entropies

$$S = (S_A + S_B + S_C)/3 \quad (4.4.12)$$

In [61] an alternative entanglement measure for three-qubit states the "entropy product" of partial entropies

$$S_P = S_A \cdot S_B \cdot S_C \quad (4.4.13)$$

is proposed.

This corresponds essentially to a geometric mean (where the third root has been omitted).

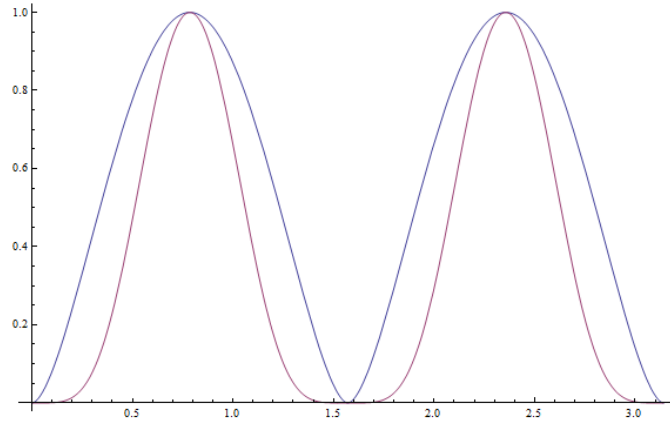


Figure 4.5: Arithmetic (blue) and geometric mean (red) entropy of generalized GHZ states

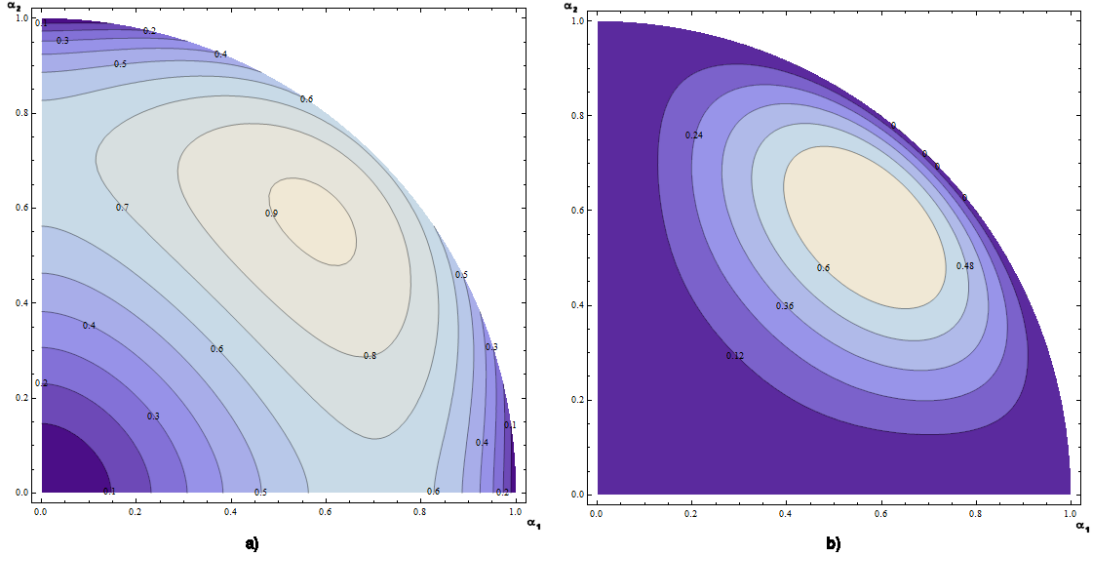


Figure 4.6: a) Arithmetic and b) geometric mean entropy of generalized W states

4.4.2.2 3-tangle and concurrence

The following entanglement measure was introduced by Coffman, Kundu and Wootters in 2000 [62]

$$\tau_3 = \tau_{ABC} = \tau_{A(BC)} - \tau_{AB} - \tau_{AC} \quad (4.4.14)$$

and τ_{XY} is the square of the concurrence (see section 3.5.2.2) of the corresponding bipartite system.

τ_3 is called the 3-tangle and is invariant under permutation. The GHZ state giving separable states for any partial trace has non-zero 3-tangle $\tau_3 = \frac{1}{4}$, whereas for the W state, where reduced states remain entangled, the corresponding 3-tangle vanishes. Since both states are of course entangled, the 3-tangle measure is not always useful for detecting differences between entangled and separable states, but it can be a distinguishing criterion between W and GHZ states.

In some way the 3-tangle is a kind of generalization of the concurrence from two to three qubits and in this form coincides with the modulus of the Cayley hyper-

determinant [8]

$$\begin{aligned}
C(|\Psi\rangle) = \text{Det}A &= a_{000}^2 a_{111}^2 + a_{001}^2 a_{110}^2 + a_{100}^2 a_{011}^2 \\
&- 2[a_{000} a_{111} (a_{001} a_{110} + a_{010} a_{101} + a_{011} a_{100}) \\
&+ a_{001} a_{010} a_{101} a_{110} + a_{001} a_{011} a_{101} a_{100} + a_{010} a_{011} a_{101} a_{100}] \\
&+ 4[a_{000} a_{011} a_{101} a_{110} + a_{001} a_{010} a_{100} a_{111}]
\end{aligned} \tag{4.4.15}$$

where the tripartite qubit can be represented as

$$|\Psi\rangle = \sum_{i,j,k=0}^1 a_{ijk} |ijk\rangle. \tag{4.4.16}$$

From this we extract the coefficient matrix $A = (a_{ijk})$.

To be able to reliably classify the different entanglement properties at least for pure states, we need more information about sub-concurrences. Building six submatrices $A_{x0} = (a_{0ij})$, $A_{y0} = (a_{i0j})$, $A_{z0} = (a_{ij0})$, $A_{x1} = (a_{1ij})$, $A_{y1} = (a_{i1j})$, $A_{z1} = (a_{ij1})$, the moduli of their determinants just give us the needed sub-concurrences:

$$C_{\alpha i} = |\det A_{\alpha i}|, (\alpha = x, y, z; i = 0, 1). \tag{4.4.17}$$

Then the ordered list

$$[|\text{Det}A|; C_{x0}; C_{x1}; C_{y0}; C_{y1}; C_{z0}; C_{z1}] \tag{4.4.18}$$

gives us a possibility to discriminate between GHZ and W states via the first term and furthermore the vanishing of the list provides a necessary and sufficient condition for separability (see [8]).

Class	S_A	S_B	S_C	τ_3
$A-B-C$	0	0	0	0
$A-BC$	0	>0	>0	0
$B-AC$	>0	0	>0	0
$C-AB$	>0	>0	0	0
W	>0	>0	>0	0
GHZ	>0	>0	>0	>0

Figure 4.7: Values of the local entropies S_A, S_B, S_C and the 3-tangle τ_3 for different classes of tripartite states (after [48])

Example 4.4.9 The 3-tangle of the GHZ state is $\tau_3(|GHZ\rangle) = \frac{1}{4}$, the concurrence vanishes. The 3-tangle for the generalized GHZ state of example 4.4.4 is given by

$$\tau_3 = (\cos \theta \cdot \sin \theta)^2. \quad (4.4.19)$$

See Figure 4.4, giving us a very similar picture as for the entropy.

In [63], [64] an n-partite generalization of the bipartite concurrence is given as

$$C_n(\psi) = 2^{1-n/2} \sqrt{(2^n - 2) - \sum_i \text{tr } \rho_i^2}, \quad (4.4.20)$$

where the ρ_i are the reduced density matrices obtained by tracing over all the different subsystems.

So, for the case of three qubits we can use

$$C_3(\psi) = \sqrt{3 - \frac{1}{2} \sum_i \text{tr } \rho_i^2}, \quad (4.4.21)$$

as a generalization of concurrence.

For product states the concurrence vanishes.

For the W state the value is

$$C_3(\rho_W) = \frac{2}{\sqrt{3}} \approx 1.1547, \quad (4.4.22)$$

for GHZ states

$$C_3(\rho_{GHZ}) = \sqrt{\frac{3}{2}} \approx 1.22474, \quad (4.4.23)$$

whereas for example the biseparable state $|\psi_{A-BC}\rangle = |0\rangle |\psi^+\rangle$ delivers the concurrence

$$C_3(\psi_{A-BC}) = 1. \quad (4.4.24)$$

It is interesting, that the generalized concurrence allows values larger than 1 for GHZ and for W states. This shows that for genuine tripartite entanglement there is an amount of entanglement that exceeds bipartite entanglement.

For the generalized W states of example 4.4.6 see a contour plot of the concurrence.

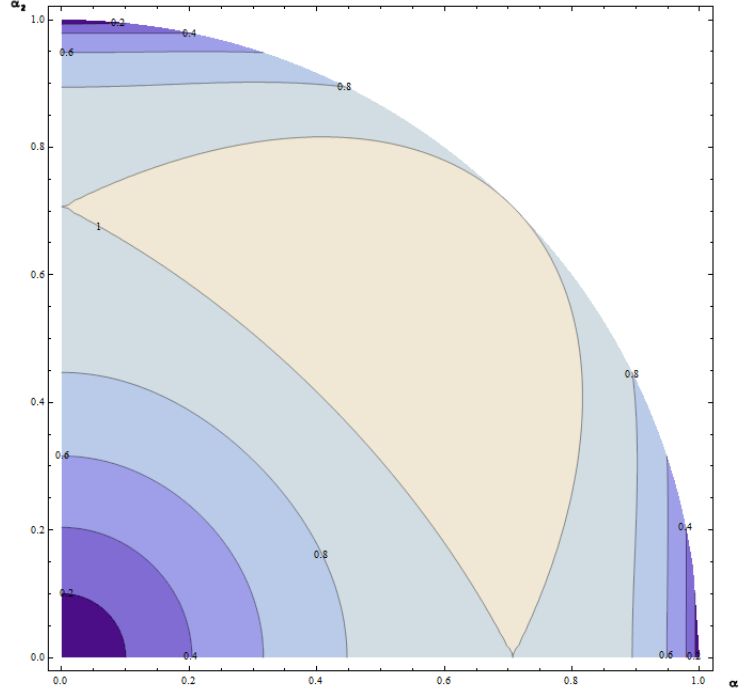


Figure 4.8: Values of the concurrence for the generalized W state $|W_{\alpha_1, \alpha_2, \alpha_3}\rangle = \alpha_1 |100\rangle + \alpha_2 |010\rangle + \alpha_3 |001\rangle$ with $0 \leq \alpha_1, \alpha_2 \leq 1, \alpha_3 = \sqrt{1 - \alpha_1^2 - \alpha_2^2}$

4.4.2.3 Negativity

In the same way as for entropies (section 4.4.2.1) we can calculate bipartite negativities by dividing our tripartite states into two parts [33].

Example 4.4.10 For a quantum system ρ consisting of three parts A, B, C , join for example parts of B and C , opposed to A and calculate the sum of negative eigenvalues of ρ^{TA} to obtain the negativity

$$N_{A-BC}(\rho) \quad (4.4.25)$$

In a similar way negativities $N_{B-AC}(\rho)$ and $N_{C-AB}(\rho)$ can be calculated for pure as well as for mixed states.

These quantities are entanglement monotones, meaning they do not increase under LOCC.

To obtain an entanglement measure, we can extend the bipartite measure in the following way [49]:

$$N_{ABC}(\rho) = (N_{A-BC} N_{B-AC} N_{C-AB})^{\frac{1}{3}} \quad (4.4.26)$$

with N_{I-JK} being bipartite negativities.

This measure can also be calculated for non-pure tripartite states.

Example 4.4.11 *Negativity for the maximally entangled GHZ state equals $\frac{1}{2}$ and for the generalized GHZ states all the above four versions are identical and we obtain*

$$N_{ABC}(\rho_\theta) = \frac{1}{2}(-1 + \cos^2 \theta + \sin^2 \theta + |\sin 2\theta|). \quad (4.4.27)$$

See Figure 4.4, especially comparing with the corresponding graphs of entropy, 3-tangle and concurrence.

Example 4.4.12 *Negativity for W states is equal to $\frac{\sqrt{2}}{3}$ for all of the above four negativity versions. For generalized W states as in Example 4.4.6 the negativities are of the form*

$$\frac{1}{2}(-1 + \alpha_i^2 + (1 - \alpha_i)^2 + 2\sqrt{|\alpha_i^2 - \alpha_i^4|}). \quad (4.4.28)$$

In Figure 4.9 the negativity of generalized W states is compared to their entropy.

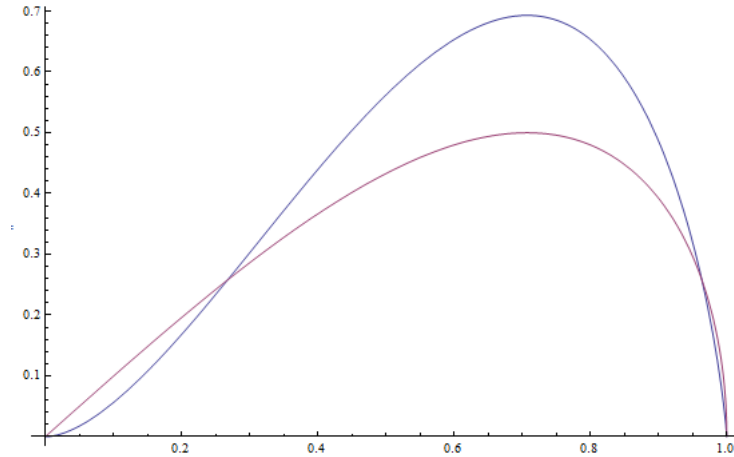


Figure 4.9: Entropy (blue) and negativity (red) of generalized W states for $0 \leq \alpha_1 \leq 1$

4.4.2.4 Entanglement witnesses

The distinction between the different entanglement classes for mixed states is not an easy task. In analogy to entanglement witnesses in the bipartite, we can construct entanglement witnesses for the tripartite case, remembering that the sets of separable (S), bipartite (B) and W states (W) are convex.

Example 4.4.13 Take for example the following witness for GHZ states:
 \mathcal{W}_{GHZ} is a hermitian operator with the following properties

$$\begin{aligned} \text{tr}(\mathcal{W}_{GHZ}\rho_{GHZ}) &< 0 \text{ for a } \rho_{GHZ} \in GHZ \setminus W \text{ and} \\ \text{tr}(\mathcal{W}_{GHZ}\rho_W) &\geq 0 \text{ for all } \rho_W \in W. \end{aligned} \quad (4.4.29)$$

For GHZ the following witness is an example:

$$\mathcal{W}_{GHZ} = \frac{3}{4}\mathbb{I} - P_{GHZ}, \quad (4.4.30)$$

where P_{GHZ} is the projector onto the GHZ state $\frac{1}{\sqrt{2}}(|000\rangle + |111\rangle)$. This witness fulfills the properties given above (see [47]).

Example 4.4.14 In an absolutely similar way a W -witness can be constructed, where the witness has negative expectation for W states, but positive or vanishing expectation value for all states in B (bi-separable or separable):

$$\mathcal{W}_W = \frac{2}{3}\mathbb{I} - P_W \quad (4.4.31)$$

with P_W the projector onto the W state $\frac{1}{\sqrt{3}}(|100\rangle + |010\rangle + |001\rangle)$.

An interesting fact is, that the pure W states form a set of measure zero, whereas the set $W \setminus B$ of mixed W states is not of measure zero. This can be seen with the help of the entanglement witness idea, showing that there is a finite ball around a state from the above set [24].

Considering again the generalized GHZ states $|GHZ_\theta\rangle = \cos\theta|000\rangle + \sin\theta|111\rangle$ from example 4.4.4, one notices (see Figure 4.10) that the entanglement witness 4.4.30 only works for states with a minimum of "entanglement" and the "right direction". This means that $\text{tr}(\mathcal{W}_{GHZ}\rho_{GHZ_\theta}) < 0$ only for

$$\arccos\left(\frac{\sqrt{2-\sqrt{3}}}{2}\right) \leq \theta \leq \arccos\left(\frac{\sqrt{2+\sqrt{3}}}{2}\right). \quad (4.4.32)$$

Where the generalized GHZ states come near to the product states $|000\rangle, |111\rangle$ or represents states similar to $|GHZ_-\rangle = \frac{1}{\sqrt{2}}(|000\rangle - |111\rangle)$ for $\theta > \frac{\pi}{2}$, the entanglement witness \mathcal{W}_{GHZ} cannot produce negative values and therefore loses the power to detect entanglement, because the operator \mathcal{W}_{GHZ} is not well fitted for these situations.

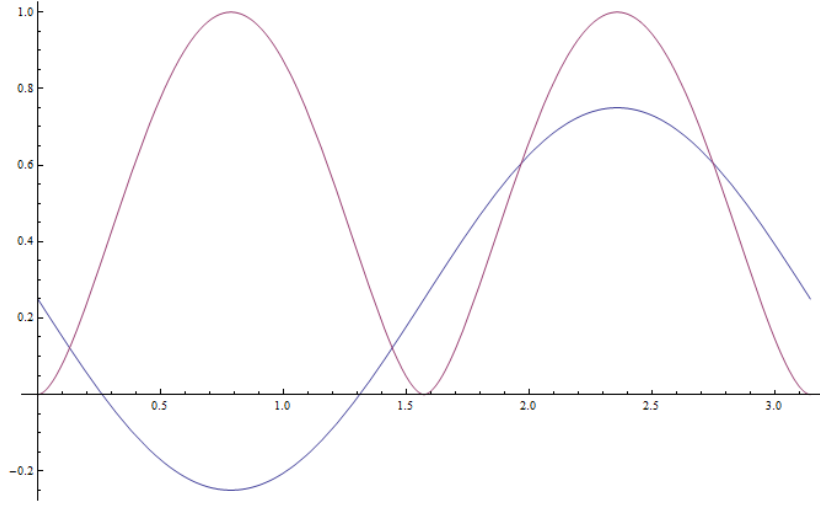


Figure 4.10: Entanglement witness (equation 4.4.30) (blue) and entropy (red) of the generalized GHZ states for $0 \leq \theta \leq \pi$

4.4.3 Entanglement type for GHZ symmetric states

Eltchka and Siewert [65] characterize the family of GHZ symmetric states by exploiting their symmetry. These states can be represented as affine combinations of the states

$$|GHZ_+\rangle = |GHZ\rangle = \frac{1}{\sqrt{2}}(|000\rangle + |111\rangle), \quad (4.4.33)$$

$$|GHZ_-\rangle = \frac{1}{\sqrt{2}}(|000\rangle - |111\rangle) \quad (4.4.34)$$

and the maximally mixed state $\frac{1}{8}\mathbb{I}$.

They fulfill the property that they are invariant under the following transformations (and also combinations):

1. qubit permutations
2. simultaneous three-qubit flips (application of $\sigma_x \otimes \sigma_x \otimes \sigma_x$)
3. qubit rotations about the z axis of the following form

$$U(\phi_1, \phi_2) = e^{i\phi_1\sigma_z} \otimes e^{i\phi_2\sigma_z} \otimes e^{-i(\phi_1+\phi_2)\sigma_z} \quad (4.4.35)$$

Density matrices ρ^S of GHZ-symmetric states can be fully specified by two independent real parameters. The following choice

$$\begin{aligned} x(\rho^S) &= \frac{1}{2}[\langle GHZ_+ | \rho^S | GHZ_+ \rangle - \langle GHZ_- | \rho^S | GHZ_- \rangle] \\ y(\rho^S) &= \frac{1}{\sqrt{3}}[\langle GHZ_+ | \rho^S | GHZ_+ \rangle + \langle GHZ_- | \rho^S | GHZ_- \rangle - \frac{1}{4}] \end{aligned} \quad (4.4.36)$$

is such that the Euclidean metric in the (x, y) plane coincides with the Hilbert-Schmidt metric for density matrices in the following way:

$$d(A, B)^2 = \frac{1}{2} \text{tr}(A - B)^\dagger (A - B) \quad (4.4.37)$$

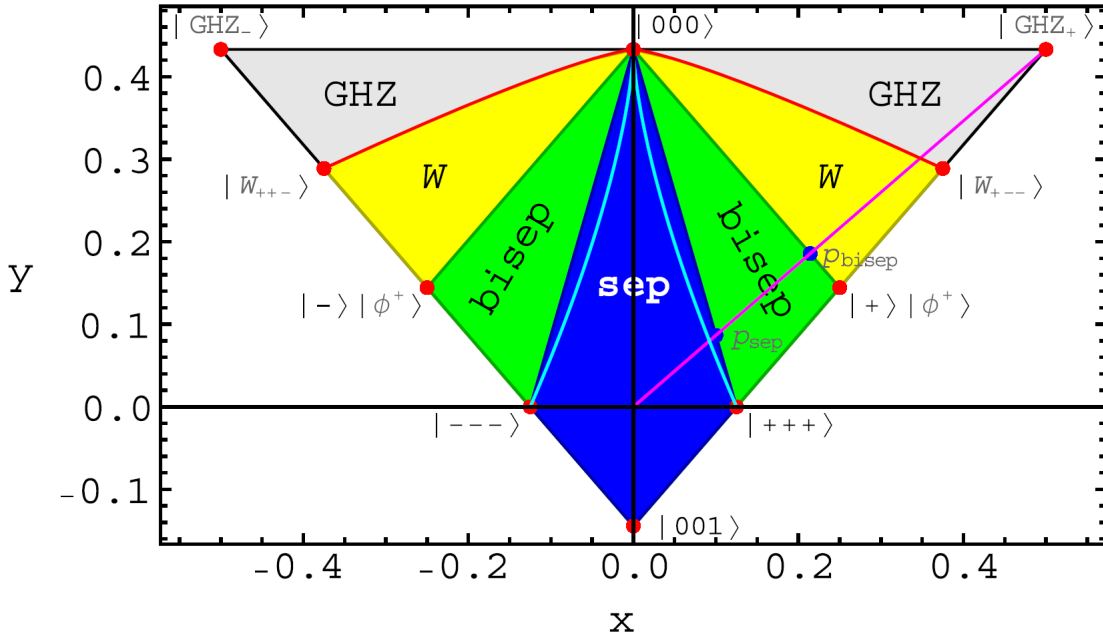


Figure 4.11: x-y representation of GHZ-symmetric states (figure from [65])

Let us now observe (mixed) states in the interior of the triangle representing the above affine combinations (see Fig. 4.11). For example, the generalized Werner states, that is the convex combinations of the maximally mixed state and a maximally entangled state (here $|GHZ\rangle$), have the following density matrix represen-

tation:

$$\begin{aligned} \rho_{WS}(p) &= p \cdot |GHZ\rangle \langle GHZ| + (1-p) \cdot \frac{1}{8} \mathbb{I}_8 \\ &= \begin{pmatrix} \frac{1+3p}{8} & 0 & 0 & 0 & 0 & 0 & 0 & \frac{p}{2} \\ 0 & \frac{1-p}{8} & 0 & 0 & 0 & 0 & 0 & 0 \\ 0 & 0 & \frac{1-p}{8} & 0 & 0 & 0 & 0 & 0 \\ 0 & 0 & 0 & \frac{1-p}{8} & 0 & 0 & 0 & 0 \\ 0 & 0 & 0 & 0 & \frac{1-p}{8} & 0 & 0 & 0 \\ 0 & 0 & 0 & 0 & 0 & \frac{1-p}{8} & 0 & 0 \\ 0 & 0 & 0 & 0 & 0 & 0 & \frac{1-p}{8} & 0 \\ \frac{p}{2} & 0 & 0 & 0 & 0 & 0 & 0 & \frac{1+3p}{8} \end{pmatrix} \end{aligned} \quad (4.4.38)$$

Using the parametrisation from [65], the representation for Werner states is given by

$$\begin{aligned} x(\rho_{WS}) &= \frac{p}{2} \\ y(\rho_{WS}) &= \frac{\sqrt{3}}{4} p \end{aligned} \quad (4.4.39)$$

and this exactly represents the Werner line $y = \frac{\sqrt{3}}{2}x$ as can be seen in the graphical representation (Fig. 4.11) of the GHZ-symmetric states, where Werner states $\rho_{WS}(p)$ can be found on the purple line.

Boundaries for the different types of entanglement can be calculated for the Werner states (see [65]), also discriminating between GHZ and W states:

- fully separable for $p \leq \frac{1}{5} = 0,2$
- biseparable $\frac{1}{5} < p \leq \frac{3}{7} \approx 0,4286$
- tripartite entangled W for $\frac{3}{7} < p \leq 0,6955$
- tripartite entangled GHZ for $p > 0,6955$

The corresponding boundaries form a sort of entanglement witnesses. This means that a state corresponding to a certain entanglement class in the graphical representation could have a "higher entanglement", but never a lower one. For example a state ρ_1^+ with $p \geq 0.696$ is a GHZ state (see boundaries in [65]), whereas a state with $\frac{3}{7} \leq p \leq 0.696$ could be a W or a GHZ state, but not biseparable.

It is interesting that all the generalized Werner states can easily be transformed to separable states. Using the unitary (non local) transformation U from example 4.4.15 of section 4.4.4 below, the density matrix of every Werner state is

transformed into a diagonal matrix, thus in any case transforming the state into a separable state:

$$U\rho_{WS}U^\dagger = \begin{pmatrix} \frac{1+7p}{8} & 0 & 0 & 0 & 0 & 0 & 0 & 0 \\ 0 & \frac{1-p}{8} & 0 & 0 & 0 & 0 & 0 & 0 \\ 0 & 0 & \frac{1-p}{8} & 0 & 0 & 0 & 0 & 0 \\ 0 & 0 & 0 & \frac{1-p}{8} & 0 & 0 & 0 & 0 \\ 0 & 0 & 0 & 0 & \frac{1-p}{8} & 0 & 0 & 0 \\ 0 & 0 & 0 & 0 & 0 & \frac{1-p}{8} & 0 & 0 \\ 0 & 0 & 0 & 0 & 0 & 0 & \frac{1-p}{8} & 0 \\ 0 & 0 & 0 & 0 & 0 & 0 & 0 & \frac{1-p}{8} \end{pmatrix} \quad (4.4.40)$$

Graphically the above unitary transformation moves the Werner states from the purple line horizontally to the y-axis into the separable domain, resulting in the coordinates:

$$\begin{aligned} x(U\rho_{WS}U^\dagger) &= 0 \\ y(U\rho_{WS}U^\dagger) &= \frac{\sqrt{3}}{4}p. \end{aligned} \quad (4.4.41)$$

If we calculate the reduced density matrices of $\rho_{WS}(p)$ we obtain (tracing over the first qubit A):

$$\begin{aligned} \text{tr}_A \rho_{WS} &= \frac{1-p}{4}\mathbb{I}_4 + \frac{p}{2} |00\rangle\langle 00| + |11\rangle\langle 11| \\ &= \begin{pmatrix} \frac{1+p}{4} & 0 & 0 & 0 \\ 0 & \frac{1-p}{4} & 0 & 0 \\ 0 & 0 & \frac{1-p}{4} & 0 \\ 0 & 0 & 0 & \frac{1+p}{4} \end{pmatrix} \end{aligned} \quad (4.4.42)$$

giving us always a mixed, not entangled state. This was to be expected from the GHZ type states, but is at first quite unexpected since the Werner states also cross the domain of the W states. But all these W states are mixed and so it seems, the property of the pure W state to produce entangled reduced density matrices, is somehow diluted.

4.4.4 Unitary transformations

Contrasting the fact that under local unitary transformations the entanglement type does not change, one can show that this is not always true for unitary transformations.

In Thirring et al. [66] (Theorem 1) it was even shown that in case of bipartite states every pure state ρ can be transformed unitarily into a separable or on the

other side into a maximally entangled state. Entanglement or separability then only depends on the choice of the factorization algebra.

For mixed states the situation is a bit more complicated. For mixed separable states a transformation to an entangled state is only possible for states below a certain amount of mixedness. For the 2×2 case one can even describe the set of absolutely separable states, the states that remain separable under every unitary transformation.

It is interesting to take a view into the geometry of states that remain separable under every unitary transformation, called the absolutely separable states. The Kuś-Życzkowski ball [67], the maximal ball which can be inscribed into the set of the mixed states for a bipartite systems is a subset of the set of absolutely separable states. Verstraete et al [68] established better constraints for the set of absolutely separable states putting some constraints on the spectrum and showing that the set of absolutely separable states is larger than the Kuś-Życzkowski ball.

The statements of [66] remain true for pure tripartite states. Example 4.4.15 illustrates this in a special case. For tripartite states it is also always possible to transform pure states into GHZ states as maximally entangled states in the sense that the GHZ maximally violates Bell's inequality. Reciprocally it is also possible to transform a pure entangled state into a separable one [69].

Example 4.4.15 *Take for example the pure and entangled GHZ state. Using the following unitary transformation (a rotation)*

$$U = \begin{pmatrix} \frac{1}{\sqrt{2}} & 0 & 0 & 0 & 0 & 0 & 0 & \frac{1}{\sqrt{2}} \\ 0 & 1 & 0 & 0 & 0 & 0 & 0 & 0 \\ 0 & 0 & 1 & 0 & 0 & 0 & 0 & 0 \\ 0 & 0 & 0 & 1 & 0 & 0 & 0 & 0 \\ 0 & 0 & 0 & 0 & 1 & 0 & 0 & 0 \\ 0 & 0 & 0 & 0 & 0 & 1 & 0 & 0 \\ 0 & 0 & 0 & 0 & 0 & 0 & 1 & 0 \\ \frac{1}{\sqrt{2}} & 0 & 0 & 0 & 0 & 0 & 0 & -\frac{1}{\sqrt{2}} \end{pmatrix}, \quad (4.4.43)$$

we obtain the separable product state:

$$U\rho_{GHZ}U^\dagger = |000\rangle\langle 000| \quad (4.4.44)$$

Open question: What are absolutely separable states in the tripartite case, states which cannot be changed into entangled states by unitary transformation and how can they be described geometrically?

4.5 Entangled Entanglement

Quantum states in which one particle is nonclassically correlated to the entangled state of the other two – similar to Bell states – are said to possess entangled entanglement. Such states have been studied and experimentally realized by Walther et al. [70].

Example 4.5.1 *Thinking of a situation where one qubit corresponds to Alice and two entangled qubits correspond to Bob, we could for example write such a state as*

$$|\Phi\rangle = \frac{1}{\sqrt{2}}(|0\rangle |\phi^-\rangle - |1\rangle |\psi^+\rangle) \quad (4.5.1)$$

where $|\phi^-\rangle$ and $|\psi^+\rangle$ are two of the bipartite Bell states.

By measuring the single particle of Alice, the properties of the relation between the two particles of Bob are defined, but not their single particle properties. These relational properties can now be measured by Bob. In [70] it is mentioned that correlations between the measurement outcomes of the polarization state of a single photon and the entangled state of two other experimentally violated the Clauser-Horne-Shimony-Holt Bell inequality, showing that entanglement itself can be entangled.

Example 4.5.2 *As another example take the following state*

$$|\Phi\rangle = \frac{1}{2}\{|R\rangle(|L\rangle|+\rangle + |R\rangle|-\rangle) + |L\rangle(|R\rangle|+\rangle + |L\rangle|-\rangle)\} \quad (4.5.2)$$

where the particles are represented with some rotated basis vectors from $\{|R\rangle, |L\rangle\}$ and $\{|+\rangle, |-\rangle\}$ defined in section 2.1, showing typical entangled entanglement in this representation. Nevertheless the state is absolutely equivalent to the original GHZ state

$$|\Phi\rangle = |\text{GHZ}\rangle = \frac{1}{\sqrt{2}}(|000\rangle + |111\rangle) \quad (4.5.3)$$

and is represented by the same density matrix!

Tracing over the first system of Alice,

$$\begin{aligned} \text{tr}_A \rho_{\text{GHZ}_{\text{rot}}} &= \frac{1}{4}\{(|RL\rangle + |LR\rangle)(\langle RL| + \langle LR|) + (|RR\rangle + |LL\rangle)(\langle RR| + \langle LL|)\} \\ &= \frac{1}{2} \begin{pmatrix} 1 & 0 & 0 & 0 \\ 0 & 0 & 0 & 0 \\ 0 & 0 & 0 & 0 \\ 0 & 0 & 0 & 1 \end{pmatrix} \end{aligned} \quad (4.5.4)$$

we obtain as residual state – again – a separable state, as was expected, since the state is in some sense indential to the GHZ state.

4.5.1 Eight entangled entanglement 2x2x2 states

For bipartite states, the Bell states can be represented as four linear independent vectors

$$|\psi^+\rangle = \begin{pmatrix} 0 \\ \frac{1}{\sqrt{2}} \\ \frac{1}{\sqrt{2}} \\ 0 \end{pmatrix}, \quad |\psi^-\rangle = \begin{pmatrix} 0 \\ \frac{1}{\sqrt{2}} \\ -\frac{1}{\sqrt{2}} \\ 0 \end{pmatrix}, \quad |\phi^+\rangle = \begin{pmatrix} \frac{1}{\sqrt{2}} \\ 0 \\ 0 \\ \frac{1}{\sqrt{2}} \end{pmatrix}, \quad |\phi^-\rangle = \begin{pmatrix} \frac{1}{\sqrt{2}} \\ 0 \\ 0 \\ -\frac{1}{\sqrt{2}} \end{pmatrix} \quad (4.5.5)$$

in the corresponding four dimensional vector space, therefore building a basis in this sense.

In a similar way, but constructing them as entangled entanglement states as in [70], let us consider the following set of eight three particle states, where the first particle (photon) is entangled with the entangled state of the second and third particle in a similar way as two particles are entangled in Bell states [71]:

$$\begin{aligned} |GHZ1^+\rangle &= \frac{1}{\sqrt{2}}(|0\rangle|\phi^-\rangle + |1\rangle|\psi^+\rangle) \\ |GHZ1^-\rangle &= \frac{1}{\sqrt{2}}(|0\rangle|\phi^-\rangle - |1\rangle|\psi^+\rangle) \\ |GHZ2^+\rangle &= \frac{1}{\sqrt{2}}(|0\rangle|\phi^+\rangle + |1\rangle|\psi^-\rangle) \\ |GHZ2^-\rangle &= \frac{1}{\sqrt{2}}(|0\rangle|\phi^+\rangle - |1\rangle|\psi^-\rangle) \\ |GHZ3^+\rangle &= \frac{1}{\sqrt{2}}(|1\rangle|\phi^-\rangle + |0\rangle|\psi^+\rangle) \\ |GHZ3^-\rangle &= \frac{1}{\sqrt{2}}(|1\rangle|\phi^-\rangle - |0\rangle|\psi^+\rangle) \\ |GHZ4^+\rangle &= \frac{1}{\sqrt{2}}(|1\rangle|\phi^+\rangle + |0\rangle|\psi^-\rangle) \\ |GHZ4^-\rangle &= \frac{1}{\sqrt{2}}(|1\rangle|\phi^+\rangle - |0\rangle|\psi^-\rangle) \end{aligned} \quad (4.5.6)$$

The vectors corresponding to these eight states are

$$|GHZ1^+\rangle = \begin{pmatrix} \frac{1}{2} \\ 0 \\ 0 \\ -\frac{1}{2} \\ 0 \\ \frac{1}{2} \\ \frac{1}{2} \\ 0 \end{pmatrix}, \quad |GHZ1^-\rangle = \begin{pmatrix} \frac{1}{2} \\ 0 \\ 0 \\ -\frac{1}{2} \\ 0 \\ -\frac{1}{2} \\ \frac{1}{2} \\ 0 \end{pmatrix}, \quad |GHZ2^+\rangle = \begin{pmatrix} \frac{1}{2} \\ 0 \\ 0 \\ -\frac{1}{2} \\ 0 \\ \frac{1}{2} \\ -\frac{1}{2} \\ 0 \end{pmatrix}, \quad |GHZ2^-\rangle = \begin{pmatrix} \frac{1}{2} \\ 0 \\ 0 \\ -\frac{1}{2} \\ 0 \\ -\frac{1}{2} \\ \frac{1}{2} \\ 0 \end{pmatrix} \quad (4.5.7)$$

$$\begin{aligned}
|GHZ3^+\rangle &= \begin{pmatrix} 0 \\ \frac{1}{2} \\ \frac{1}{2} \\ 0 \\ \frac{1}{2} \\ 0 \\ 0 \\ -\frac{1}{2} \end{pmatrix}, |GHZ3^-\rangle = \begin{pmatrix} 0 \\ -\frac{1}{2} \\ -\frac{1}{2} \\ 0 \\ \frac{1}{2} \\ 0 \\ 0 \\ -\frac{1}{2} \end{pmatrix}, |GHZ4^+\rangle = \begin{pmatrix} 0 \\ \frac{1}{2} \\ -\frac{1}{2} \\ 0 \\ \frac{1}{2} \\ 0 \\ 0 \\ \frac{1}{2} \end{pmatrix}, |GHZ4^-\rangle = \begin{pmatrix} 0 \\ -\frac{1}{2} \\ \frac{1}{2} \\ 0 \\ \frac{1}{2} \\ 0 \\ 0 \\ \frac{1}{2} \end{pmatrix}
\end{aligned} \tag{4.5.8}$$

again eight linear independent vectors, forming a basis in the eight dimensional vector space.

These eight states form the vertices of a "magic simplex" \mathbb{S} in the corresponding Hilbert space similar to the tetrahedron of states described in [35] or [72].

The set \mathbb{S} consists of the convex combinations of all the corresponding density matrices $\rho_{GHZi^\pm} = |GHZi^\pm\rangle\langle GHZi^\pm|, i = 1, \dots, 4$

$$\mathbb{S} = \left\{ \rho = \sum_{i=1, \dots, 4; k=+, -} \lambda_i^k \rho_{GHZi^k}, \quad \lambda_i^\pm \geq 0, \quad \sum \lambda_i^\pm = 1 \right\}. \tag{4.5.9}$$

The result of the convex combination forms a simplex with the maximally mixed state $\frac{1}{8}\mathbb{I}$ at its center and all the density matrices inside this simplex represent valid quantum states: The eigenvalues of every state $\rho = \sum_{i=1, \dots, 4; k=+, -} \lambda_i^k \rho_{GHZi^k}$ in the simplex are just equal to the eight coefficients λ_i^k . For elements of \mathbb{S} , we know – by construction – that $\lambda_i^\pm \geq 0$ and $\sum \lambda_i^\pm = 1$, so that inside the simplex all the eigenvalues are non-negative and the trace of ρ equals 1. Therefore $\rho \in \mathbb{S}$ is a valid density matrix.

On the other hand we know that matrices outside the simplex \mathbb{S} have to violate one of the above properties and therefore do not form density matrices of physical states. So we made sure that in the corresponding Hilbert space the valid density matrices are exactly represented by elements of the simplex \mathbb{S} .

Example 4.5.3 Take the density matrices on a one-dimensional facet, e.g. $\rho_{Facet_{\alpha}1+1-} = \alpha\rho_{GHZ1+} + (1 - \alpha)\rho_{GHZ1-}$, $0 \leq \alpha \leq 1$.

Then the following density matrix (a state on a ray from the maximally mixed to a state on the facet)

$$\rho = \frac{1}{8}\mathbb{I} + \mu(\rho_{Facet_{\alpha}1+1-} - \frac{1}{8}\mathbb{I}) = \mu\rho_{Facet_{\alpha}1+1-} + (1 - \mu)\frac{1}{8}\mathbb{I} \text{ with } \mu \geq 0$$

has eigenvalues $\frac{1-\mu}{8}$ (6 times), $\frac{1+7\mu-8\alpha\mu}{8}$ and $\frac{1-\mu+8\alpha\mu}{8}$.

Obviously all the Eigenvalues are nonnegative for $\mu \leq 1$, but crossing the border of \mathbb{S} by setting $\mu > 1$, we obtain negative eigenvalues, since then $\frac{1-\mu}{8}$ is obviously negative.

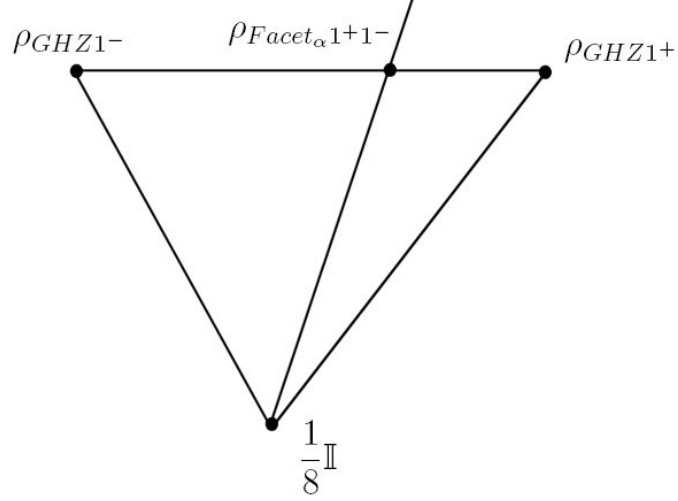


Figure 4.12: Illustration (projection into a subspace) for states in- and outside the simplex \mathbb{S}

4.5.2 Local unitary transformation of entangled entanglement states

Analyzing the eight states $|GHZi^{\pm}\rangle$ more closely, we note that the states $|GHZ1^{-}\rangle$ and $|GHZ3^{+}\rangle$ can easily be represented as GHZ type states using the basis of right and left circularly polarized photons $|R\rangle$ and $|L\rangle$:

$$\begin{aligned} |GHZ1^{-}\rangle &= \frac{1}{\sqrt{2}}(|RRR\rangle + |LLL\rangle) \\ |GHZ3^{+}\rangle &= -\frac{i}{\sqrt{2}}(|RRR\rangle - |LLL\rangle) \end{aligned} \quad (4.5.10)$$

For the other six states such a representation is possible in a similar way.

$$\begin{aligned} |GHZ1^{+}\rangle &= \frac{1}{\sqrt{2}}(|RLL\rangle + |LRR\rangle) \\ |GHZ2^{+}\rangle &= \frac{1}{\sqrt{2}}(|RRL\rangle + |LLR\rangle) \\ |GHZ2^{-}\rangle &= \frac{1}{\sqrt{2}}(|RLR\rangle + |LRL\rangle) \\ |GHZ3^{-}\rangle &= -\frac{i}{\sqrt{2}}(|RLL\rangle - |LLR\rangle) \\ |GHZ4^{+}\rangle &= -\frac{i}{\sqrt{2}}(|RLR\rangle - |LRL\rangle) \\ |GHZ4^{-}\rangle &= -\frac{i}{\sqrt{2}}(|RRL\rangle - |LLR\rangle) \end{aligned} \quad (4.5.11)$$

Using transformations of the form

$$U = U_A \otimes U_B \otimes U_C \quad (4.5.12)$$

with U_i local unitary transformations (listed below 4.5.14), we can obtain all these eight states from the GHZ state $\frac{1}{\sqrt{2}}(|000\rangle + |111\rangle)$:

$$U |GHZ\rangle = |GHZi^\pm\rangle, i = 1, \dots, 4. \quad (4.5.13)$$

	U_A	U_B	U_C
ρ_{GHZ1^-}	U_{09}	U_{09}	U_{09}
ρ_{GHZ1^+}	U_{09}	U_{13}	U_{13}
ρ_{GHZ2^-}	U_{09}	U_{13}	U_{09}
ρ_{GHZ2^+}	U_{09}	U_{09}	U_{13}
ρ_{GHZ3^-}	U_{09}	U_{13}	U_{55}
ρ_{GHZ3^+}	U_{09}	U_{09}	U_{51}
ρ_{GHZ4^-}	U_{09}	U_{09}	U_{55}
ρ_{GHZ4^+}	U_{09}	U_{13}	U_{51}

(4.5.14)

Remark 4.5.1 *To find suitable unitary transformations, we listed eighty different unitary 2×2 matrices covering many different patterns, see Appendix B. This is of course no complete enumeration, but with help of Mathematica and this list, appropriate unitary transformations could be found easily.*

Example 4.5.4 *For example we obtain $U |GHZ\rangle = |GHZ1^-\rangle$ with the following transformation $U = U_A \otimes U_B \otimes U_C$ with*

$$U_A = U_B = U_C = U_{09} = \frac{1}{\sqrt{2}} \begin{pmatrix} 1 & 1 \\ i & -i \end{pmatrix} \quad (4.5.15)$$

Remark 4.5.2 *These transformations are not unique.*

This means all eight states are in some way equivalent to the GHZ state and they form a simplex in the corresponding Hilbertspace.

Subjecting all states of this simplex to one of those unitary transformations U (same for all the corners), for example the transformation U from example 4.5.4 by which we transformed $|GHZ\rangle$ to $|GHZ1^-\rangle$, we obtain a new simplex formed

by the following states:

$$\begin{aligned}
U |GHZ1^-\rangle &= -\frac{1-i}{2} |+++\rangle - \frac{1+i}{2} |--+\rangle \\
U |GHZ1^+\rangle &= \frac{1-i}{2} |+-+\rangle + \frac{1+i}{2} |-++\rangle \\
U |GHZ2^-\rangle &= \frac{1+i}{2} |+-+\rangle + \frac{1-i}{2} |-+-\rangle \\
U |GHZ2^+\rangle &= \frac{1+i}{2} |++-\rangle + \frac{1-i}{2} |--+\rangle \\
U |GHZ3^-\rangle &= -\frac{1+i}{2} |+-+\rangle - \frac{1-i}{2} |-++\rangle \\
U |GHZ3^+\rangle &= \frac{1+i}{2} |+++\rangle + \frac{1-i}{2} |--+\rangle \\
U |GHZ4^-\rangle &= \frac{1-i}{2} |++-\rangle + \frac{1+i}{2} |--+\rangle \\
U |GHZ1^+\rangle &= \frac{1-i}{2} |+-+\rangle + \frac{1+i}{2} |-+-\rangle
\end{aligned} \tag{4.5.16}$$

Applying this same unitary transformation U a second time, we again obtain a simplex of GHZ type states:

$$\begin{aligned}
U^2 |GHZ1^-\rangle &= -\frac{1-i}{2} (|000\rangle + |111\rangle) \\
U^2 |GHZ1^+\rangle &= -\frac{1-i}{2} (|011\rangle + |100\rangle) \\
U^2 |GHZ2^-\rangle &= -\frac{1-i}{2} (|010\rangle + |101\rangle) \\
U^2 |GHZ2^+\rangle &= -\frac{1-i}{2} (|001\rangle + |110\rangle) \\
U^2 |GHZ3^-\rangle &= \frac{1+i}{2} (|011\rangle - |100\rangle) \\
U^2 |GHZ3^+\rangle &= \frac{1+i}{2} (|000\rangle - |111\rangle) \\
U^2 |GHZ4^-\rangle &= \frac{1+i}{2} (|001\rangle - |110\rangle) \\
U^2 |GHZ1^+\rangle &= \frac{1+i}{2} (|010\rangle - |101\rangle)
\end{aligned} \tag{4.5.17}$$

Finally applying the unitary transformation U a third time, we return to the states where we started from, in the sense that the corresponding density matrices are identical:

$$\begin{aligned}
U^3 |GHZ1^-\rangle &= -\frac{1-i}{2} (|RRR\rangle + |LLL\rangle) = -\frac{1-i}{\sqrt{2}} |GHZ1^-\rangle \\
U^3 |GHZ1^+\rangle &= -\frac{1-i}{2} (|RLL\rangle + |LRR\rangle) = -\frac{1-i}{\sqrt{2}} |GHZ1^+\rangle \\
U^3 |GHZ2^-\rangle &= -\frac{1-i}{2} (|RLR\rangle + |LRL\rangle) = -\frac{1-i}{\sqrt{2}} |GHZ2^-\rangle \\
U^3 |GHZ2^+\rangle &= -\frac{1-i}{2} (|RRL\rangle + |LRR\rangle) = -\frac{1-i}{\sqrt{2}} |GHZ2^+\rangle \\
U^3 |GHZ3^-\rangle &= \frac{1+i}{2} (|RLL\rangle - |LRR\rangle) = -\frac{1-i}{\sqrt{2}} |GHZ3^-\rangle \\
U^3 |GHZ3^+\rangle &= \frac{1+i}{2} (|RRR\rangle - |LLL\rangle) = -\frac{1-i}{\sqrt{2}} |GHZ3^+\rangle \\
U^3 |GHZ4^-\rangle &= \frac{1+i}{2} (|RRL\rangle - |LLR\rangle) = -\frac{1-i}{\sqrt{2}} |GHZ4^-\rangle \\
U^3 |GHZ1^+\rangle &= \frac{1+i}{2} (|RLR\rangle - |LRL\rangle) = -\frac{1-i}{\sqrt{2}} |GHZ4^+\rangle
\end{aligned} \tag{4.5.18}$$

Applying the above transformation three times reveals a certain symmetry, similar to a rotation that returns after three applications to the original state. In such a way we obtain three simplices. Their intersection is restricted to one element – the totally mixed state.

4.5.3 Entanglement construction

Entangled states with more than three qubits can be constructed in a similar way.

Example 4.5.5 *The states $|GHZ1^-\rangle$ and $|GHZ3^+\rangle$ are entangled. Now we entangle them in a similar way as before with the help of $|0\rangle$ and $|1\rangle$, obtaining the following two states:*

$$\begin{aligned} |\Psi_1\rangle &= \frac{1}{\sqrt{2}}(|0\rangle |GHZ1^-\rangle - |1\rangle |GHZ3^+\rangle) \\ |\Psi_2\rangle &= \frac{1}{\sqrt{2}}(|0\rangle |GHZ3^+\rangle + |1\rangle |GHZ1^-\rangle) \end{aligned} \quad (4.5.19)$$

Similar to the results in the previous section, we notice that the state $|\Psi_1\rangle$ is absolutely identical to the four particle GHZ state in the basis $\{|R\rangle, |L\rangle\}$

$$|\Psi_1\rangle = |\Psi^+\rangle = \frac{1}{\sqrt{2}}(|RRRR\rangle + |LLLL\rangle) \quad (4.5.20)$$

and in a similar way

$$|\Psi_2\rangle = |\Psi^-\rangle = \frac{-i}{\sqrt{2}}(|RRRR\rangle - |LLLL\rangle). \quad (4.5.21)$$

With the help of states with entangled entanglement and using them as building blocks in a considerate and careful way, we can construct GHZ type states in higher dimensions.

We can show very generally that for every number of particles, it is possible to construct GHZ type entangled states in the above way. To this end we introduce the following notations:

$$\begin{aligned} |\varphi_1^1\rangle &= |0\rangle & |\varphi_1^2\rangle &= |1\rangle \\ |\varphi_2^1\rangle &= \frac{1}{\sqrt{2}}(|0\rangle |\varphi_1^1\rangle - |1\rangle |\varphi_1^2\rangle) & |\varphi_2^2\rangle &= \frac{1}{\sqrt{2}}(|0\rangle |\varphi_1^2\rangle + |1\rangle |\varphi_1^1\rangle) \\ &= |\varphi^-\rangle & &= |\varphi^+\rangle \\ |\varphi_3^1\rangle &= \frac{1}{\sqrt{2}}(|0\rangle |\varphi_2^1\rangle - |1\rangle |\varphi_2^2\rangle) & |\varphi_3^2\rangle &= \frac{1}{\sqrt{2}}(|0\rangle |\varphi_2^2\rangle + |1\rangle |\varphi_2^1\rangle) \\ &= |GHZ1^-\rangle & &= |GHZ3^+\rangle \end{aligned} \quad (4.5.22)$$

And generally

$$\begin{aligned} |\varphi_n^1\rangle &= \frac{1}{\sqrt{2}}(|0\rangle |\varphi_{n-1}^1\rangle - |1\rangle |\varphi_{n-1}^2\rangle) \\ |\varphi_n^2\rangle &= \frac{1}{\sqrt{2}}(|0\rangle |\varphi_{n-1}^2\rangle + |1\rangle |\varphi_{n-1}^1\rangle) \end{aligned} \quad (4.5.23)$$

If we denote by $|RL_n^\pm\rangle$ the GHZ states in the $\{|R\rangle, |L\rangle\}$ basis

$$|RL_n^\pm\rangle = \frac{1}{\sqrt{2}}(\underbrace{|RR\dots R\rangle}_n \pm \underbrace{|LL\dots L\rangle}_n) \quad (4.5.24)$$

we can for example write for $n = 3$ the equalities from the last section

$$|\varphi_3^1\rangle = |GHZ1^-\rangle = |RL_3^+\rangle \text{ and } |\varphi_3^2\rangle = |GHZ3^+\rangle = |RL_3^-\rangle \quad (4.5.25)$$

in a compact way.

By mathematical induction we can now show for all $n \geq 3$ that

$$|\varphi_n^1\rangle = |RL_n^+\rangle \text{ and } |\varphi_n^2\rangle = -i |RL_n^-\rangle. \quad (4.5.26)$$

Assume $|\varphi_n^1\rangle = |RL_n^+\rangle$ and $|\varphi_n^2\rangle = -i |RL_n^-\rangle$ then it follows that

$$\begin{aligned} |\varphi_{n+1}^1\rangle &= \frac{1}{\sqrt{2}}(|0\rangle |\varphi_n^1\rangle - |1\rangle |\varphi_n^2\rangle) \\ &= \frac{1}{\sqrt{2}}(|0\rangle |RL_n^+\rangle + i |1\rangle |RL_n^-\rangle) \\ &= \frac{1}{\sqrt{2}}(|0\rangle \frac{1}{\sqrt{2}}(\underbrace{|RR\dots R\rangle}_n + \underbrace{|LL\dots L\rangle}_n) + i |1\rangle \frac{1}{\sqrt{2}}(\underbrace{|RR\dots R\rangle}_n - \underbrace{|LL\dots L\rangle}_n)) \\ &= \frac{1}{\sqrt{2}}(\frac{(|0\rangle+i|1\rangle)}{\sqrt{2}} \underbrace{|RR\dots R\rangle}_n + \frac{(|0\rangle-i|1\rangle)}{\sqrt{2}} \underbrace{|LL\dots L\rangle}_n) \\ &= \frac{1}{\sqrt{2}}(|R\rangle \underbrace{|RR\dots R\rangle}_n + |L\rangle \underbrace{|LL\dots L\rangle}_n) \\ &= \frac{1}{\sqrt{2}}(\underbrace{|RR\dots R\rangle}_{n+1} + \underbrace{|LL\dots L\rangle}_{n+1}) \\ &= |RL_{n+1}^+\rangle \end{aligned}$$

$|\varphi_{n+1}^2\rangle = -i |RL_{n+1}^-\rangle$ follows in an absolutely similar way.

Thus it is now obviously possible to construct in a systematic way GHZ states of arbitrary many states in the $\{|R\rangle, |L\rangle\}$ basis using the process of entangling states that are already entangled.

4.6 Bloch representation in the tripartite case

4.6.1 Unitary 2x2x2 transformations and density matrices

Density matrices and unitary $2 \otimes 2 \otimes 2$ transformations can be represented with the help of Pauli matrices:

$$\begin{aligned} \sigma_0 = \mathbb{I} &= \begin{pmatrix} 1 & 0 \\ 0 & 1 \end{pmatrix}, \sigma_1 = \begin{pmatrix} 0 & 1 \\ 1 & 0 \end{pmatrix}, \sigma_2 = \begin{pmatrix} 0 & -i \\ i & 0 \end{pmatrix}, \sigma_3 = \begin{pmatrix} 1 & 0 \\ 0 & -1 \end{pmatrix} \\ U &= \sum_{i=0}^3 \sum_{j=0}^3 \sum_{k=0}^3 u_{ijk} \cdot \sigma_i \otimes \sigma_j \otimes \sigma_k \end{aligned} \quad (4.6.1)$$

Remark 4.6.1 *The following examples of Bloch representations in the $2 \times 2 \times 2$ case have been calculated with help of a Mathematica Tool (see Appendix A)*

Example 4.6.1 *Bloch representation of the unitary transformation U from example 4.4.15, that transforms the entangled GHZ state into the separable product state $|000\rangle\langle 000|$:*

$$\begin{aligned}
U = \frac{1}{4} & (3\mathbb{I} \otimes \mathbb{I} \otimes \mathbb{I} \\
& + \frac{1}{\sqrt{2}}(\sigma_1 \otimes \sigma_1 \otimes \sigma_1 + \sigma_3 \otimes \sigma_3 \otimes \sigma_3) \\
& + \frac{1}{\sqrt{2}}(\mathbb{I} \otimes \mathbb{I} \otimes \sigma_3 + \mathbb{I} \otimes \sigma_3 \otimes \mathbb{I} + \sigma_3 \otimes \mathbb{I} \otimes \mathbb{I}) \\
& - (\mathbb{I} \otimes \sigma_3 \otimes \sigma_3 + \sigma_3 \otimes \mathbb{I} \otimes \sigma_3 + \sigma_3 \otimes \sigma_3 \otimes \mathbb{I}) \\
& - \frac{1}{\sqrt{2}}(\sigma_1 \otimes \sigma_2 \otimes \sigma_2 + \sigma_2 \otimes \sigma_1 \otimes \sigma_2 + \sigma_2 \otimes \sigma_2 \otimes \sigma_1))
\end{aligned} \tag{4.6.2}$$

Example 4.6.2 *The density matrix of the GHZ state $\rho_{GHZ} = |GHZ\rangle\langle GHZ|$ can be written in Bloch representation in the following way:*

$$\begin{aligned}
\rho_{GHZ} = \frac{1}{8} & (\sigma_1 \otimes \sigma_1 \otimes \sigma_1 - \sigma_2 \otimes \sigma_2 \otimes \sigma_1 - \sigma_1 \otimes \sigma_2 \otimes \sigma_2 - \sigma_2 \otimes \sigma_1 \otimes \sigma_2 + \\
& \mathbb{I} \otimes \sigma_3 \otimes \sigma_3 + \sigma_3 \otimes \mathbb{I} \otimes \sigma_3 + \sigma_3 \otimes \sigma_3 \otimes \mathbb{I} + \mathbb{I} \otimes \mathbb{I} \otimes \mathbb{I})
\end{aligned} \tag{4.6.3}$$

and for example one of the states with entangled entanglement shows the following Bloch decomposition

$$\begin{aligned}
\rho_{GHZ1+} = \frac{1}{8} & (\sigma_1 \otimes \sigma_3 \otimes \sigma_1 - \sigma_3 \otimes \sigma_1 \otimes \sigma_1 - \sigma_2 \otimes \mathbb{I} \otimes \sigma_2 + \mathbb{I} \otimes \sigma_2 \otimes \sigma_2 + \\
& \sigma_1 \otimes \sigma_1 \otimes \sigma_3 + \sigma_3 \otimes \sigma_3 \otimes \sigma_3 - \sigma_2 \otimes \sigma_2 \otimes \mathbb{I} + \mathbb{I} \otimes \mathbb{I} \otimes \mathbb{I})
\end{aligned} \tag{4.6.4}$$

4.6.2 Pure 2x2x2 states

One qubit can be geometrically represented as a point in the Bloch ball. Pure states correspond to points on the Bloch sphere mentioned in section 2.3, mixed states lie inside the ball.

In the bipartite case, for two qubits, the Bloch representation from section 3.7

$$\rho = \frac{1}{4} (\mathbb{I} \otimes \mathbb{I} + \vec{a} \cdot \vec{\sigma} \otimes \mathbb{I} + \mathbb{I} \otimes \vec{b} \cdot \vec{\sigma} + \sum_i t_{ii} \sigma_i \otimes \sigma_i) \tag{4.6.5}$$

is already more complicated.

For states that can be represented as convex combination of only four special constituents, namely $\mathbb{I} \otimes \mathbb{I}$, $\sigma_1 \otimes \sigma_1$, $\sigma_2 \otimes \sigma_2$ and $\sigma_3 \otimes \sigma_3$, the Bell-diagonal states

$$\rho = \frac{1}{4}(\mathbb{I} \otimes \mathbb{I} + a \cdot \sigma_x \otimes \sigma_x + b \cdot \sigma_y \otimes \sigma_y + c \cdot \sigma_z \otimes \sigma_z) \quad (4.6.6)$$

the corresponding geometrical representation is the tetrahedron or magic simplex (Figure 3.4) with the Bell states at the corners. In Fig. 4.13 this tetrahedron is illustrated in combination with the ball of all pure states.

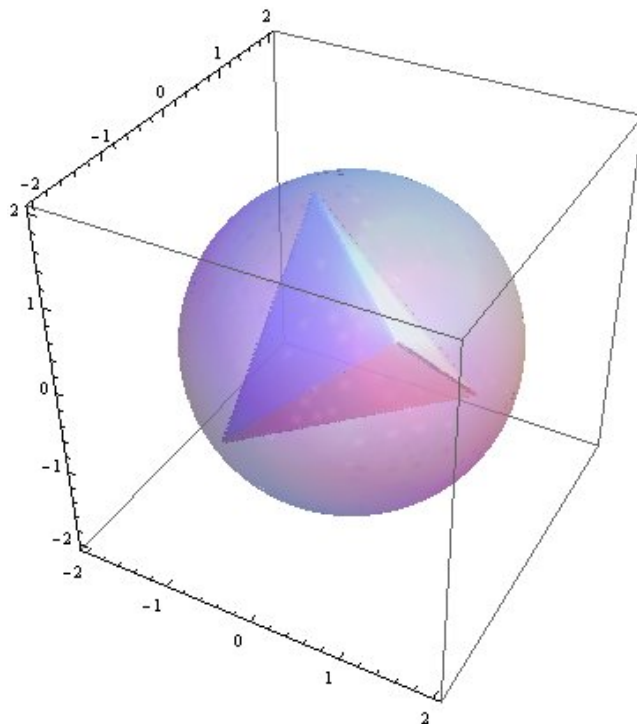


Figure 4.13: Tetrahedron of physical states and ball of pure states for two qubits

The borders have been defined by checking the eigenvalues and determining where they are non-negative. To find pure states, we calculate $\text{tr}(\rho^2) = \frac{1}{4}(1 + a^2 + b^2 + c^2)$ and set it equal to 1. Only states that fulfill $\frac{1}{4}(1 + a^2 + b^2 + c^2) = 1$ or equivalently $a^2 + b^2 + c^2 = 3$ are pure states.

In our case the only points in the intersection of the tetrahedron of physical states and the ball of pure states are the corners of the tetrahedron. So only the four Bell states at the corners are pure states, all other states in this special setting are mixed.

In the tripartite case the situation is still more complicated. Many more terms are possible as could already be seen in the last section. If we restrict ourselves again

to similar terms as before $\mathbb{I} \otimes \mathbb{I} \otimes \mathbb{I}$, $\sigma_1 \otimes \sigma_1 \otimes \sigma_1$, $\sigma_2 \otimes \sigma_2 \otimes \sigma_2$ and $\sigma_3 \otimes \sigma_3 \otimes \sigma_3$, the corresponding state is

$$\rho = \frac{1}{8}(\mathbb{I} \otimes \mathbb{I} \otimes \mathbb{I} + a\sigma_x \otimes \sigma_x \otimes \sigma_x + b\sigma_y \otimes \sigma_y \otimes \sigma_y + c\sigma_z \otimes \sigma_z \otimes \sigma_z) \quad (4.6.7)$$

with a very symmetrical density matrix form

$$\rho = \begin{pmatrix} \frac{1+c}{8} & 0 & 0 & 0 & 0 & 0 & 0 & \frac{a-ib}{8} \\ 0 & \frac{1-c}{8} & 0 & 0 & 0 & 0 & \frac{a+ib}{8} & 0 \\ 0 & 0 & \frac{1-c}{8} & 0 & 0 & \frac{a+ib}{8} & 0 & 0 \\ 0 & 0 & 0 & \frac{1+c}{8} & \frac{a-ib}{8} & 0 & 0 & 0 \\ 0 & 0 & 0 & \frac{a+ib}{8} & \frac{1-c}{8} & 0 & 0 & 0 \\ 0 & 0 & \frac{a-ib}{8} & 0 & 0 & \frac{1+c}{8} & 0 & 0 \\ 0 & \frac{a-ib}{8} & 0 & 0 & 0 & 0 & \frac{1+c}{8} & 0 \\ \frac{a+ib}{8} & 0 & 0 & 0 & 0 & 0 & 0 & \frac{1-c}{8} \end{pmatrix} \quad (4.6.8)$$

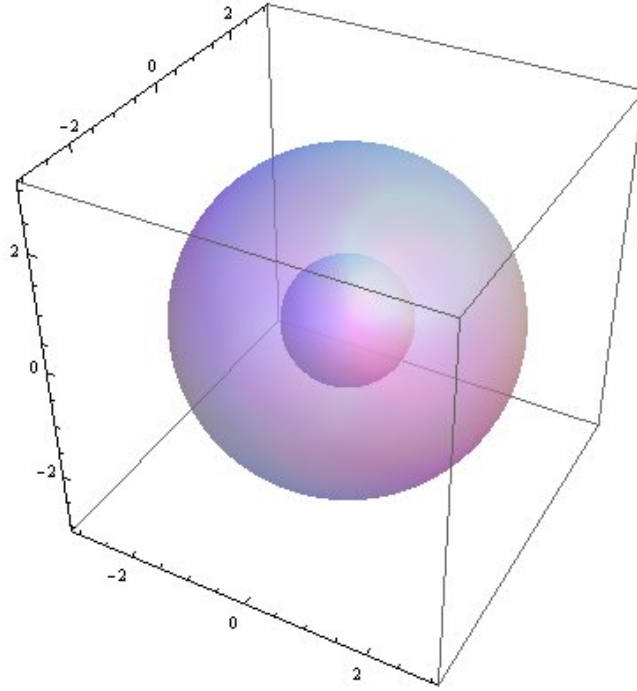


Figure 4.14: Ball of physical states and ball of pure states for three qubits

The eigenvalues are $\frac{1}{8}(1 - \sqrt{a^2 + b^2 + c^2})$ and $\frac{1}{8}(1 + \sqrt{a^2 + b^2 + c^2})$. To obtain valid density matrices, non-negative eigenvalues are necessary, therefore we obtain the

constraint $\sqrt{a^2 + b^2 + c^2} \leq 1$. This means in our situation that the set of valid density matrices is again represented by a ball.

Only for pure states we would need $\text{tr}(\rho^2) = \frac{1}{8}(1 + a^2 + b^2 + c^2) = 1$, corresponding to states on the ball $a^2 + b^2 + c^2 = 7$. This clearly is not possible, so in this case the set of states with this restricted set of Bloch terms does not include any pure state.

In the case of four particles, geometry changes again and we obtain for states of the form

$$\rho = \frac{1}{8}(\mathbb{I}^{\otimes 4} + a\sigma_x^{\otimes 4} + b\sigma_y^{\otimes 4} + c\sigma_z^{\otimes 4}) \quad (4.6.9)$$

a tetrahedron as in the case of two particles (actually compared to the two particle case we obtain here a flipped tetrahedron). But as in the case before, this tetrahedron of physical states does not contain any pure states; the condition for purity being $a^2 + b^2 + c^2 = 15$ in this case, contradicting the conditions for non-negative eigenvalues.

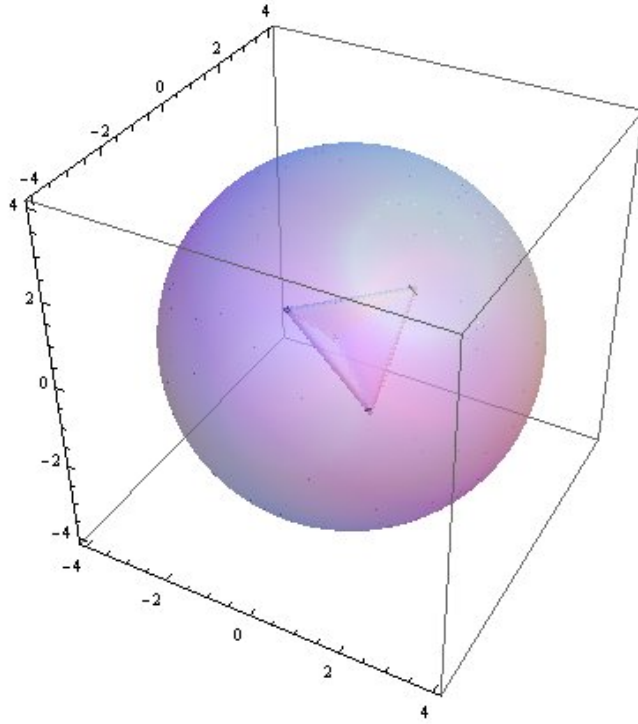


Figure 4.15: Tetrahedron of physical states and ball of pure states for four qubits

This alternation between tetrahedra and balls can be shown to hold generally, see Appendix C.

All in all, we can say that for n particle states of the simple structure

$$\rho = \frac{1}{8}(\mathbb{I}^{\otimes n} + a \cdot \sigma_x^{\otimes n} + b \cdot \sigma_y^{\otimes n} + c \cdot \sigma_z^{\otimes n}) \quad (4.6.10)$$

the corresponding geometrical Bloch representation is a tetrahedron for n even and a ball for n odd. For $n \geq 3$ this set of states does not include any pure states.

4.6.3 States with entangled entanglement

For the states with entangled entanglement we obtain the following Bloch representations:

$$\begin{aligned}
\rho_{GHZ1^-} &= |GHZ1^-\rangle \langle GHZ1^-| \\
&= \frac{1}{8}(-\sigma_3 \otimes \sigma_1 \otimes \sigma_1 - \sigma_1 \otimes \sigma_3 \otimes \sigma_1 + \mathbb{I} \otimes \sigma_2 \otimes \sigma_2 \\
&\quad + \sigma_2 \otimes \mathbb{I} \otimes \sigma_2 - \sigma_1 \otimes \sigma_1 \otimes \sigma_3 + \sigma_3 \otimes \sigma_3 \otimes \sigma_3 \\
&\quad + \sigma_2 \otimes \sigma_2 \otimes \mathbb{I} + \mathbb{I} \otimes \mathbb{I} \otimes \mathbb{I}) \\
\rho_{GHZ1^+} &= |GHZ1^+\rangle \langle GHZ1^+| \\
&= \frac{1}{8}(-\sigma_3 \otimes \sigma_1 \otimes \sigma_1 + \sigma_1 \otimes \sigma_3 \otimes \sigma_1 + \mathbb{I} \otimes \sigma_2 \otimes \sigma_2 \\
&\quad - \sigma_2 \otimes \mathbb{I} \otimes \sigma_2 + \sigma_1 \otimes \sigma_1 \otimes \sigma_3 + \sigma_3 \otimes \sigma_3 \otimes \sigma_3 \\
&\quad - \sigma_2 \otimes \sigma_2 \otimes \mathbb{I} + \mathbb{I} \otimes \mathbb{I} \otimes \mathbb{I}) \\
\rho_{GHZ2^-} &= |GHZ2^-\rangle \langle GHZ2^-| \\
&= \frac{1}{8}(\sigma_3 \otimes \sigma_1 \otimes \sigma_1 - \sigma_1 \otimes \sigma_3 \otimes \sigma_1 - \mathbb{I} \otimes \sigma_2 \otimes \sigma_2 \\
&\quad + \sigma_2 \otimes \mathbb{I} \otimes \sigma_2 + \sigma_1 \otimes \sigma_1 \otimes \sigma_3 + \sigma_3 \otimes \sigma_3 \otimes \sigma_3 \\
&\quad - \sigma_2 \otimes \sigma_2 \otimes \mathbb{I} + \mathbb{I} \otimes \mathbb{I} \otimes \mathbb{I}) \\
\rho_{GHZ2^+} &= |GHZ2^+\rangle \langle GHZ2^+| \\
&= \frac{1}{8}(\sigma_3 \otimes \sigma_1 \otimes \sigma_1 + \sigma_1 \otimes \sigma_3 \otimes \sigma_1 - \mathbb{I} \otimes \sigma_2 \otimes \sigma_2 \\
&\quad - \sigma_2 \otimes \mathbb{I} \otimes \sigma_2 - \sigma_1 \otimes \sigma_1 \otimes \sigma_3 + \sigma_3 \otimes \sigma_3 \otimes \sigma_3 \\
&\quad + \sigma_2 \otimes \sigma_2 \otimes \mathbb{I} + \mathbb{I} \otimes \mathbb{I} \otimes \mathbb{I}) \\
\rho_{GHZ3^-} &= |GHZ3^-\rangle \langle GHZ3^-| \\
&= \frac{1}{8}(\sigma_3 \otimes \sigma_1 \otimes \sigma_1 - \sigma_1 \otimes \sigma_3 \otimes \sigma_1 + \mathbb{I} \otimes \sigma_2 \otimes \sigma_2 \\
&\quad - \sigma_2 \otimes \mathbb{I} \otimes \sigma_2 - \sigma_1 \otimes \sigma_1 \otimes \sigma_3 - \sigma_3 \otimes \sigma_3 \otimes \sigma_3 \\
&\quad - \sigma_2 \otimes \sigma_2 \otimes \mathbb{I} + \mathbb{I} \otimes \mathbb{I} \otimes \mathbb{I}) \\
\rho_{GHZ3^+} &= |GHZ3^+\rangle \langle GHZ3^+| \\
&= \frac{1}{8}(\sigma_3 \otimes \sigma_1 \otimes \sigma_1 + \sigma_1 \otimes \sigma_3 \otimes \sigma_1 + \mathbb{I} \otimes \sigma_2 \otimes \sigma_2 \\
&\quad + \sigma_2 \otimes \mathbb{I} \otimes \sigma_2 + \sigma_1 \otimes \sigma_1 \otimes \sigma_3 - \sigma_3 \otimes \sigma_3 \otimes \sigma_3 \\
&\quad + \sigma_2 \otimes \sigma_2 \otimes \mathbb{I} + \mathbb{I} \otimes \mathbb{I} \otimes \mathbb{I}) \\
\rho_{GHZ4^-} &= |GHZ4^-\rangle \langle GHZ4^-| \\
&= \frac{1}{8}(-\sigma_3 \otimes \sigma_1 \otimes \sigma_1 - \sigma_1 \otimes \sigma_3 \otimes \sigma_1 - \mathbb{I} \otimes \sigma_2 \otimes \sigma_2 \\
&\quad - \sigma_2 \otimes \mathbb{I} \otimes \sigma_2 + \sigma_1 \otimes \sigma_1 \otimes \sigma_3 - \sigma_3 \otimes \sigma_3 \otimes \sigma_3 \\
&\quad + \sigma_2 \otimes \sigma_2 \otimes \mathbb{I} + \mathbb{I} \otimes \mathbb{I} \otimes \mathbb{I}) \\
\rho_{GHZ4^+} &= |GHZ4^+\rangle \langle GHZ4^+| \\
&= \frac{1}{8}(-\sigma_3 \otimes \sigma_1 \otimes \sigma_1 + \sigma_1 \otimes \sigma_3 \otimes \sigma_1 - \mathbb{I} \otimes \sigma_2 \otimes \sigma_2 \\
&\quad + \sigma_2 \otimes \mathbb{I} \otimes \sigma_2 - \sigma_1 \otimes \sigma_1 \otimes \sigma_3 - \sigma_3 \otimes \sigma_3 \otimes \sigma_3 \\
&\quad - \sigma_2 \otimes \sigma_2 \otimes \mathbb{I} + \mathbb{I} \otimes \mathbb{I} \otimes \mathbb{I})
\end{aligned} \tag{4.6.11}$$

All these states include only terms of the following set:

$$\begin{aligned}
B0 &= \mathbb{I} \otimes \mathbb{I} \otimes \mathbb{I} \\
B1 &= \sigma_3 \otimes \sigma_1 \otimes \sigma_1 \\
B2 &= \sigma_1 \otimes \sigma_3 \otimes \sigma_1 \\
B3 &= \mathbb{I} \otimes \sigma_2 \otimes \sigma_2 \\
B4 &= \sigma_2 \otimes \mathbb{I} \otimes \sigma_2 \\
B5 &= \sigma_1 \otimes \sigma_1 \otimes \sigma_3 \\
B6 &= \sigma_3 \otimes \sigma_3 \otimes \sigma_3 \\
B7 &= \sigma_2 \otimes \sigma_2 \otimes \mathbb{I}
\end{aligned} \tag{4.6.12}$$

The $GHZi^\pm$ states can be represented as a linear combination of these terms $B0, \dots, B7$ with the following $+$ and $-$ signs, see (4.6.11)

	$B0$	$B1$	$B2$	$B3$	$B4$	$B5$	$B6$	$B7$
ρ_{GHZ1-}	+	-	-	+	+	-	+	+
ρ_{GHZ1+}	+	-	+	+	-	+	+	-
ρ_{GHZ2-}	+	+	-	-	+	+	+	-
ρ_{GHZ2+}	+	+	+	-	-	-	+	+
ρ_{GHZ3-}	+	+	-	+	-	-	-	-
ρ_{GHZ3+}	+	+	+	+	+	+	-	+
ρ_{GHZ4-}	+	-	-	-	-	+	-	+
ρ_{GHZ4+}	+	-	+	-	+	-	-	-

(4.6.13)

As it is not possible to draw pictures in these high dimensional spaces, one can take smaller subsets or projections to gain some insights into the geometry. If we take – for example – a subset of four of the entangled entanglement states from section 4.5.1, for example $\rho_{GHZ1-}, \rho_{GHZ1+}, \rho_{GHZ3-}$ and ρ_{GHZ3+} and adjust the reference states to the following "directions",

$D1$	$=$	$B0 + B3$
$D2$	$=$	$B2 + B5$
$D3$	$=$	$B1 - B6$
$D4$	$=$	$B4 + B7$

(4.6.14)

we can represent the above states geometrically in three dimensions by a tetrahedron, actually again a kind of "magic simplex" with $D1$ in the center and the three dimensional directions $D2, D3$ and $D4$.

ρ_{GHZ1-}	$=$	$(D1 - D2 - D3 + D4)/8$
ρ_{GHZ1+}	$=$	$(D1 + D2 - D3 - D4)/8$
ρ_{GHZ3-}	$=$	$(D1 - D2 + D3 - D4)/8$
ρ_{GHZ3+}	$=$	$(D1 + D2 + D3 + D4)/8$

(4.6.15)

The states $\rho_{GHZ1-}, \rho_{GHZ1+}, \rho_{GHZ3-}$ and ρ_{GHZ3+} are then the corners of the corresponding magic simplex. The states inside the simplex take the form

$$\rho = \lambda_1 \rho_{GHZ1-} + \lambda_2 \rho_{GHZ1+} + \lambda_3 \rho_{GHZ3-} + \lambda_4 \rho_{GHZ3+}, \lambda_i \geq 0, \sum_i \lambda_i = 1 \quad (4.6.16)$$

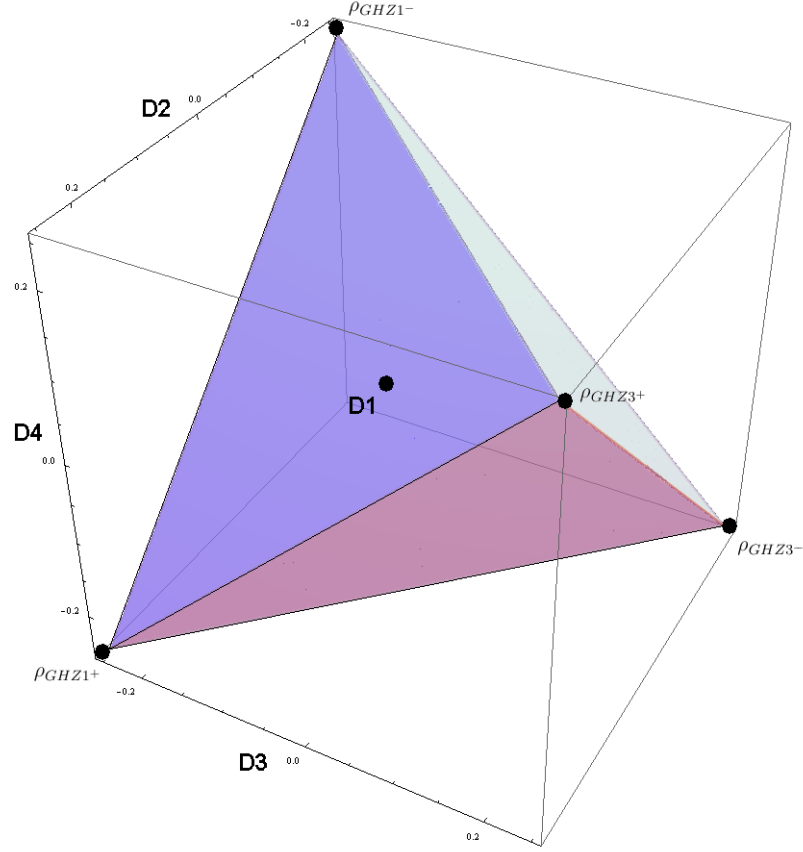


Figure 4.16: Magic simplex of 4 GHZ states with entangled entanglement

The state

$$D1 = (\rho_{GHZ1-} + \rho_{GHZ1+} + \rho_{GHZ3-} + \rho_{GHZ3+})/4 = \mathbb{I} \otimes \mathbb{I} \otimes \mathbb{I} + \mathbb{I} \otimes \sigma_2 \otimes \sigma_2 \quad (4.6.17)$$

lies at the center of the simplex.

We can analyze states on a ray from the center $D1$ to one of the facets, e.g. $\{\rho_{GHZ1-}, \rho_{GHZ1+}, \rho_{GHZ3+}\}$,

$$(1 - \lambda) \cdot D1 + \lambda \cdot (\alpha_1 \rho_{GHZ1-} + \alpha_2 \rho_{GHZ1+} + \alpha_3 \rho_{GHZ3+}) \quad (4.6.18)$$

with $\sum_{i=1}^3 \alpha_i = 1$. One notices that at least one eigenvalue is of the form $\frac{1-\lambda}{4}$ and so we observe that – as expected – states outside the simplex ($\lambda > 1$) are in fact not physical, they possess at least one negative eigenvalue.

To gain insight into the geometry of these states, we now take another point of view. This time we take only three corner states, e.g. $\{\rho_{GHZ1-}, \rho_{GHZ1+}, \rho_{GHZ3+}\}$ as above, but now we study the relation to the whole polytope built from all eight states $\{\rho_{GHZ1-}, \rho_{GHZ1+}, \rho_{GHZ2-}, \rho_{GHZ2+}, \rho_{GHZ3-}, \rho_{GHZ3+}, \rho_{GHZ4-}, \rho_{GHZ4+}\}$, not only a subset as shown in Figure 4.16.

Take the state at the center of the facet $[\rho_{GHZ1-}, \rho_{GHZ1+}, \rho_{GHZ3+}]$

$$\rho_c = \frac{1}{3}(\rho_{GHZ1-} + \rho_{GHZ1+} + \rho_{GHZ3+}). \quad (4.6.19)$$

Connecting it with the maximally mixed state $\frac{1}{8}\mathbb{I}$ and extending this ray to the "other side" of the polytope of physical states, we end up having the following state

$$\rho_d = \frac{1}{5}(\rho_{GHZ2-} + \rho_{GHZ2+} + \rho_{GHZ3-} + \rho_{GHZ4-} + \rho_{GHZ4+}) \quad (4.6.20)$$

which is at the center of the "opposite" facet of the polytope (this facet cannot be represented in our picture due to dimensionality restrictions).

A further exploration along a ray from a point between $\frac{1}{8}\mathbb{I}$ and ρ_c

$$\rho_\alpha = \alpha \frac{1}{8}\mathbb{I} + (1 - \alpha)\rho_c, \quad 0 \leq \alpha \leq 1 \quad (4.6.21)$$

to the "center"

$$\rho_m = \frac{1}{3}(\rho_{GHZ1-} + \rho_{GHZ1+} + \frac{1}{8}\mathbb{I}) \quad (4.6.22)$$

of the facet $[\rho_{GHZ1-}, \rho_{GHZ1+}, \frac{1}{8}\mathbb{I}]$ of the polytope with the corners $\{\rho_{GHZ1-}, \rho_{GHZ1+}, \rho_{GHZ3+}, \frac{1}{8}\mathbb{I}\}$ delivers the point

$$\rho_b = \lambda \rho_m + (1 - \lambda)\rho_\alpha. \quad (4.6.23)$$

For example if $\alpha = \frac{1}{2}$ the state ρ_b has the following eigenvalues:

$$\frac{1}{48}(11 - 9\lambda), \quad \frac{3 - \lambda}{48}(5\times), \quad \frac{11 + 7\lambda}{48}(2\times). \quad (4.6.24)$$

So the physical states on this ray end with $\lambda = \frac{11}{9}$ and this corresponding state is just on the facet $[\rho_{GHZ1-}, \rho_{GHZ1+}, \rho_d]$

$$\rho_b = \frac{11}{27}\rho_{GHZ1-} + \frac{11}{27}\rho_{GHZ1+} + \frac{5}{27}\rho_d \quad (4.6.25)$$

with eigenvalues

$$\frac{11}{27}(2\times), \frac{1}{27}(5\times) \text{ and } 0. \quad (4.6.26)$$

This again shows that the physical states can only be inside the "magic" polytope. As soon as we reach the border, at least one eigenvalue turns zero and obtains negative values outside.

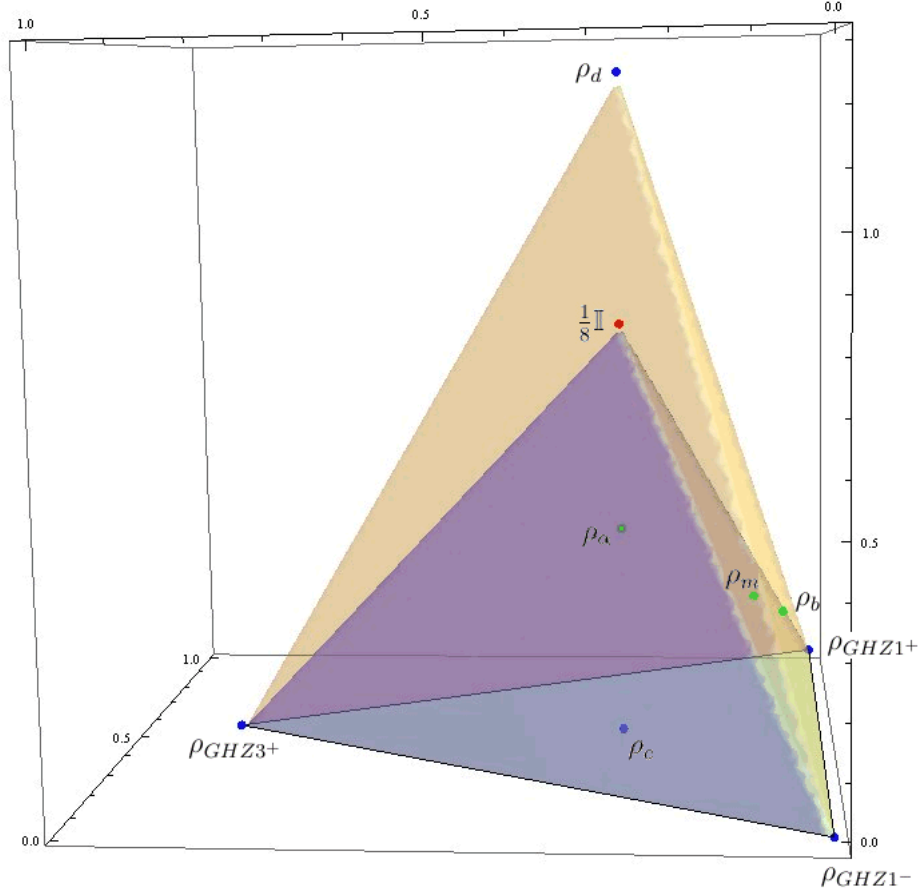


Figure 4.17: Part of the magic simplex of 3 GHZ states and their "opposite"

4.6.4 Entanglement in the magic simplex

Entanglement classification for mixed states being very difficult, we suggest a method to find entanglement types at least for some special cases in the simplex of the entangled entanglement simplex.

According to section 4.5.2 it is possible to map the $\rho_{GHZi\pm}$ to ρ_{GHZ} via local unitary transformations. For some pairs of states $\rho_{GHZi\pm}$ a common local unitary transformation $U = U_A \otimes U_B \otimes U_C$ can be found that transforms these states to the pair ρ_{GHZ} and ρ_{GHZ-}

Example 4.6.3 *Of the eight states with entangled entanglement there are four pairs of states that can be converted to the pair ρ_{GHZ} and ρ_{GHZ-} .*

With local unitaries $U = U_A \otimes U_B \otimes U_C$, the following transformations can be executed

$$\begin{array}{ccc} U_{03} \otimes U_{03} \otimes U_{03} & & \\ \rho_{GHZ1-} & \rightarrow & \rho_{GHZ} \\ \rho_{GHZ3+} & \rightarrow & \rho_{GHZ-}, \end{array} \quad (4.6.27)$$

$$\begin{array}{ccc} U_{03} \otimes U_{04} \otimes U_{03} & & \\ \rho_{GHZ2-} & \rightarrow & \rho_{GHZ} \\ \rho_{GHZ4+} & \rightarrow & \rho_{GHZ-}, \end{array} \quad (4.6.28)$$

$$\begin{array}{ccc} U_{03} \otimes U_{04} \otimes U_{08} & & \\ \rho_{GHZ3-} & \rightarrow & \rho_{GHZ} \\ \rho_{GHZ1+} & \rightarrow & \rho_{GHZ-}, \end{array} \quad (4.6.29)$$

$$\begin{array}{ccc} U_{03} \otimes U_{03} \otimes U_{08} & & \\ \rho_{GHZ4-} & \rightarrow & \rho_{GHZ} \\ \rho_{GHZ2+} & \rightarrow & \rho_{GHZ-}, \end{array} \quad (4.6.30)$$

This means: Using the same transformation $U = U_{03} \otimes U_{03} \otimes U_{03}$ for ρ_{GHZ1-} and ρ_{GHZ3+} , we obtain

$$\begin{aligned} U |GHZ1-\rangle \langle GHZ1-| U^\dagger &= |GHZ\rangle \langle GHZ| \\ U |GHZ3+\rangle \langle GHZ3+| U^\dagger &= |GHZ-\rangle \langle GHZ-| \end{aligned} \quad (4.6.31)$$

From that we deduce that we can also identify every state in the triangle $(\frac{1}{8}\mathbb{I}, \rho_{GHZ1-}, \rho_{GHZ3+})$ with a corresponding state in the triangle $(\frac{1}{8}\mathbb{I}, \rho_{GHZ}, \rho_{GHZ-})$ from [65].

$$a_1 \frac{1}{8}\mathbb{I} + a_2 \rho_{GHZ1-} + a_3 \rho_{GHZ3+} \xrightarrow{U} a_1 \frac{1}{8}\mathbb{I} + a_2 \rho_{GHZ} + a_3 \rho_{GHZ-} \quad (4.6.32)$$

The local unitary mapping between these states should not change their entanglement type, so that we can identify mixed states from the first triangle of entangled entanglement states to states from the Fig. 2 in the Eltschka/Siewert paper [65], where areas for the different types of entanglement classes are specified and infer the same type of entanglement for our mixed states.

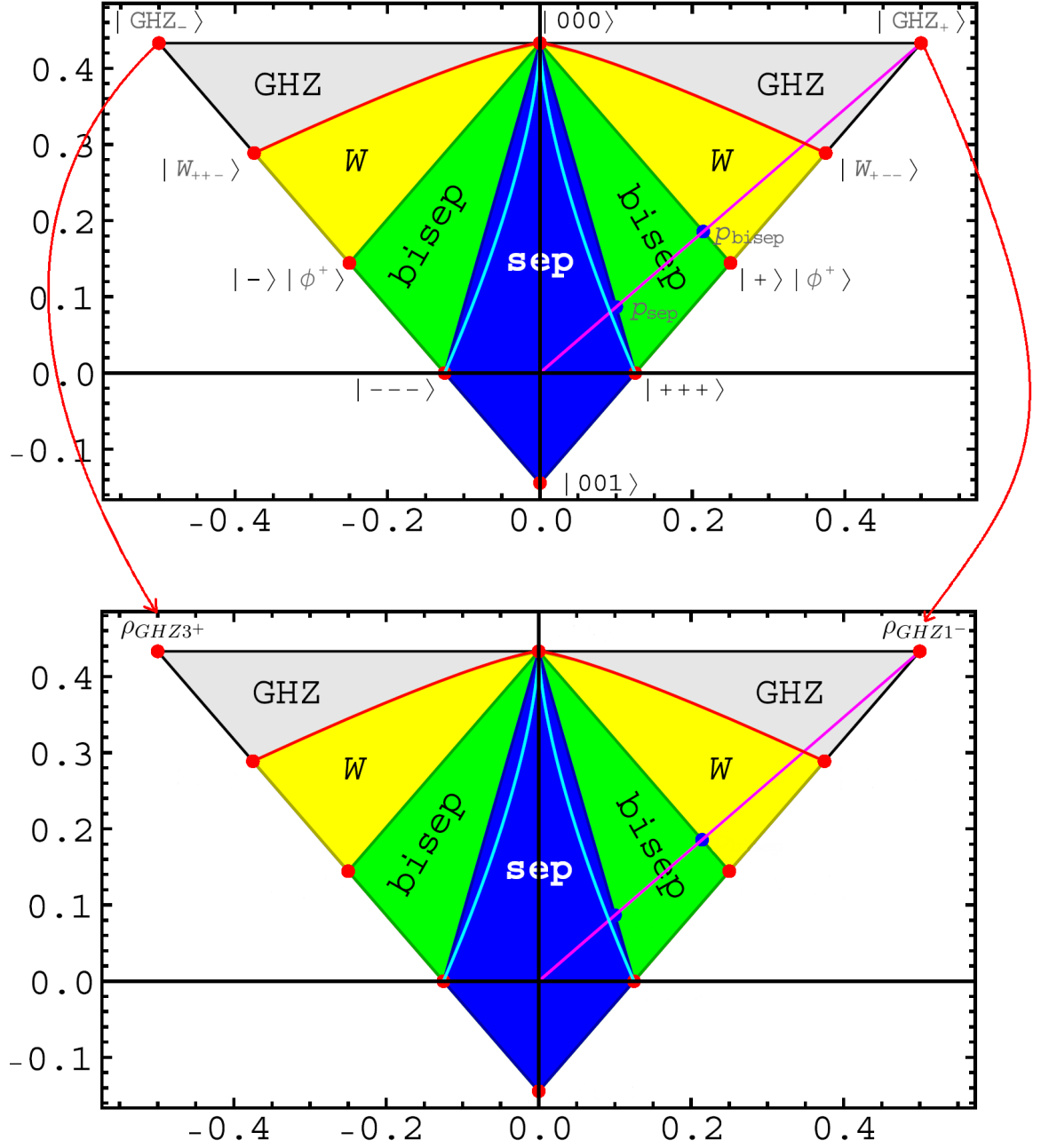


Figure 4.18: Correspondence of states in the entangled entanglement simplex and the entanglement classes from [65]

Example 4.6.4 *Werner like states*

$$\rho_{WS}^{1-} = p |GHZ1^-\rangle \langle GHZ1^-| + \frac{1-p}{8} \mathbb{I} \quad (4.6.33)$$

can then be identified with the corresponding generalized Werner states $\rho_{WS} = p |GHZ\rangle \langle GHZ| + \frac{1-p}{8} \mathbb{I}$ in [65] via the above unitary transformation. Therefore assigning the same separation values for p at the regions separating separable, bi-separable, W and GHZ states:

$$\begin{aligned} \rho_{WS}^{1-} \text{ separable for} & \quad 0 \leq p \leq \frac{1}{5} \\ \rho_{WS}^{1-} \text{ bi-separable for} & \quad \frac{1}{5} < p \leq \frac{3}{7} \\ \rho_{WS}^{1-} \text{ } W \text{ state for} & \quad \frac{3}{7} < p \leq 0.6955427... \\ \rho_{WS}^{1-} \text{ } GHZ \text{ state for} & \quad 0.6955427... < p \leq 1 \end{aligned}$$

Chapter 5

Conclusion

Entanglement being one of the most important properties of quantum systems, considerable work has been done in this field. Bipartite and especially bipartite qubit states are quite well studied. A very powerful criterion, the PPT criterion, exists for 2×2 and 2×3 states, that can exactly discriminate between separable and entangled states. For higher dimensions and multipartite states we still have no such general tool, although for some special cases and some families of states, entanglement properties can successfully be detected.

This work is concentrated on tripartite qubit states. Three qubit states have a much richer entanglement structure than two qubit states and so many of the well known entanglement measures for bipartite states cannot be used, at least not in the usual way. Nevertheless in the last years entanglement measures, also for the multipartite case, have been developed. We have studied some of these entanglement measures especially for generalized GHZ and W states.

Using symmetries is investigated and for GHZ symmetric states it is possible to determine the entanglement status, even giving border lines or regions for the different types of entanglement.

Also due to richer possibilities in the tripartite case we had the possibility to study the entanglement of entangled states and some of their geometrical structures. In a similar way as for two qubit states the geometrical structure of simplices plays a central role with maximally entangled states at their corners and the maximally mixed state in the center. Local unitary transformations applied to these simplices reveal another interesting symmetry: after three applications – similar to a rotation – we again recover the original states.

The notion of entangled entanglement can be inductively generalized to generate many-particle GHZ type states in a very easy and constructive way. We use some

of our basis states similar to building blocks, entangle them in a special way and obtain GHZ type states for arbitrary many particles.

Finally the Bloch representation for these tripartite states was established. This kind of representation is in general much more complicated in its structure compared to the bipartite case, but nevertheless gave us some interesting, especially geometrical insights.

The GHZ type states being very important for many applications in quantum information, certainly much more investigation will be effectuated in the near future. The investigations in this work are only very small glimpses in a very wide field and the situation somehow feels like in the old indian story of the blind men and the elephant. A group of blind men touch an elephant on different parts of his body. Every man now tells a different story of how the elephant feels, having touched only a small part. Like them we only have partial information and not yet a view of the whole situation!

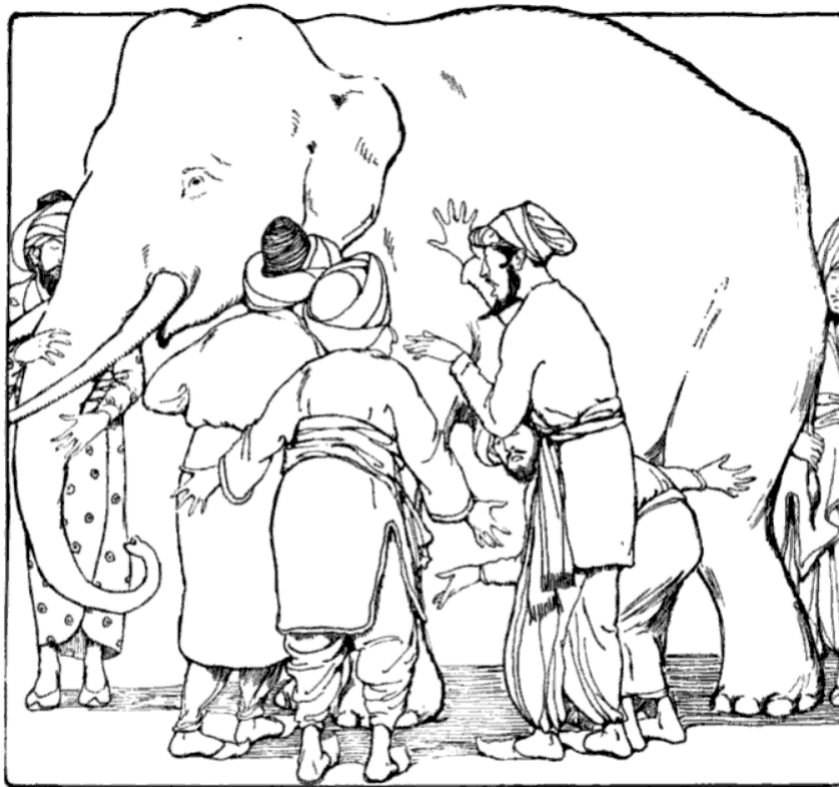


Figure 5.1: The blind men and the elephant
(Source: Martha Adelaide Holton & Charles Madison Curry, Holton-Curry readers, Rand McNally & Co. (Chicago), p. 108, Illustrator unknown, 1914)

Appendix A

Mathematica Tool

To calculate the Bloch representation of $2 \times 2 \times 2$ states, the following Mathematica tool is sometimes useful.

The density matrix of the state for which we want to evaluate the Bloch representation is submitted to a variable called "state".

The Bloch basis consists of the Pauli matrices and the identity matrix in the following notation

$$\sigma_1 = \begin{pmatrix} 0 & 1 \\ 1 & 0 \end{pmatrix}, \sigma_2 = \begin{pmatrix} 0 & -i \\ i & 0 \end{pmatrix}, \sigma_3 = \begin{pmatrix} 1 & 0 \\ 0 & -1 \end{pmatrix}, \sigma_4 = \mathbb{I} = \begin{pmatrix} 1 & 0 \\ 0 & 1 \end{pmatrix} \quad (\text{A.0.1})$$

By pressing the Button "Evaluate" the calculation is started and the representation of the state in the following form

$$\rho = \frac{1}{8} \sum_{i=1}^4 \sum_{j=1}^4 \sum_{k=1}^4 t_{ijk} \cdot \sigma_i \otimes \sigma_j \otimes \sigma_k \quad (\text{A.0.2})$$

is calculated.

The coefficients are given in four matrices in the following way:

The first matrix consists of the coefficients t_{ij1} , the second of t_{ij2} and so on. For the example in Figure A.1, which denotes the state ρ_{GHZ1+} , this means:

$$\begin{aligned} \rho_{GHZ1+} = & \left(\begin{array}{l} \sigma_1 \otimes \sigma_3 \otimes \sigma_1 - \sigma_3 \otimes \sigma_1 \otimes \sigma_1 - \\ \sigma_2 \otimes \sigma_4 \otimes \sigma_2 + \sigma_4 \otimes \sigma_2 \otimes \sigma_2 + \\ \sigma_1 \otimes \sigma_1 \otimes \sigma_3 + \sigma_3 \otimes \sigma_3 \otimes \sigma_3 - \\ \sigma_2 \otimes \sigma_2 \otimes \sigma_4 + \sigma_4 \otimes \sigma_4 \otimes \sigma_4 \end{array} \right) / 8 \end{aligned} \quad \begin{array}{l} \text{from the first matrix} \\ \text{from the second matrix} \\ \text{from the third matrix} \\ \text{from the fourth matrix} \end{array} \quad (\text{A.0.3})$$

In[1]:= (*
 Bloch decomposition for qubit states. Used basis are Pauli matrices.
 *)

$$\text{state} = \begin{pmatrix} \frac{1}{4} & 0 & 0 & -\frac{1}{4} & 0 & \frac{1}{4} & \frac{1}{4} & 0 \\ 0 & 0 & 0 & 0 & 0 & 0 & 0 & 0 \\ 0 & 0 & 0 & 0 & 0 & 0 & 0 & 0 \\ -\frac{1}{4} & 0 & 0 & \frac{1}{4} & 0 & -\frac{1}{4} & -\frac{1}{4} & 0 \\ 0 & 0 & 0 & 0 & 0 & 0 & 0 & 0 \\ \frac{1}{4} & 0 & 0 & -\frac{1}{4} & 0 & \frac{1}{4} & \frac{1}{4} & 0 \\ \frac{1}{4} & 0 & 0 & -\frac{1}{4} & 0 & \frac{1}{4} & \frac{1}{4} & 0 \\ 0 & 0 & 0 & 0 & 0 & 0 & 0 & 0 \end{pmatrix};$$

Out[2]=

EVALUATE

Out[5]= General state $\rightarrow \frac{1}{8} \left\{ \sum_{i=1}^4 \sum_{j=1}^4 \sum_{k=1}^4 t_{ijk} \sigma_i \otimes \sigma_j \otimes \sigma_k \right\}$

Out[8]= Bloch basis \rightarrow

$\begin{pmatrix} 0 & 1 \\ 1 & 0 \end{pmatrix}$	$\begin{pmatrix} 0 & -i \\ i & 0 \end{pmatrix}$
$\begin{pmatrix} 1 & 0 \\ 0 & -1 \end{pmatrix}$	$\begin{pmatrix} 1 & 0 \\ 0 & 1 \end{pmatrix}$

Out[10]= Given state \rightarrow

$$\begin{pmatrix} \frac{1}{4} & 0 & 0 & -\frac{1}{4} & 0 & \frac{1}{4} & \frac{1}{4} & 0 \\ 0 & 0 & 0 & 0 & 0 & 0 & 0 & 0 \\ 0 & 0 & 0 & 0 & 0 & 0 & 0 & 0 \\ -\frac{1}{4} & 0 & 0 & \frac{1}{4} & 0 & -\frac{1}{4} & -\frac{1}{4} & 0 \\ 0 & 0 & 0 & 0 & 0 & 0 & 0 & 0 \\ \frac{1}{4} & 0 & 0 & -\frac{1}{4} & 0 & \frac{1}{4} & \frac{1}{4} & 0 \\ \frac{1}{4} & 0 & 0 & -\frac{1}{4} & 0 & \frac{1}{4} & \frac{1}{4} & 0 \\ 0 & 0 & 0 & 0 & 0 & 0 & 0 & 0 \end{pmatrix}$$

Out[19]= Coefficients f. k=1, 2, 3, 4 \rightarrow

$\begin{pmatrix} 0 & 0 & 1 & 0 \\ 0 & 0 & 0 & 0 \\ -1 & 0 & 0 & 0 \\ 0 & 0 & 0 & 0 \end{pmatrix}$	$\begin{pmatrix} 0 & 0 & 0 & 0 \\ 0 & 0 & 0 & -1 \\ 0 & 0 & 0 & 0 \\ 0 & 1 & 0 & 0 \end{pmatrix}$	$\begin{pmatrix} 1 & 0 & 0 & 0 \\ 0 & 0 & 0 & 0 \\ 0 & 0 & 1 & 0 \\ 0 & 0 & 0 & 0 \end{pmatrix}$	$\begin{pmatrix} 0 & 0 & 0 & 0 \\ 0 & -1 & 0 & 0 \\ 0 & 0 & 0 & 0 \\ 0 & 0 & 0 & 1 \end{pmatrix}$
---	---	--	---

Out[21]= Normalization \rightarrow State is Normalized

Figure A.1: User Interface of a Mathematica tool for Bloch representation of a 2x2x2 state

```
Cell[BoxData[{
RowBox[{"Button", "[",
RowBox[{"\"\\<EVALUATE\\>\"", ",",
RowBox[{"FrontEndExecute", "[",
RowBox[{"{",
RowBox[{"
RowBox[{"
RowBox[{"FrontEnd`NotebookFind", "[",
RowBox[{"
RowBox[{"FrontEnd`InputNotebook", "[", "]", "}], ",", "\"\\<Input\\>\"",
",", "All", ",", "CellStyle"}], "]", "}], ",",
RowBox[{"FrontEndToken", "[",
RowBox[{"
RowBox[{"FrontEnd`InputNotebook", "[", "]", "}], ",",
"\"\\<EvaluateCells\\>\"", "]", "}]"]], "}]"]], "]", "}], ",",
RowBox[{"Active", "->", "True"}], ",",
RowBox[{"ImageSize", "->",
RowBox[{"{",
RowBox[{"100", ",", "50"}], "}]"]}], "\n",
RowBox[{"
RowBox[{"
RowBox[{"T", "[",
RowBox[{"x_", ",", "y_"}], "]", "="},
RowBox[{"KroneckerProduct", "[",
RowBox[{"x", ",", "y"}], "]", ";"}], "\n",
RowBox[{"
RowBox[{"
RowBox[{"T3", "[",
RowBox[{"x_", ",", "y_", ",", "z_"}], "]", "="},
RowBox[{"KroneckerProduct", "[",
RowBox[{"x", ",",
RowBox[{"KroneckerProduct", "[",
RowBox[{"y", ",", "z"}], "]", "}]"]], ";"}], "\n",
RowBox[{"HoldForm", "[",
RowBox[{"Style", "[",
RowBox[{"
RowBox[{"\"\\<General state\\>\"", "->",
RowBox[{"
FractionBox["1", "8"], " ",
```



```

        RowBox[{"-", "I"}]}}], "}"}}], ",",
    RowBox[{"{"},
        RowBox[{"I", ",", "0"}] , "}"}}] , "}"}}] , ";" ,
RowBox[{
    RowBox[{"m", "[", "3", "]" }], "=",
    RowBox[{"{",
        RowBox[{
            RowBox[{"{",
                RowBox[{"1", ",", "0"}] , "}"}}], ",",
            RowBox[{"{",
                RowBox[{"0", ",",
                    RowBox[{"-", "1"}]}}] , "}"}}] , "}"}}] , ";" }], "\n",
RowBox[{
    RowBox[{"temp", "=",
        RowBox[{"Grid", "[",
            RowBox[{
                RowBox[{"{",
                    RowBox[{
                        RowBox[{"{",
                            RowBox[{
                                RowBox[{"MatrixForm", "[",
                                    RowBox[{"m", "[", "1", "]" }], "]" }], ",",
                                    RowBox[{"MatrixForm", "[",
                                        RowBox[{"m", "[", "2", "]" }], "]" }]]], "}"}}], ",",
                                RowBox[{"{",
                                    RowBox[{
                                        RowBox[{"MatrixForm", "[",
                                            RowBox[{"m", "[", "3", "]" }], "]" }], ",",
                                            RowBox[{"MatrixForm", "[",
                                                RowBox[{"m", "[", "4", "]" }], "]" }]]], "}"}}]]], "}"}}] , ",",
                                    RowBox[{"Frame", "->", "All"}]}}] , "]" }]]], ";" }], "\n",
RowBox[{"Style", "[",
    RowBox[{
        RowBox[{"\"<Bloch basis>\"", "->", "temp"}] , ",",
        RowBox[{"FontSize", "->", "20"}]}}] , "]" }], "\n",
RowBox[{
    RowBox[{"temp", "=",
        RowBox[{"MatrixForm", "[", "state", "]" }]]], ";" }], "\n",
RowBox[{"Style", "[",
    RowBox[{

```

```

RowBox[{"\"<Given state>\", "->", "temp"}], ",",
RowBox[{"FontSize", "->", "20"}]]], ""]], "\n",
RowBox[{
RowBox[{"allgZustand", "=",
RowBox[{
FractionBox["1", "8"], " ",
RowBox[{
UnderoverscriptBox["\[Sum]",
RowBox[{"i", "=", "1"}], "4"],
RowBox[{
UnderoverscriptBox["\[Sum]",
RowBox[{"j", "=", "1"}], "4"],
RowBox[{
UnderoverscriptBox["\[Sum]",
RowBox[{"k", "=", "1"}], "4"],
RowBox[{
RowBox[{"t", "[",
RowBox[{"i", "+",
RowBox[{"4", " ", "j"}], "+",
RowBox[{"16", " ", "k"}], "- ", "20"}], ""]], " ",
RowBox[{"T3", "[",
RowBox[{
RowBox[{"m", "[", "i", ""]}], ",",
RowBox[{"m", "[", "j", ""]}], ",",
RowBox[{"m", "[", "k", ""]}], ""]]]], ";"}], "\n",
RowBox[{
RowBox[{"temp", "=",
RowBox[{"Solve", "[",
RowBox[{
RowBox[{"allgZustand", "==", "state"}], ",",
RowBox[{"Array", "[",
RowBox[{"t", ",", "64"}], ""]}], ";"}], "\n",
RowBox[{
RowBox[{"sol", "=",
RowBox[{"FullSimplify", "[",
RowBox[{
RowBox[{"Array", "[",
RowBox[{"t", ",", "64"}], ""]], "/.", " ", "temp"}], ""]}], ";"}], "\n",
RowBox[{
RowBox[{"tmatrix1", "=",

```



```

RowBox[{"MatrixForm", "["],
RowBox[{"Table", "["],
RowBox[{
RowBox[{"sol", "["],
RowBox[{"1", ",",
RowBox[{"i", "+"},
RowBox[{"4", " ", "j"}], "-", "4"}]], "]]"], ",",
RowBox[{"{",
RowBox[{"i", ",", "1", ",", "4"}], "}"}, ",",
RowBox[{"{",
RowBox[{"j", ",", "1", ",", "4"}], "}"}}], "];", "\n",
RowBox[{
RowBox[{"tmatrix2", "="},
RowBox[{"MatrixForm", "["],
RowBox[{"Table", "["],
RowBox[{
RowBox[{"sol", "["],
RowBox[{"1", ",",
RowBox[{"i", "+"},
RowBox[{"4", " ", "j"}], "+", "12"}]], "]]"], ",",
RowBox[{"{",
RowBox[{"i", ",", "1", ",", "4"}], "}"}, ",",
RowBox[{"{",
RowBox[{"j", ",", "1", ",", "4"}], "}"}}], "];", "\n",
RowBox[{
RowBox[{"tmatrix3", "="},
RowBox[{"MatrixForm", "["],
RowBox[{"Table", "["],
RowBox[{
RowBox[{"sol", "["],
RowBox[{"1", ",",
RowBox[{"i", "+"},
RowBox[{"4", " ", "j"}], "+", "28"}]], "]]"], ",",
RowBox[{"{",
RowBox[{"i", ",", "1", ",", "4"}], "}"}, ",",
RowBox[{"{",
RowBox[{"j", ",", "1", ",", "4"}], "}"}}], "];", "\n",
RowBox[{
RowBox[{"tmatrix4", "="},
RowBox[{"MatrixForm", "["],

```

```

RowBox[{"Table", "["],
RowBox[{
RowBox[{"sol", "["],
RowBox[{"1", ",",
RowBox[{"i", "+",
RowBox[{"4", " ", "j"}], "+", "44"}]]], "]]"}], ",",
RowBox[{"{",
RowBox[{"i", ",", "1", ",", "4"}], "}"}, ",",
RowBox[{"{",
RowBox[{"j", ",", "1", ",", "4"}], "}"}, "]}], ";"}],
"\n",
RowBox[{
RowBox[{"temp", "="},
RowBox[{"Grid", "["],
RowBox[{
RowBox[{"{",
RowBox[{"{",
RowBox[{"tmatrix1", ",", "tmatrix2", ",", "tmatrix3", ",",
"tmatrix4"}], "}"}, "}"}, ",",
RowBox[{"Frame", "->", "All"}]]], "}"}, "}"}, ";"}], "\n",
RowBox[{"Style", "["],
RowBox[{
RowBox[{"\"\\<Coefficients f. k=1, 2, 3, 4 \>\"", "->", "temp"}], ",",
RowBox[{"FontSize", "->", "20"}]]], "}"}, "\n",
RowBox[{
RowBox[{"temp", "="},
RowBox[{"If", "["],
RowBox[{
RowBox[{
RowBox[{"sol", "["],
RowBox[{"1", ",", "64"}], "]]"}], "===", "1"}], ",",
"\"\\<State is Normalized\\>\"", ",",
RowBox[{"sol", "["],
RowBox[{"1", ",", "64"}], "]]"}]]], "}"}, "}"}, ";"}], "\n",
RowBox[{"Style", "["],
RowBox[{
RowBox[{"\"\\<Normalization\\>\"", "->", "temp"}], ",",
RowBox[{"FontSize", "->", "20"}]]], "}"}, "Input"

```

Appendix B

Unitary transformation matrices

The following 64 plus 16, therefore 80 unitary matrices were used to find suitable local unitary transformations in a fast and easy way. These might not describe entirely all possible cases, but proved to be a very useful subset.

$$\begin{array}{llll}
 U_{01} = \frac{1}{2} \begin{pmatrix} 1 & 1 \\ 1 & -1 \end{pmatrix} & U_{02} = \frac{1}{2} \begin{pmatrix} 1 & -1 \\ 1 & 1 \end{pmatrix} & U_{03} = \frac{1}{2} \begin{pmatrix} 1 & i \\ 1 & -i \end{pmatrix} & U_{04} = \frac{1}{2} \begin{pmatrix} 1 & -i \\ 1 & i \end{pmatrix} \\
 U_{05} = \frac{1}{2} \begin{pmatrix} 1 & 1 \\ -1 & 1 \end{pmatrix} & U_{06} = \frac{1}{2} \begin{pmatrix} 1 & -1 \\ -1 & 1 \end{pmatrix} & U_{07} = \frac{1}{2} \begin{pmatrix} 1 & i \\ -1 & i \end{pmatrix} & U_{08} = \frac{1}{2} \begin{pmatrix} 1 & -i \\ -1 & -i \end{pmatrix} \\
 U_{09} = \frac{1}{2} \begin{pmatrix} 1 & 1 \\ i & -i \end{pmatrix} & U_{10} = \frac{1}{2} \begin{pmatrix} 1 & -1 \\ i & i \end{pmatrix} & U_{11} = \frac{1}{2} \begin{pmatrix} 1 & i \\ i & 1 \end{pmatrix} & U_{12} = \frac{1}{2} \begin{pmatrix} 1 & -i \\ i & -1 \end{pmatrix} \\
 U_{13} = \frac{1}{2} \begin{pmatrix} 1 & 1 \\ -i & i \end{pmatrix} & U_{14} = \frac{1}{2} \begin{pmatrix} 1 & -1 \\ -i & -i \end{pmatrix} & U_{15} = \frac{1}{2} \begin{pmatrix} 1 & i \\ -i & -1 \end{pmatrix} & U_{16} = \frac{1}{2} \begin{pmatrix} 1 & -i \\ -i & 1 \end{pmatrix} \\
 U_{17} = \frac{1}{2} \begin{pmatrix} -1 & 1 \\ 1 & 1 \end{pmatrix} & U_{18} = \frac{1}{2} \begin{pmatrix} -1 & -1 \\ 1 & -1 \end{pmatrix} & U_{19} = \frac{1}{2} \begin{pmatrix} -1 & i \\ 1 & i \end{pmatrix} & U_{20} = \frac{1}{2} \begin{pmatrix} -1 & -i \\ 1 & -i \end{pmatrix} \\
 U_{21} = \frac{1}{2} \begin{pmatrix} -1 & 1 \\ -1 & -1 \end{pmatrix} & U_{22} = \frac{1}{2} \begin{pmatrix} -1 & -1 \\ -1 & 1 \end{pmatrix} & U_{23} = \frac{1}{2} \begin{pmatrix} -1 & i \\ -1 & -i \end{pmatrix} & U_{24} = \frac{1}{2} \begin{pmatrix} -1 & -i \\ -1 & i \end{pmatrix} \\
 U_{25} = \frac{1}{2} \begin{pmatrix} -1 & 1 \\ i & i \end{pmatrix} & U_{26} = \frac{1}{2} \begin{pmatrix} -1 & -1 \\ i & -i \end{pmatrix} & U_{27} = \frac{1}{2} \begin{pmatrix} -1 & i \\ i & -1 \end{pmatrix} & U_{28} = \frac{1}{2} \begin{pmatrix} -1 & -i \\ i & 1 \end{pmatrix} \\
 U_{29} = \frac{1}{2} \begin{pmatrix} -1 & 1 \\ -i & -i \end{pmatrix} & U_{30} = \frac{1}{2} \begin{pmatrix} -1 & -1 \\ -i & i \end{pmatrix} & U_{31} = \frac{1}{2} \begin{pmatrix} -1 & i \\ -i & 1 \end{pmatrix} & U_{32} = \frac{1}{2} \begin{pmatrix} -1 & -i \\ -i & -1 \end{pmatrix}
 \end{array}$$

$$\begin{aligned}
U_{33} &= \frac{1}{2} \begin{pmatrix} i & 1 \\ 1 & i \end{pmatrix} & U_{34} &= \frac{1}{2} \begin{pmatrix} i & -1 \\ 1 & -i \end{pmatrix} & U_{35} &= \frac{1}{2} \begin{pmatrix} i & i \\ 1 & -1 \end{pmatrix} & U_{36} &= \frac{1}{2} \begin{pmatrix} i & -i \\ 1 & 1 \end{pmatrix} \\
U_{37} &= \frac{1}{2} \begin{pmatrix} i & 1 \\ -1 & -i \end{pmatrix} & U_{38} &= \frac{1}{2} \begin{pmatrix} i & -1 \\ -1 & i \end{pmatrix} & U_{39} &= \frac{1}{2} \begin{pmatrix} i & i \\ -1 & 1 \end{pmatrix} & U_{40} &= \frac{1}{2} \begin{pmatrix} i & -i \\ -1 & -1 \end{pmatrix} \\
U_{41} &= \frac{1}{2} \begin{pmatrix} i & 1 \\ i & -1 \end{pmatrix} & U_{42} &= \frac{1}{2} \begin{pmatrix} i & -1 \\ i & 1 \end{pmatrix} & U_{43} &= \frac{1}{2} \begin{pmatrix} i & i \\ i & -i \end{pmatrix} & U_{44} &= \frac{1}{2} \begin{pmatrix} i & -i \\ i & i \end{pmatrix} \\
U_{45} &= \frac{1}{2} \begin{pmatrix} i & 1 \\ -i & 1 \end{pmatrix} & U_{46} &= \frac{1}{2} \begin{pmatrix} i & -1 \\ -i & -1 \end{pmatrix} & U_{47} &= \frac{1}{2} \begin{pmatrix} i & i \\ -i & i \end{pmatrix} & U_{48} &= \frac{1}{2} \begin{pmatrix} i & -i \\ -i & -i \end{pmatrix} \\
U_{49} &= \frac{1}{2} \begin{pmatrix} -i & 1 \\ 1 & -i \end{pmatrix} & U_{50} &= \frac{1}{2} \begin{pmatrix} -i & -1 \\ 1 & i \end{pmatrix} & U_{51} &= \frac{1}{2} \begin{pmatrix} -i & i \\ 1 & 1 \end{pmatrix} & U_{52} &= \frac{1}{2} \begin{pmatrix} -i & -i \\ 1 & -1 \end{pmatrix} \\
U_{53} &= \frac{1}{2} \begin{pmatrix} -i & 1 \\ -1 & i \end{pmatrix} & U_{54} &= \frac{1}{2} \begin{pmatrix} -i & -1 \\ -1 & -i \end{pmatrix} & U_{55} &= \frac{1}{2} \begin{pmatrix} -i & i \\ -1 & -1 \end{pmatrix} & U_{56} &= \frac{1}{2} \begin{pmatrix} -i & -i \\ -1 & 1 \end{pmatrix} \\
U_{57} &= \frac{1}{2} \begin{pmatrix} -i & 1 \\ i & 1 \end{pmatrix} & U_{58} &= \frac{1}{2} \begin{pmatrix} -i & -1 \\ i & -1 \end{pmatrix} & U_{59} &= \frac{1}{2} \begin{pmatrix} -i & i \\ i & i \end{pmatrix} & U_{60} &= \frac{1}{2} \begin{pmatrix} -i & -i \\ i & -i \end{pmatrix} \\
U_{61} &= \frac{1}{2} \begin{pmatrix} -i & 1 \\ -i & -i \end{pmatrix} & U_{62} &= \frac{1}{2} \begin{pmatrix} -i & -1 \\ -i & 1 \end{pmatrix} & U_{63} &= \frac{1}{2} \begin{pmatrix} -i & i \\ -i & -i \end{pmatrix} & U_{64} &= \frac{1}{2} \begin{pmatrix} -i & -i \\ -i & i \end{pmatrix} \\
U_{65} &= \begin{pmatrix} 1 & 0 \\ 0 & 1 \end{pmatrix} & U_{66} &= \begin{pmatrix} 1 & 0 \\ 0 & -1 \end{pmatrix} & U_{67} &= \begin{pmatrix} -1 & 0 \\ 0 & 1 \end{pmatrix} & U_{68} &= \begin{pmatrix} -1 & 0 \\ 0 & -1 \end{pmatrix} \\
U_{69} &= \begin{pmatrix} 0 & 1 \\ 1 & 0 \end{pmatrix} & U_{70} &= \begin{pmatrix} 0 & 1 \\ -1 & 0 \end{pmatrix} & U_{71} &= \begin{pmatrix} 0 & -1 \\ 1 & 0 \end{pmatrix} & U_{72} &= \begin{pmatrix} 0 & -1 \\ -1 & 0 \end{pmatrix} \\
U_{73} &= \begin{pmatrix} i & 0 \\ 0 & i \end{pmatrix} & U_{74} &= \begin{pmatrix} i & 0 \\ 0 & -i \end{pmatrix} & U_{75} &= \begin{pmatrix} -i & 0 \\ 0 & i \end{pmatrix} & U_{76} &= \begin{pmatrix} -i & 0 \\ 0 & -i \end{pmatrix} \\
U_{77} &= \begin{pmatrix} 0 & i \\ i & 0 \end{pmatrix} & U_{78} &= \begin{pmatrix} 0 & i \\ -i & 0 \end{pmatrix} & U_{79} &= \begin{pmatrix} 0 & -i \\ i & 0 \end{pmatrix} & U_{80} &= \begin{pmatrix} 0 & -i \\ -i & 0 \end{pmatrix}
\end{aligned}$$

Appendix C

Bloch representation and pure states

In section 4.6.2 the representation of states of the form (n number of particles)

$$\rho = \frac{1}{8}(\mathbb{I}^{\otimes n} + a\sigma_x^{\otimes n} + b\sigma_y^{\otimes n} + c\sigma_z^{\otimes n})$$

was discussed.

We can easily represent these states as density matrices for different cases:

1. $n = 4k, k \in \mathbb{N}$

$$\rho = \begin{pmatrix} 1+c & 0 & \cdots & \cdots & \cdots & \cdots & 0 & a+b \\ 0 & 1-c & \cdots & \cdots & \cdots & \cdots & a-b & 0 \\ \vdots & & \ddots & & & & & \vdots \\ \vdots & & & 1-c & a-b & & & \vdots \\ \vdots & & & a-b & 1-c & & & \vdots \\ \vdots & & \ddots & & & \ddots & & \vdots \\ 0 & a-b & \cdots & \cdots & \cdots & \cdots & 1-c & 0 \\ a+b & 0 & \cdots & \cdots & \cdots & \cdots & 0 & 1+c \end{pmatrix}$$

2. $n = 4k + 1, k \in \mathbb{N}$

$$\rho = \begin{pmatrix} 1+c & 0 & \cdots & \cdots & \cdots & \cdots & 0 & a+ib \\ 0 & 1-c & \cdots & \cdots & \cdots & \cdots & a-ib & 0 \\ \vdots & & \ddots & & & & \ddots & \vdots \\ \vdots & & & 1+c & a-ib & & & \vdots \\ \vdots & & & a+ib & 1-c & & & \vdots \\ \vdots & & \ddots & & & \ddots & & \vdots \\ 0 & a+ib & \cdots & \cdots & \cdots & \cdots & 1+c & 0 \\ a-ib & 0 & \cdots & \cdots & \cdots & \cdots & 0 & 1-c \end{pmatrix}$$

3. $n = 4k + 2, k \in \mathbb{N}$

$$\rho = \begin{pmatrix} 1+c & 0 & \cdots & \cdots & \cdots & \cdots & 0 & a-b \\ 0 & 1-c & \cdots & \cdots & \cdots & \cdots & a+b & 0 \\ \vdots & & \ddots & & & & \ddots & \vdots \\ \vdots & & & 1-c & a+b & & & \vdots \\ \vdots & & & a+b & 1-c & & & \vdots \\ \vdots & & \ddots & & & \ddots & & \vdots \\ 0 & a+b & \cdots & \cdots & \cdots & \cdots & 1-c & 0 \\ a-b & 0 & \cdots & \cdots & \cdots & \cdots & 0 & 1+c \end{pmatrix}$$

4. $n = 4k + 3, k \in \mathbb{N}$

$$\rho = \begin{pmatrix} 1+c & 0 & \cdots & \cdots & \cdots & \cdots & 0 & a-ib \\ 0 & 1-c & \cdots & \cdots & \cdots & \cdots & a+ib & 0 \\ \vdots & & \ddots & & & & \ddots & \vdots \\ \vdots & & & 1+c & a+ib & & & \vdots \\ \vdots & & & a-ib & 1-c & & & \vdots \\ \vdots & & \ddots & & & \ddots & & \vdots \\ 0 & a-ib & \cdots & \cdots & \cdots & \cdots & 1+c & 0 \\ a+ib & 0 & \cdots & \cdots & \cdots & \cdots & 0 & 1-c \end{pmatrix}$$

We obtain different factors in the characteristic polynome and from there can calculate the eigenvalues for the four cases. The factors and eigenvalues are of the following form:

1. $n = 4k, k \in \mathbb{N}$: Factors $(\frac{1+c}{2^n} - \lambda)^2 - (\frac{a+b}{2^n})^2$ and $(\frac{1-c}{2^n} - \lambda)^2 - (\frac{a-b}{2^n})^2$
 Eigenvalues: $\lambda = \frac{1+c \pm (a+b)}{2^n}$ or $\lambda = \frac{1-c \pm (a-b)}{2^n}$, giving us finally four different eigenvalues
 $\lambda_1 = \frac{1}{2^n}(1 + a + b + c), \lambda_2 = \frac{1}{2^n}(1 - a - b + c),$
 $\lambda_3 = \frac{1}{2^n}(1 + a - b - c), \lambda_4 = \frac{1}{2^n}(1 - a + b - c)$
2. $n = 4k + 2, k \in \mathbb{N}$ Factors $(\frac{1+c}{2^n} - \lambda)^2 - (\frac{a-b}{2^n})^2$ and $(\frac{1-c}{2^n} - \lambda)^2 - (\frac{a+b}{2^n})^2$
 Eigenvalues: $\lambda = \frac{1+c \pm (a-b)}{2^n}$ or $\lambda = \frac{1-c \pm (a+b)}{2^n}$, giving us again four different eigenvalues
 $\lambda_1 = \frac{1}{2^n}(1 + a - b + c), \lambda_2 = \frac{1}{2^n}(1 - a + b + c),$
 $\lambda_3 = \frac{1}{2^n}(1 + a + b - c), \lambda_4 = \frac{1}{2^n}(1 - a - b - c)$
3. $n = 4k+1, k \in \mathbb{N}$ and $n = 4k+3, k \in \mathbb{N}$ have the same factors and eigenvalues
 All factors are of the form $(\frac{1+c}{2^n} - \lambda)(\frac{1-c}{2^n} - \lambda) - (\frac{a+ib}{2^n})(\frac{a-ib}{2^n})$, therefore the characteristic polynome is

$$\lambda^2 - \frac{1}{2^{n-1}} \cdot \lambda + \frac{1 - a^2 - b^2 - c^2}{2^n} = 0$$

Eigenvalues: $\lambda_{1,2} = \frac{1}{2^n} \pm \frac{1}{2^n} \sqrt{a^2 + b^2 + c^2}$, giving us two different eigenvalues in this case.

From the above results we conclude, ensuring that the eigenvalues are non negative, that we obtain the following geometrical representations

1. $n = 4k, k \in \mathbb{N}$: A tetrahedron with constraints
 $1 + a + b + c \geq 0, 1 - a - b + c \geq 0,$
 $1 + a - b - c \geq 0, 1 - a + b - c \geq 0$
2. $n = 4k + 2, k \in \mathbb{N}$: A tetrahedron with constraints
 $1 + a - b + c \geq 0, 1 - a + b + c \geq 0,$
 $1 + a + b - c \geq 0, 1 - a - b - c \geq 0$
3. $n = 4k + 1, k \in \mathbb{N}$ and $n = 4k + 3, k \in \mathbb{N}$:
 The ball $\sqrt{a^2 + b^2 + c^2} \leq 1$

List of Figures

2.1	Bloch sphere (image from Wikimedia commons)	7
3.1	Schematic picture of the set of all states with the set of separable states as a convex subset. It should be stressed that the extremal points of the set of separable states (the pure product states), are also extremal points of the set of all physical states (taken from Gühne/Toth's review article [17])	15
3.2	Schematic overview for an entanglement witness. The nearest separable state is ρ_0 and the optimal entanglement witness A_{opt}	25
3.3	Source emitting two particles, from [7] (slightly adapted)	27
3.4	Magic tetrahedron	30
4.1	Types of tripartite entanglement after [47]	34
4.2	Graphic representation of entanglement types in pure states of three-qubit systems	36
4.3	Graphic representation of entanglement types in mixed states of three-qubit systems	36
4.4	Entropy (blue), 3-tangle (red), concurrence (yellow) and negativity (green) of the generalized GHZ state	41
4.5	Arithmetic (blue) and geometric mean (red) entropy of generalized GHZ states	42
4.6	a) Arithmetic and b) geometric mean entropy of generalized W states . .	43
4.7	Values of the local entropies S_A, S_B, S_C and the 3-tangle τ_3 for different classes of tripartite states (after [48])	44
4.8	Values of the concurrence for the generalized W state $ W_{\alpha_1, \alpha_2, \alpha_3}\rangle = \alpha_1 100\rangle + \alpha_2 010\rangle + \alpha_3 001\rangle$ with $0 \leq \alpha_1, \alpha_2 \leq 1, \alpha_3 = \sqrt{1 - \alpha_1^2 - \alpha_2^2}$.	46

4.9	Entropy (blue) and negativity (red) of generalized W states for $0 \leq \alpha_1 \leq 1$	47
4.10	Entanglement witness (equation 4.4.30) (blue) and entropy (red) of the generalized GHZ states for $0 \leq \theta \leq \pi$	49
4.11	x-y representation of GHZ-symmetric states (figure from [65])	50
4.12	Illustration (projection into a subspace) for states in- and outside the simplex \mathbb{S}	57
4.13	Tetrahedron of physical states and ball of pure states for two qubits	63
4.14	Ball of physical states and ball of pure states for three qubits	64
4.15	Tetrahedron of physical states and ball of pure states for four qubits	65
4.16	Magic simplex of 4 GHZ states with entangled entanglement	69
4.17	Part of the magic simplex of 3 GHZ states and their "opposite"	71
4.18	Correspondence of states in the entangled entanglement simplex and the entanglement classes from [65]	73
5.1	The blind men and the elephant (Source: Martha Adelaide Holton & Charles Madison Curry, Holton-Curry readers, Rand McNally & Co. (Chicago), p. 108, Illustrator unknown, 1914)	76
A.1	User Interface of a Mathematica tool for Bloch representation of a 2x2x2 state	78

Bibliography

- [1] D.M. Greenberger, M.A. Horne, A. Zeilinger *Going Beyond Bell's Theorem*, in: M. Kafatos (ed.), *Bells Theorem, Quantum Theory, and Conception of the Universe*, Kluwer Academic, 6972 (1989)
- [2] K. Yang, L. Huang, W. Yang, F. Song *Quantum Teleportation via GHZ-like State*, Int. J. Theor. Phys. 48, 516521 (2009)
- [3] C.-Y. Lu, T. Yang, J.-W. Pan *Experimental Multiparticle Entanglement Swapping for Quantum Networking*, Phys. Rev. Let. 103, 020501 (2009)
- [4] D. Gottesmann, I.L. Chuang *Demonstrating the viability of universal quantum computation using teleportation and single-qubit operations*, Nature 402, 390-393 (1999)
- [5] K. Chen, H.-K. Lo *Multi-partite quantum cryptographic protocols with noisy GHZ states*, Quantum Information and Computation 7, 689-715 (2007)
- [6] D. Bouwmeester, J.-W. Pan, M. Daniell, H. Weinfurter, A. Zeilinger *Observation of Three-Photon Greenberger-Horne-Zeilinger Entanglement*, Phys. Rev. Let. 82, Nr. 7, 1345 (1999)
- [7] D.M. Greenberger, M. Horne, A. Shimony, A. Zeilinger *Bells Theorem without inequalities*, Am. J. of Phys. 58 (12), 1131 (1990)
- [8] A.I. Solomon, C.-L. Ho *Condition for tripartite entanglement*, Journal of Physics: Conference Series 343, 012114 (2012)
- [9] M.B. Plenio, S. Virmani *An introduction to entanglement measures*, Quantum Information and Computation 7, 1-51 (2007)
- [10] D.J. Griffiths *Introduction to Quantum Mechanics*, Pearson Prentice Hall (2005).
- [11] K. Blum *Density Matrix Theory and Applications*, Springer (1996)

- [12] R.B. Griffiths *Consistent Quantum Theory*, Cambridge University Press (2002).
- [13] G.H. Golub, C.F. Van Loan *Matrix Computations*, Johns Hopkins University Press (1996)
- [14] M.A.Nielsen, I.L. Chuang *Quantum Computation and Quantum Information*, Cambridge University Press (2000)
- [15] J.H. Eberly *Schmidt Analysis of Pure-State Entanglement* Laser Physics 16, 921–926 (2006)
- [16] L. Gurvits *Classical complexity and quantum entanglement*, J. of Computer and System Sciences 69, pp. 448–484 (2004)
- [17] O. Gühne, G. Tóth *Entanglement detection*, Physics Reports 474, 1 (2009)
- [18] R.F. Werner *Quantum states with Einstein-Podolsky-Rosen correlations admitting a hidden-variable model*, Physical Review A 40 (8), 42774281 (1989)
- [19] M. Horodecki, P. Horodecki, R. Horodecki *Reduction criterion of separability and limits for a class of distillation protocols*, Phys. Rev. A 59, 4206–4216 (1999)
- [20] A. Peres *Separability criterion for density matrices*, Phys. Rev. Lett. 77, 1413 (1996)
- [21] M. Horodecki, P. Horodecki, R. Horodecki *Separability of mixed states: necessary and sufficient conditions*, Phys. Lett. 223, 1–8 (1996)
- [22] D. Bruß, C. Macchiavello *How the First Partial Transpose was Written*, Found. Phys. 35, Nr 11, 1921-1926, (2005)
- [23] V. Vedral, M.B. Plenio, M.A. Rippin, P.L. Knight *Quantifying Entanglement*, Phys. Rev. Lett. 78, 2275 (1997)
- [24] D. Bruß *Characterizing entanglement* J. Math. Phys., Vol. 43, No. 9, 4237–4251 (2002)
- [25] A. Gabriel *Quantum Entanglement and Geometry*, Diploma Thesis, University of Vienna (2009)
- [26] C.H. Bennett, D.P. Di Vincenzo, J.A. Smolin, W.K. Wootters *Mixed-state entanglement and quantum error correction*, Phys. Rev. A 54, No. 5, 3824–3851 (1996)

- [27] W.K. Wootters, *Entanglement of Formation of an Arbitrary State of Two Qubits*, Phys. Rev. Lett. 80, 2245 (1998)
- [28] S. Hill and W.K. Wootters, *Entanglement of a Pair of Quantum Bits*, Phys. Rev. Lett. 78, 5022 (1997)
- [29] W.K. Wootters, *Entanglement of Formation and Concurrence*, Quantum Information and Computation, Vol. 1, No. 1, 2744 (2001)
- [30] P.M. Hayden, M. Horodecki, B.M. Terhal *The Asymptotic Entanglement Cost of Preparing a Quantum State*, J. Phys. A: Math. Gen., 34, 6891 (2001)
- [31] E.M. Rains *Rigorous treatment of distillable entanglement*, Phys. Rev. A 60, 173 (1999)
- [32] M. Ozawa *Entanglement measures and the Hilbert-Schmidt distance*, Physics Letters A 268, 158–160 (2000)
- [33] G. Vidal, R. F. Werner *Computable measure for entanglement*, Phys. Rev. A, 65, 032314 (2002)
- [34] B.M. Terhal *Bell inequalities and the separability criterion*, Phys. Lett. A 271, 319–326 (2000)
- [35] R.A. Bertlmann, H. Narnhofer, W. Thirring *Geometric picture of entanglement and Bell inequalities*, Phys. Rev. A 66, 032319 (2002)
- [36] A. Einstein, B. Podolsky, N. Rosen *Can quantum-mechanical description of physical reality be considered complete?*, Phys. Rev. 47, 777 – 780 (1935)
- [37] J.S. Bell *On the Einstein-Podolsky-Rosen paradox*, Physics, 1, 195 – 200 (1964)
- [38] S.J. Freedman, J.F. Clauser *Experimental test of local hidden-variable theories*, Phys. Rev. Lett. 28, 938 (1972)
- [39] A. Aspect, P. Grangier, G. Roger *Experimental Tests of Realistic Local Theories via Bell's Theorem*, Phys. Rev. Lett. 47, 460 (1981)
- [40] J.F. Clauser, M.A. Horne, A. Shimony, R.A. Holt *Proposed Experiment to Test Local Hidden-Variable Theories* Physical Review Letters 23, Nr. 15, 880–884 (1969)
- [41] G. Weihs *Ein Experiment zum Test der Bellschen Ungleichung unter Einsteinscher Lokalität*, Doctoral Thesis, University of Vienna 1999

- [42] R. Horodecki, M. Horodecki *Information-theoretic aspects of inseparability of mixed states*, Phys. Rev. A 54, Nr. 3, 1838–1843 (1996)
- [43] R. Horodecki, P. Horodecki, M. Horodecki *Violating Bell inequality by mixed spin- $\frac{1}{2}$ states: necessary and sufficient condition*, Phys. Let. A 200, 340–344 (1995)
- [44] R.A. Bertlmann, P. Krammer *Bloch vectors for qudits*, J. Phys. A: Math. Theor. 41, 235303 (2008)
- [45] B. Baumgartner, B.C. Hiesmayr, H. Narnhofer *A special simplex in the state space for entangled qudits*, J. Phys. A: Math. Theor. 40, 7919 (2007)
- [46] B. Baumgartner, B.C. Hiesmayr, H. Narnhofer *The geometry of bipartite qutrits including bound entanglement*, Physics Letters A 372, 21902195 (2008)
- [47] A. Acín, D. Bruß, M. Lewenstein, A. Sanpera *Classification of Mixed Three-Qubit States*, Phys. Rev. Let. 87, Nr. 4 (2001)
- [48] W. Dür, G. Vidal, J.I. Cirac *Three qubits can be entangled in two inequivalent ways*, Phys. Rev. A 62, 062314 (2000)
- [49] C. Sabín, G. García-Alcaine *A classification of entanglement in three-qubit systems*, Eur. Phys. J. D 48, pp 435–442 (2008)
- [50] A. Peres, *Higher order Schmidt decompositions*, Physics Letters A 202, 16-17 (1995)
- [51] A. Acín, A. Adrianov, L. Costa, E. Jané, J.I. Latorre, R. Tarrach *Generalized Schmidt Decomposition and Classification of Three-Quantum-Bit States*, Physical Review Letters 85, Nr. 7, 1560 (2000)
- [52] H.A. Carteret, A. Higuchi, A. Sudbery *Multipartite generalization of the Schmidt decomposition*, J. Math. Phys. 41, 7932 (2000)
- [53] J. Kempe, *Multiparticle entanglement and its applications to cryptography*, Phys. Rev. A 60, 910 (1999)
- [54] R.W. Spekkens, J E. Sipe, *Non-orthogonal preferred projectors for modal interpretations of quantum mechanics*, arXiv:quant-ph/0003092 (2000)
- [55] A. Sudbery, *On local invariants of pure three-qubit states*, J. Phys. A: Math. Gen. 34, 643 (2001)
- [56] L. Tamaryan, D. Park, S. Tamaryan, *Generalized Schmidt decomposition based on injective tensor norm*, arXiv:quant-ph/0809.1290 (2008)

- [57] N.D. Mermin *Quantum mysteries revisited*, Am. J. of Phys. 58 (8), 731 (1990)
- [58] P.G. Kwiat, L. Hardy *The mystery of the quantum cakes*, Am. J. Phys. 68 (1), 33 (2000)
- [59] P.K. Aravind *Quantum mysteries revisited again*, Am. J. Phys. 72 (19), 1303 (2004)
- [60] F. Pan, D. Liu, G. Lu, J.P. Draayer *Simple Entanglement Measure for Multipartite Pure States*, Int. J. Theor. Phys. 43, 1241 (2004)
- [61] W. Cao, D. Liu, F. Pan, G. Long *Entropy product measure for multipartite pure states*, Science in China Ser. G 49, 606 (2006)
- [62] V. Coffman, J. Kundu, W.K. Wootters *Distributed entanglement*, Physical Review A 61, 052306 (2000)
- [63] A.R.R. Carvalho, F. Mintert, A. Buchleitner *Decoherence and Mutlipartite Entanglement*, PRL 93, 230501 (2004)
- [64] F. Mintert, M. Kuś, A. Buchleitner *Concurrence of Mixed Multipartite Quantum States*, PRL 95, 260502 (2005)
- [65] C. Eltschka, J. Siewert *Entanglement of Three-Qubit Greenberger-Horne-Zeilinger Symmetric States*, PRL 108, 020502 (2012)
- [66] W. Thirring, R. A. Bertlmann, P. Köhler, H. Narnhofer *Entanglement or separability - The choice of how to factorize the algebra of a density matrix*, Eur. Phys. J. D64, 181 (2011)
- [67] M. Kuś, K. Życzkowski *Geometry of entangled states*, Physical Review A 63.3 (2001)
- [68] F. Verstraete, K. Audenaert, B. DeMoor *Maximally Entangled Mixed States of Two Qubits*, Phys. Rev. A 64, 012316 (2001)
- [69] V. Scarani, N. Gisin *Spectral decomposition of Bells operators for qubits*, J. Phys. A: Math. Gen. 34, 60436053 (2001)
- [70] P. Walther, K. J. Resch, C. Brukner, and A. Zeilinger *Experimental Entangled Entanglement*, PRL 97, 020501 (2006)
- [71] R.A. Bertlmann *Private communication*
- [72] B. Baumgartner, B.C. Hiesmayr, H. Narnhofer *State space for two qutrits has a phase space structure in its core*, Phys. Rev. A 74, 032327 (2006)

Abstract

For tripartite states there is still no general tool to discriminate between separability and different types of entanglement. Some special entanglement measures, adjusted to the usage for multipartite system were studied, and especially applied to generalized GHZ and W states.

States with entangled entanglement and some of their corresponding geometrical structures are examined. Similar to the magic simplex in the two qubit case the geometrical structure of simplices plays an important role in the investigation of relations, symmetries and entanglement properties of tripartite qubit states.

For GHZ symmetric states the entanglement status and border lines for regions of different types of entanglement can be found [65]. Via local unitary transformation these informations could also be used for a simplex of states with entangled entanglement.

Using basis states as building blocks and entangling them in a special way we are able to construct GHZ type state for arbitrary many particles in a very straightforward method.

Finally with help of a Bloch representation we gained some interesting geometrical insights into the structure of tripartite qubit states.

Zusammenfassung

Für tripartite Quantenzustände gibt es bisher noch kein allgemeines Kriterium, das eine Unterscheidung zwischen separablen und verschiedenartig verschränkten Zuständen zuläßt. Einige spezielle Größen erlauben es – auch für multipartite Systeme – das Ausmaß von Verschränkung zu bestimmen. Diese wurden untersucht und speziell auf verallgemeinerte GHZ und W Zustände angewandt.

Auch Zustände mit verschränkter Verschränkung und deren entsprechend geometrische Struktur wurden untersucht. Wie beim "magischen Simplex" im Zwei-Qubit Fall spielt die geometrische Struktur eine wichtige Rolle bei der Untersuchung von Zusammenhängen, Symmetrien und Verschränkungs-Eigenschaften tripartiter Zustände.

Für GHZ-symmetrische Zustände können Verschränkungs-Eigenschaften und ihre Bereiche bestimmt werden [65]. Mit Hilfe von lokalen unitären Transformationen kann dieses Wissen auch auf einen Simplex von Zuständen mit verschränkter Verschränkung angewendet werden.

Verwendet man Basis-Zustände als Bauklötze und verschränkt diese in spezieller Art, so kann man auf einfache Weise GHZ Zustände mit einer beliebigen Anzahl von Teilchen erhalten.

Mit Hilfe der Bloch-Darstellung kann man weitere Einsichten in die Geometrie und Struktur von tripartiten Qubit-Zuständen gewinnen.

Curriculum vitae

Personal

Name: Gabriele E. Uchida

Education

1978	Matura (Baccalauréat), Lycée français de Vienne
1983	Diploma in Business Informatics (Wirtschaftsinformatik), University of Vienna
1988	Doctorate in Business Informatics (Wirtschaftsinformatik), University of Vienna
1994	Habilitation in Operations Research, University of Vienna
Since 2005	Studies of Physics at University of Vienna

Positions held

1982-1983	Research Associate, University of Vienna
1983-1994	Assistant Professor, University of Vienna
1994-	Associate Professor, University of Vienna